Effects of Prenatal Stress on Circadian Rhythms and Metabolism in Adult Rat Offspring

by

Alyssa Murray

A thesis submitted in partial fulfillment
of the requirements for the degree of
Master of Science (MSc) in Biology

The Faculty of Graduate Studies
Laurentian University
Sudbury, Ontario, Canada

Abstract

Circadian clocks developed in organisms as a way of estimating the time of day and control many vital aspects of physiology from the sleep-wake cycle to metabolism. The circadian clock operates through transcriptional-translational feedback loops. The normal circadian signaling relies on a 'master clock', located in the suprachiasmatic nucleus (SCN), which synchronizes peripheral oscillators. Here, glucocorticoid receptor (GR) signaling has the ability to reset the phase of peripheral clocks. It has been shown that maternal exposure to the stress hormone, glucocorticoids (GCs), can lead to modification of hypothalamic-pituitary-adrenal (HPA) function and impact stress-related behaviours and a hypertensive state via GR activation. We previously demonstrated altered circadian rhythm signaling in the adrenal glands of offspring exposed to the synthetic glucocorticoid, dexamethasone (Dex). Results from the current study show that prenatal exposure to Dex, affects circadian rhythm gene expression in a tissue and sex specific manner in molecular oscillators of the amygdala, hippocampus, paraventricular nucleus and prefrontal cortex as well as the main oscillator in the SCN. Results also show that spontaneously hypertensive rats (SHRs) exhibited dysregulated circadian rhythms in these same brain regions compared with normotensive Wistar-Kyoto rats (WKYs), although the pattern of dysregulation was markedly different from that seen in the Dex model. Metabolomic and gene expression results in the livers of GC-exposed offspring revealed sex specific metabolic profiles with females displaying increased lipid and glutathione metabolism, increased triglyceride concentration and decreased purine metabolism while males saw increased purine metabolism and evidence of an adaptation for increased lipid metabolism.

Keywords: Circadian rhythms, fetal programming, metabolism, hypertension, spontaneously hypertensive rat (SHR), dexamethasone

Acknowledgements

There are a number of individuals to whom I would like to thank and express my gratitude to for their contribution and support in the development and completion of this project. I would like to thank Dr. T.C. Tai and Dr. Sujeenthar Tharmalingam for their supervision and the professional guidance they have provided to me for the experimental design and conceptualization of this project. I would also like to thank Dr. Sandhya Khurana for the supervision and assistance she provided me in the training process as well as her support in my experimental work in the laboratory throughout this project. I also thank my committee members Dr. Aseem Kumar and Dr. Kabwe Nkongolo for their support of this project. I would like to thank my lab mate Christine Lalonde for her expertise in the micro-punching of the brain regions of the animals used in my gene expression experiments and for her assistance in the RNA extractions of these tissues. I would also like to thank my other lab mates and researchers at the Northern Ontario School of Medicine research laboratory for being extremely willing to answer questions and provide assistance. Important thanks is extended to previous Master's students in the Tai Lab, Phong Nguyen and Julie Grandbois, who performed excellent studies to acquire the brains, livers and plasma of the animals I have been fortunate enough to use for my thesis project.

I would also like to recognize and thank my family and friends for all the love and support they provided me throughout this process. I thank them for their unconditional love and unfailing support in all I do.

Table of Contents

List of Figures

List of Tables

List of Appendices

List of Abbreviations

ACADL – Acyl-CoA dehydrogenase long chain
ACADM – Acyl-CoA dehydrogenase medium chain
ACAT1 - Thiolase
ACTH – Adrenal-corticotropic hormone
ACSL1 – Acyl-CoA synthetase
ADA – Adenosine deaminase
ADHD – Attention deficit hyperactivity disorder
APS – Ammonium persulfate
Bmal1 – Brain-muscle-arnt-like protein 1
cAMP – Cyclic adenosine monophosphate
CAT – Catalase
CBP – CREB protein-binding protein
Clock – Circadian locomotor output cycle kaput
CPT1A – Carnitine palmitoyltransferase 1 alpha
CPT2 – Carnitine palmitoyltransferase 2
CRAT – Carnitine Acetyl-transferase
CRD – Circadian rhythm disorder
CREB – cAMP/Ca^{2+} response element binding protein
CRH – Corticotrophin-releasing hormone
Cry1 – Cryptochrome Circadian Regulator 1
Cry2 – Cryptochrome Circadian Regulator 2
CSNK1D – Casein kinase 1 delta
CSNK1E – Casein kinase 1 epsilon
Ct – Cycle threshold
CycA – Cyclin A
Dbp – D-Box Binding PAR BZIP Transcription Factor
DECR1 – 2, 4-dienoyl-CoA reductase
DEPC – diethylpyrocarbonate
Dex – Dexamethasone
E-box – Enhancer box
ECH1 – Enoyl-CoA hydratase
ECI1 – Enoyl-CoA isomerase
ECL – Enhanced chemiluminescence
FBXL3 – F-Box and Leucine Rich Repeat Protein 3
GAPDH – Glyceraldehyde 3-phosphate dehydrogenase
GC – Glucocorticoid
GDE1 – Glycerophosphodiester phosphodiesterase
GGT1 – Glutathione hydrolase
GPX1 – Gluthathione peroxidase
GR – Glucocorticoid Receptor
GRE – Glucocorticoid response element
GSR – Glutathione reductase
HADH – L-hydroxyacyl-CoA dehydrogenase
HESI-II – Heated-electrospray ionization probe
HPA axis – Hypothalamic-Pituitary-Adrenal Axis

HRP – Horseradish peroxidase
IQR – Interquartile range
IT – Injection time
KEGG – Kyoto Encyclopedia of Genes and Genomes
LC/MS – Liquid chromatography/mass spectrometry
MCEE – Methylmalonyl-CoA racemase
Mettl3 – Methyltransferase Like 3
MMUT – Methylmalonyl-CoA mutase
m/z – mass/charge
NCE – normalized collision energy
Npas2 – Neuronal PAS Domain Protein 2
NT5C2 – 5'-nucleotidase
PAGE – Polyacrylamide gel electrophoresis
PCCA – Propionyl-CoA carboxylase A
PCCB – Propionyl-CoA carboxylase B
PEMT – Phosphatidylethanolamine N-Methyltransferase
Per1 – Period Circadian Regulator 1
Per2 – Period Circadian Regulator 2
Per3 – Period Circadian Regulator 3
PFC – Prefrontal cortex
PLA1A – Phospholipase A1
PLA2G2A – Phospholipase A2
PLCG1 – Phospholipase C
PLD1 – Phospholipase D
PNP – Purine nucleoside phosphorylase
PPARα/γ/δ - Peroxisome proliferator activated receptor alpha/gamma/delta
PVN – Paraventricular nucleus
Rev-Erb-α – Nuclear receptor subfamily 1 group D member 1
Rev-Erb-β – Nuclear receptor subfamily 1 group D member 2
RIPA – Radioimmunoprecipitation assay
RORα/γ – Retanoic acid receptor-related orphan receptor alpha/gamma
Rpl32 – Ribosomal protein L32
RT-qPCR – Reverse transcriptase quantitative PCR
SCN – Suprachiasmatic nucleus
SDS – Sodium dodecyl sulfate
SHR – Spontaneously hypertensive rat
SMS – Spermine synthase
SOD1/2/3 – Superoxide dismutase 1/2/3
TEMED – Tetramethylethylenediamine
TG – Triglyceride
UHPLC – Ultra-high performance liquid chromatography
UOX – Uricase
WKY rat – Wistar Kyoto rat
XDH – Xanthine oxidase/dehydrogenase
YTHDF2 – YTH N6-methyladenosine RNA binding protein 2
Ywhaz – Tyrosine 3-monooxygenase/tryptophan 5-monooxygenase activation protein zeta

1. Introduction

Society puts great pressure and expectation on pregnant women to take care of themselves and to follow a set of guidelines such as the consumption of various supplements, the avoidance of alcohol or smoking, and overall healthy maintenance[1]. These guidelines have been put in place for good reason. What is currently recognized as fetal programming was first postulated in the seminal works of Barker and Hales,[2,3] who linked impaired gestational growth and development with the increased risk of several major diseases in later life [4–7]. The Barker hypothesis postulates that many organ systems undergo 'programming' in utero and that this is crucial in determining physiological and metabolic responses into adult life. There are many types of stressors that can induce negative programming such as changes in nutrition, endocrine status, and environmental pollutants throughout gestation and result in structural, physiological, metabolic and epigenetic changes[8].

Circadian disruption or misalignment is another such stressor that can invoke negative effects on the offspring. While much less is known about the fetal circadian system in comparison to that of the adult, it is known that the development of circadian rhythms is key to the development of the offspring and is influenced by the maternal circadian system[9]. While still a subject of study, most findings suggest that the expression of circadian rhythms does not occur until after birth in mammals[10–12]. It has been shown that the development of offspring can still occur normally in the absence of a functional maternal suprachiasmatic nucleus (SCN), however, signals of circadian timing from the mothers are required to synchronize rhythms postnatally[9,13]. The close proximity of mammalian mothers to their offspring, acts to influence their development in an action imitation manner[9,12]. It appears that entrainment of the fetal circadian system is influenced by the maternal circadian system either directly in a prenatal manner, or through learning cues in a postnatal

manner[9,12,13]. While there are many methods of inducing prenatal stress in an animal model such as malnutrition or environmental stressors (fetal hypoxia), this investigation examined the effects of prenatal stress, experienced through glucocorticoid (GC) administration, on the circadian rhythm system of rat offspring. Additionally, we investigated and compared circadian rhythms in the fetal programming model of hypertension and the genetic model of hypertension by examining the circadian system in the spontaneously hypertensive rat. Lastly, we assessed circadian rhythm signaling and metabolic function in the livers of glucocorticoid offspring through untargeted metabolomics.

1.1 Circadian Rhythm Clocks

Circadian rhythm clocks are regulators of the internal biological clock of the body. These clocks are what ensure the body awakens in the morning, becomes tired at night, and hungers at certain times of the day. The body's clock is trained to become activated by external stimuli such as light or temperature with light being the largest influence[14]. Nearly every cell in our body contains a molecular oscillator which allows it to tell the time[15]. In mammals, the circadian system is organized into a master clock located in the SCN of the hypothalamus, which commands peripheral clocks located in almost every tissue of the body including the liver, the lungs, peripheral leukocytes and the adrenal glands[16]. Peripheral clocks can be synchronized through external factors such as food or temperature or internal cues such as hormones, cytokines, metabolites, body temperature and sympathetic nervous activation[17].

Light stimuli enter through the eyes and are registered by the cells of the SCN[14,18]. At the cellular level, transcription-translation feedback loops of the clock genes Bmal1, Clock, Per1, Per2 and Per3, as well as Cry1 and Cry2, and their protein products result in the circadian oscillation of

clock genes and of genes involved in many cellular functions[14,15,18]. The proteins Bmal1 and Clock, or a Clock homolog called Npas2, make up the positive part of the circadian oscillator[16]. After they are translated, they dimerize and bind to E-box (enhancer box) response elements within the promoter regions of the Cry and Per genes; stimulating the transcription of these other essential clock genes[16,18]. Subsequently, Cry and Per protein products then form the negative limb of the circadian oscillator[18]. These proteins accumulate, form a complex with CSNK1D and CSNK1E, are phosphorylated, and translocate to the nucleus where they inhibit their own transcription through interfering with the Bmal1/Clock complex; thereby creating a negative feedback loop[14,18] (see Figure 1 for a visual overview of this process). With diurnal stimuli, this negative feedback loop acts to maintain a rhythmic oscillation of gene expression that cycles approximately every 24 hours and influences biological activities involved in the sleep/wake cycle, blood pressure, metabolism and immune functioning[15,19].

In addition to this main or core feedback loop described above, there are secondary or auxiliary feedback loops, which help to maintain the core loop activity[20]. There are many of these accessory feedback loops and levels of regulation to stabilize oscillatory patterns and fine-tune the cycle[14]. These systems of molecular clock machinery are found in all nucleus-containing cells within an organism and the central and peripheral clocks function through similar cellular processes.

It has been shown that 43% of all protein coding genes in mice show a circadian pattern in their transcription in at least one organ of the body[21]. On the organ level, it was found that the liver displayed the most gene cycling in a circadian fashion with 3,186 while the hypothalamus had the lowest amount at 642[21]. While 43% of all genes were found to oscillate, only 10 were found to oscillate in all organs and these 10 included core circadian genes such as Bmal1, Per1,

Per2 and Per3 as well as circadian rhythm activator Dbp and circadian rhythm repressors Rev-Erbα and Rev-Erbβ[21].

The importance of circadian rhythms can most effectively be seen through what happens when they are disrupted. Shift workers, frequent travelers and chronically stressed individuals often see the effects of this disruption through the development of metabolic problems[22]. Metabolic syndrome effectively describes a group of disorders that can co-occur including obesity, dyslipidemia, hyperglycemia and hypertension[23]. Disruptions in circadian rhythms have been implicated in many diseases such as breast cancer[24], obesity and type 2 diabetes[25,26], cardiometabolic disorders[27] and an overall higher risk of being immunocompromised[19]. The cell cycle and circadian rhythms are closely interrelated and clock genes contribute to the development of tumors through their interference with or regulation of c-Myc, p53 and p21, which are key cell-cycle related genes[17].

Many pharmacological drugs are also under circadian control with their metabolism and transport capacity differing with time of day. It is widely known that dosing time can account for variabilities in drug efficacy and specific schedules have been made for over 300 medications[28]. This is likely due to the target gene products of many drugs being products of circadian genes.

Aside from damaging the circadian rhythm system through the sleep/wake cycle in shift work or unbalanced stress hormone profile, circadian rhythms can also be disrupted through eating at unusual times[14], consuming alcohol, or taking antidepressants[29]. Misalignment of the circadian rhythm system can also have implications on behaviour with mood disorders as well as other mental health problems thought to be impacted by the circadian cycle[30,31]. This is especially important in the developing brains of pubescents, where sleep quality and circadian disruption have been shown to lead to an increased susceptibility of mood and substance use disorders[17].

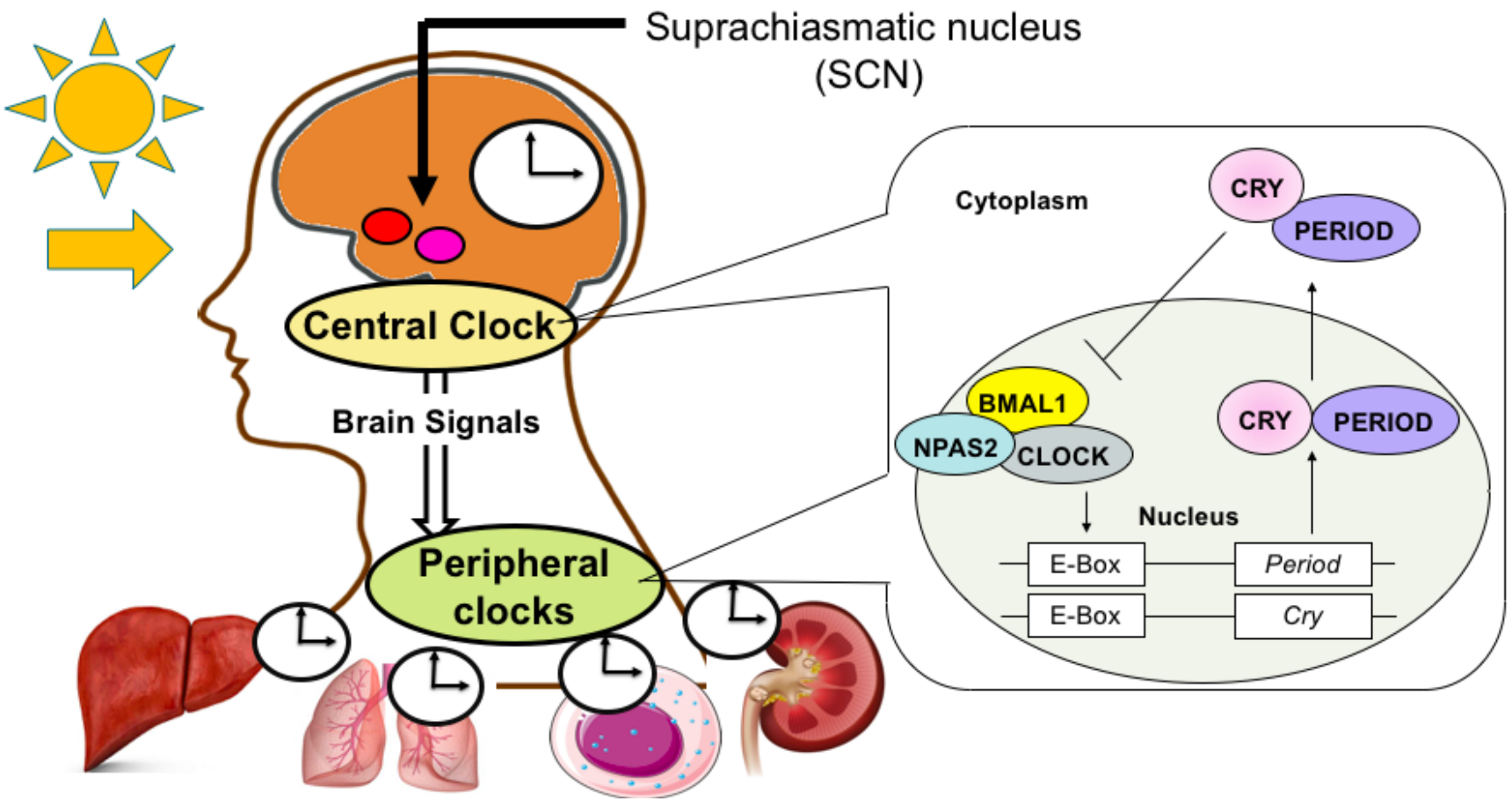

Figure 1. Visual representation of the circadian rhythm system on both a systemic and molecular level. The central clock in the SCN directs peripheral clocks in other organs and systems throughout the body. At the molecular level, transcription/translation feedback loops of Bmal1 and Clock as well as the Per and Cry genes drive the rhythmic timing of many bodily functions. Adapted from Nakao et al. 2015 [16].

1.2 Glucocorticoids

Glucocorticoids (GCs) such as cortisol (humans) or corticosterone (rodents) are typically labelled as stress hormones and are involved in the fight or flight response[18]. Under situations of stress, GCs are released through the activation of the hypothalamic-pituitary-adrenal (HPA) axis, which then coordinates the body's physiological response to stress via neuroendocrine mechanism. Signals from the SCN, the hippocampus, the prefrontal cortex (PFC) and the amygdala are transferred to the paraventricular nucleus (PVN) in the hypothalamus, which then activates the HPA axis[20,32]. This activation leads to the production of corticotrophin-releasing hormone (CRH) from the PVN, which binds to receptors on the anterior pituitary and initiates the secretion of adrenal-corticotropic hormone (ACTH) into the bloodstream[14,18,20]. This then triggers the production and release of GCs from the adrenal gland. These GCs are capable of binding to glucocorticoid receptors (GR) present in almost all tissues throughout the body activating a variety of responses generally involved in the maintenance of metabolism and energy[14]. This normally occurs through a negative feedback loop whereby the GCs in the bloodstream inhibit further stimulation of the HPA axis[33] (see Figure 2 for a visual representation of this process). When GC release becomes ill-timed, however, the high levels of cortisol can lead to metabolic effects, which in turn causes stress on the body and perpetuates the cycle. It is therefore imperative for the body to retain relatively good control over the release of GCs.

The glucocorticoid receptor (GR) interacts with GCs, and is central to the regulation of numerous genes involved in the stress response, the immune response and metabolism[14,18]. GR is expressed in nearly all tissues, with the notable exception of the SCN[34]. Once stimulated by GCs, the GR/GC complex can translocate to the nucleus and bind to glucocorticoid response elements (GREs) in the promoter regions of many genes, thereby influencing their expression[14]. The

circadian rhythm genes Per1 and Per2 have GREs present in their promoter regions, allowing for transcriptional control of these rhythmic genes by the level of GCs in the body[34,35]. Stress responses in the body tend to depend on the time of day. It has been noted that chronic stress seems to be more harmful when applied during the inactive or dark phase[14,34]. Dysregulation of GC release can be triggered by the shortening of daylight, constant light, and unnatural food intake times with these disruptions shown to lead to a variety of adverse health effects[27]. Previous findings have suggested that while GR influences the transcription of Clock and Bmal1 that the Clock/Bmal1 heterodimer itself can also affect GR levels. The Clock/Bmal1 complex acts as a negative regulator of GR in peripheral target tissues, and can actually mimic the physiologic actions of fluctuating cortisol[36]. This illustrates the significant amount of interplay that is present between the circadian rhythm and GR/GC systems.

GCs are one of many hormones which are typically released based on circadian signaling and are under the control of the SCN[34]. As previously mentioned, GR is not expressed in SCN cells with the exception of a short period around birth[34]. This fact allows for the central and peripheral clocks in the body to not always be running at the exact same time. Stress mediated release of high levels of GC are capable of interacting with GR in cells other than the SCN, changing the circadian gene expression levels and causing shifts in the normal rhythms in the body[18,34]. Shifts in rhythms can occur through food restriction, or the administration of exogenous GCs[37]. The adrenal glands have core circadian oscillators in their cells which have activity independent of SCN signaling via the pituitary gland[34,38]. The adrenal circadian clock is capable of inducing rhythms in other peripheral tissues via the release of catecholamines, glucocorticoids and sex steroids[14,39,40]. It has been found that the destruction of the central clock abolishes the synchronization of peripheral clocks in different organs, however, the circadian rhythm in each

peripheral clock is maintained[41]. This suggests that peripheral clocks have conditional autonomy from the central clock. When central clock and peripheral oscillators become uncoupled, GCs have been found to be secreted at high concentrations, which acts to try and overcome the discrepancy between the two clocks, providing a protective yet maladaptive response to stress[20].

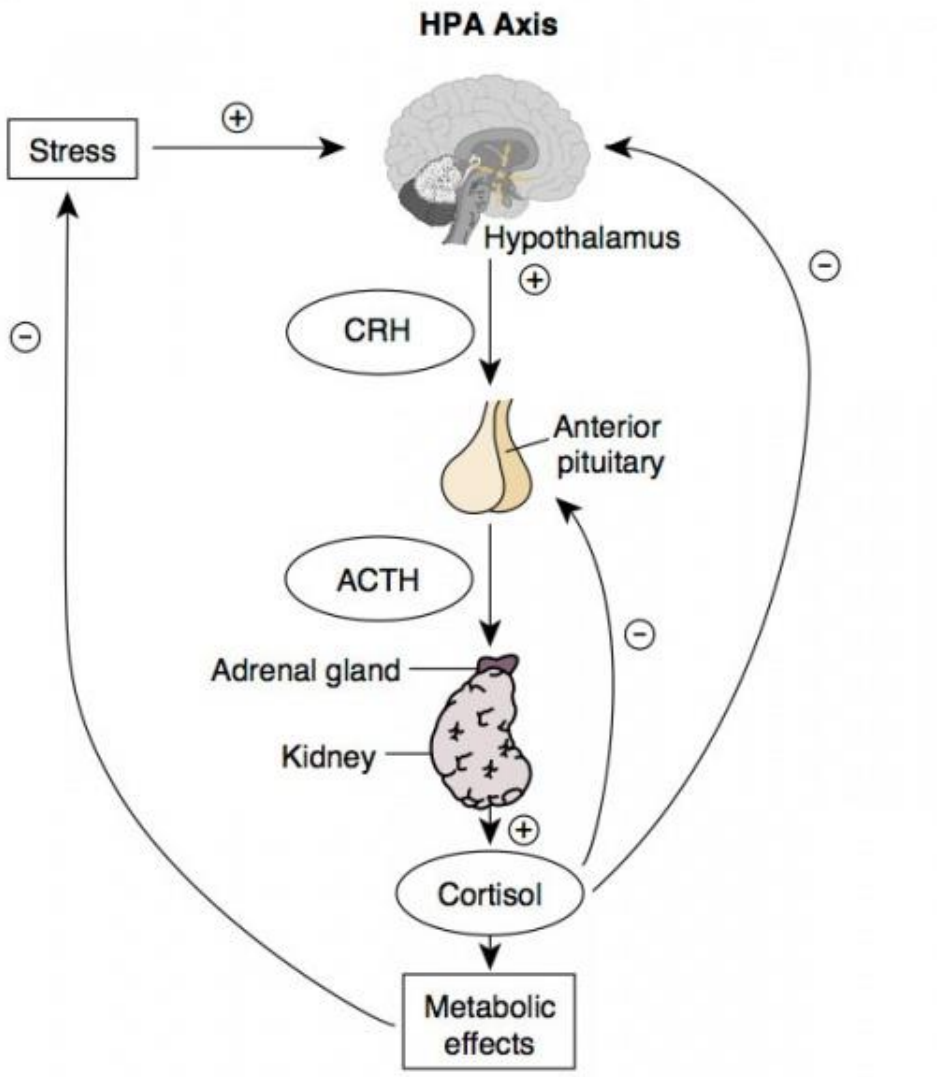

Figure 2. Visual representation of the HPA axis and the stress response system. Under times of high and continual stress, the negative feedback loop of the HPA axis is inhibited and continual release of Cortisol (GCs) occur; leading to metabolic effects and perpetuating the cycle. Retrieved from UNSW Embryology[42].

1.3 Fetal Programming Stress Model

One model that we used to study circadian rhythm dysregulation was the fetal programming stress model. While it has been shown that immediate stressors have an effect on circadian rhythms, the role of a fetal programmed state of stress is unclear. As previously mentioned, the Barker hypothesis, established in the 90s, states that under situations of maternal stress, many fetal organ systems and functions can undergo "programming" *in utero* that is crucial in determining physiologic and metabolic responses into adult life[6,7]. There are many types of prenatal stressors such as maternal undernutrition, the dysregulation of hormones, and other environmental factors such as not getting enough sleep or drug use[43], that can induce a negative programming and result in structural, physiologic, metabolic and epigenetic changes in the offspring. The expression of circadian rhythms does not occur until after birth in mammals and timing signals from the mothers in addition to the environment are required to synchronize these rhythms postnatally[9,44]. Resilience to stressors is decreased and vulnerability is increased by adverse childhood or fetal experiences that lead to a biological embedding of response to stressful life events. This vulnerability leads to an increased risk of physical and mental health disorders over life,[8] perhaps through an epigenetic mechanism. Epigenetics are thought to play a role in fetal programming as transgenerational effects are seen[32,45,46]. Subsequent offspring of fetal programmed animals, who themselves were not subjected to adverse conditions *in utero*, receive the programming from their parents and tend to display the effects of prenatal stress.

Some of the earliest examples of fetal programming can be found from the aftermath of two widespread famines, the Dutch Hunger Winter in the North of Holland and the Leningrad famine, both of which took place during World War II. A comparison of these two famines lead to surprising results. In the Dutch famine, offspring subjected to restricted nutrition *in utero* during

early pregnancy had more coronary heart disease, increased blood lipid levels, higher obesity and altered clotting compared to those not exposed[47]. Interestingly, the Leningrad study did not find the same results. There were differences in these populations that may have accounted for this, such as length of famine (Leningrad-3 years, Dutch-6 months) and also the previous nutrition status of the population. This lead researchers to hypothesize that long-term effects of adaptations to a sub-optimal intrauterine environment may prove more detrimental if a mismatch occurred between the predicted postnatal environment developed *in utero* and the actual postnatal environment encountered[47]. Infants that have a rapid catch-up growth period after delivery have been found to have an increased risk of several components of metabolic syndrome in adulthood; including hypertension[48].

In adult mammals, GCs regulate a variety of important cardiovascular, metabolic and immunologic functions[5,8], however, in the fetus, GCs appear to be important in fetal development. GRs are expressed in fetal tissues from mid-gestation onwards and in the placenta[32]. Clinically, injections of a synthetic GC, dexamethasone (Dex), are given to mothers at high risk of preterm labour to accelerate the maturation of fetal lung tissue, decrease the likelihood of respiratory distress syndrome and improve survival[49]. Exogenous GC administration can lead to increased plasma corticosterone levels and prematurely induce significant maturational events[32]. High GC exposure can also occur endogenously, such as if a mother experiences high levels of stress. The severity of the programming is often dependent on the dose and the timing of the GC exposure[43]. While high levels of GCs during pregnancy leads to a reduction in birth weight (a key identifier in fetal programmed offspring), programming effects can also be seen in the absence of low birth weight[8]. Short term prenatal exposure to Dex or corticosterone is associated with programmed effects on blood pressure, and renal development[50]. There are also a variety of critical periods in

development during which the administration of GCs may have a more detrimental effect[32,43]. *In utero* exposure to GCs during the last trimester of pregnancy reduces GR levels in the hippocampus of the offspring, which is thought to decrease the sensitivity of stimulus feedback and altering the baseline of the HPA axis[32]. Prenatal Dex exposure increases the levels of CRH in the amygdala, which has been shown to have a relationship with the expression of fear and an increase in anxiety-like behaviour[32].

Limited research has been done surrounding the long-term effects prenatal stress has on the circadian rhythm functioning of the offspring and the potential implications an impaired functioning could have in overall health and disease. The development of this project began with a fetal programming study where pregnant female WKY rats were given injections of Dex through the third trimester of their pregnancy[51]. A whole transcriptome analysis of the adrenal glands highlighted the disruption of circadian rhythm signaling genes in animals that were prenatally exposed to Dex, compared to the naïve or saline groups[52]. This study showed that the genes Bmal1 and Npas2 were significantly upregulated and the genes Per2 and Per3 were significantly downregulated. These results suggest an altered mechanism of circadian signaling in the adrenal glands of the GC exposed offspring where Bmal1 and Npas2 control the expression of the Pers and Crys rather than the normal Clock/Bmal1 system[14,40]. Since the Npas2 protein is a homolog of clock and has been shown to be associated with hypertension, Bmal1 and Npas2 may interact together in this prenatally programmed dysregulated system and drive the phenotypic effects of hypertension seen in these animals[53].

Circulating GCs tend to demonstrate a rhythmic pattern in the body with peak secretion levels occurring in the morning, which is important in synchronizing central and peripheral clocks[40]. It has been shown that children exposed to antenatal GCs lacked the peak morning

secretion, known as a cortisol awakening response, and displayed a flattened rhythm throughout the day[54]. Fetal programming studies with the stressor of maternal undernutrition have shown that programmed animals lost the variation in blood pressure between day and night, which reflects a loss of circadian rhythm[47]. This is significant as it is known that individuals that do not display a circadian pattern of blood pressure have been associated with hypertension and cardiovascular disease[55].

1.4 Spontaneously Hypertensive Rat (SHR) Model

As previously mentioned, it has been shown that a chronic disruption in circadian rhythms can lead to certain pathological states, including hypertension[23]. Therefore, the other model that we used to study circadian rhythm dysregulation was the WKY/SHR system, which is a genetic model for hypertension. Hypertension, also known as the 'silent killer', refers to a chronic rise in blood pressure over time and leads to an increased risk of cardiovascular disease and death[56] and is estimated to affect 25% of the world's adult population. The spontaneously hypertensive rat (SHR) is the most commonly used animal model for hypertension and is genetically related to the Wistar-Kyoto (WKY) rat from which it was genetically modified to be hypertensive[57]. These genetically modified animals have significantly increased blood pressure compared to their normotensive counterparts. SHR rats develop pre-tensive blood pressures around 6 weeks of life and demonstrate full hypertension at 12-14 weeks of life[58]. Mean arterial blood pressure in male SHRs typically reach around 180 mmHg while female SHRs reach blood pressures of 150-160 mmHg[59]. It is also well documented that male SHR rats have a much more rapid and severe development of hypertension than the females, which is similar to the trend seen in humans between adult males and pre-menopausal women[59]. Due to these differences, it is thought that sex

hormones must play a role in either facilitating a rise in blood pressure in males or protecting against hypertension in females. As it has been shown that ovariectomy does not contribute to an increased risk of hypertension on its own, it is thought that higher levels of androgens promote a state of hypertension[59].

Blood pressure is tied to its own rhythm and SHRs have a blood pressure rhythm that is shifted compared to WKYs. Interestingly, the activity period in SHR animals is shifted 1.5 hours earlier than WKYs and their response to life cycle shifts is changed, which indicates that they have aberrant circadian functioning at some level[60]. A key piece of evidence linking the circadian system with the pathogenesis of hypertension in SHRs is the presence of a single nucleotide polymorphism in the Bmal1 gene[61]. We have previously shown that many of the core and accessory circadian rhythm genes including Bmal1 are dysregulated in the adrenal glands of SHRs compared to their WKY controls and that these changes are much different than those seen in the Dex model[52]. While the Dex model of hypertension showed upregulations in the positive limb of the circadian oscillator (Bmal1 and Npas2) and downregulations in the negative limb (Per and Cry genes), the SHR model of hypertension showed the opposite, which suggests that while these animals have dysregulated circadian rhythms it is not in the same manner. In fact, previous studies have shown that SHR adrenal glands display a circadian phase advance compared to their WKY counterparts[62] and in our previous study, when examining the normal circadian oscillation patterns in comparison to time of animal sacrifice, results showed that increased Bmal1 and Npas2 transcripts occurred earlier than expected in SHR animals and later than expected in Dex animals.

1.5 Hypertension and Circadian Rhythms

Since both investigated models result in a hypertensive state and have been shown to have dysregulated circadian rhythms, it is possible that an altered circadian entrainment may play a role in the development of hypertension in both two animals models examined. It has been long known that blood pressure exhibits a circadian rhythm as it lowers at night, has a surge in the morning and peaks in late afternoon[55]. Not only does blood pressure have its own circadian rhythm, but it also is affected by the circadian clock as well. Chronic shift workers who experience circadian misalignment display a significant increase in both diastolic and systolic blood pressures as well as C-reactive protein; a marker of systemic inflammation[63]. This study demonstrated a direct link between circadian disruption and increased risk of cardiovascular disease.

There have been many rodent models which demonstrate a link between the circadian clock in the regulation of blood pressure. Every clock gene mutant or knockout studied has exhibited an abnormal blood pressure phenotype[55]. Bmal1 knockout mice have been shown to have a lowered blood pressure and an unnatural rhythm with blood pressure remaining lowered throughout the entire 24 h cycle[64]. Sympathoadrenal function was also disrupted, which indicated the control of enzymes related to the synthesis (phenylethanolamine *N*-methyltransferase) and degradation of catecholamines (monoamine oxidase B and catechol-*O*-methyl transferase) is tied to the circadian clock[64]. Clock knockout mice exhibit a lowered blood pressure compared to wild type controls, however, it is not as pronounced as that seen in Bmal1 knockouts likely due to the ability of Npas2 to substitute for Clock in the heterodimer with Bmal1[55,64]. In a study by Woon *et al*. a strong association was found between Bmal1 and an increased susceptibility to type 2 diabetes and hypertension as the result of two single nucleotide polymorphisms (SNPs) in the Bmal1 gene, which lowered transcription efficiency[61]. A human kidney transcriptome study between

normotensive and hypertensive individuals found the Per1 was significantly upregulated in those with hypertension[65]. Collectively, these studies show that the circadian rhythm genes play an important role in blood pressure control in humans and rodent models.

1.6 Circadian Rhythms and Metabolism

There is a significant link between circadian rhythm and metabolism as evidenced by chronic shift workers and frequent travellers. Circadian disruption is strongly associated with metabolic imbalance and an increased risk of metabolic syndrome; which currently describes a group of disorders that often co-occur such as central obesity, insulin resistance dyslipidemia, hyperglycemia and hypertension[66,67].

Factors such as nutrient-lacking high-energy foods along with decreased energy expenditure and a sedentary life-style contribute to metabolic disorders[68]. It has been shown, however, that environmental circadian disruption and genetic aberrant variants in circadian machinery can lead to metabolic disorders[69]. The body is remarkable in its ability to maintain its energy equilibrium but when energy intake exceeds energy expenditure, metabolic fuel is stored as liver glycogen, muscle protein and adipose tissue[66]. This is further complicated if energy intake does not coincide with gene expression for metabolic homeostasis. Many metabolic pathways in the muscle, adipose, liver and pancreas follow a circadian rhythm in their expression and if feeding does not occur at the correct time, the mechanisms of metabolic fuel use and energy storage are disrupted[70,71]. The SCN has been shown to contribute to the circadian rhythmicity of eating and drinking since ablation of the SCN destroys the rhythms of both these processes[72].

Further evidence for the rhythmic nature of metabolism comes from studies that examined rhythmic gene expression that occurs in the absence of environmental cues such as a light-dark

cycle. By holding mice under constant darkness, it was reported that 15% of the expressed transcripts in the liver exhibited a circadian rhythm and although these transcriptional rhythms were attributed to the circadian clock, they were sustained even in the absence of light[73]. Interesting results were also reported with regards to feeding in the presence of an absent internal clock. The cyclic activities of metabolic regulators are loosely associated with the circadian clock, however, time restricted feeding can promote their rhythmic activity even in the absence of an internal clock[73]. In this same study, rhythmic feeding was shown to increase the amplitude of circadian clock oscillations and their target, which in turn modified and enhanced transcriptional responses to feeding with respect to metabolism. This example shows the large amount of interplay that occurs at the molecular level between circadian rhythms and metabolism.

Due to the importance of the liver in the homeostasis of glucose and lipid metabolism, its involvement in the circadian system is extremely important to metabolic physiology[66]. Circadian clock proteins in the liver have other intracellular roles apart from the classical loop seen in Figure 1 (see Figure 3). For example, Per2 has been found to bind to nuclear receptors PPARα, PPARγ and Rev-Erbα, which controls white adipose and liver tissue metabolism[74,75]. Cry1 has also been shown to have a role in cAMP signaling and gluconeogenesis[76]. Rev-Erbα, one of the targets of Per2 in the liver, is a circadian clock gene that can repress Bmal1. It is also an important metabolic regulator in the liver where it modulates lipid, glucose and bile acid metabolism and contributes to processes such as adipogenesis and inflammation[70]. Many rate-limiting metabolic enzymes in the liver are directly controlled by core circadian transcription factors[68]. For example, peak expression of glucose transporters and the glucagon receptor is observed in the early evening, which is when most animals ingest the majority of their daily food[68]. The liver is a key player in lipid metabolism and while the circadian clock regulates most aspects of hepatic lipid metabolism,

it has been found that lipids also regulate circadian rhythms[77]. RORα, RORγ and PPAR(α, γ and δ) regulate the transcription of Bmal1 while at the same time participate in the control of lipid metabolism[77]. RORα and RORγ are themselves transcriptionally regulated by cholesterol and oxysterols while PPAR isoforms are bound by eicosanoids and various fatty acids[77]. This study provides evidence of a metabolic feedback loop within the liver circadian clock mechanism, which involves intermediates of lipid metabolism.

1.7 Stress, GCs and Metabolism

GCs primarily contribute to the stress response through the activation of the HPA axis. Stress is defined as a state of threat to homeostasis or disharmony within the body and results in a variety of physiologic and behavioural responses which attempt to restore balance within the body[78]. With regard to metabolism, the stress response adapts to the threatening situation by mobilizing the body's energy stores[79]. There are two categories of stress; acute and chronic. Acute stress has been shown to favour an anorexigenic response where food intake and body weight are reduced in a manner directly proportional to the stress severity[80]. Interestingly, body-weight lowering effects can be extremely long lasting when the stressor has been encountered repeatedly. Even after 80 days after a 3-day stressor, rats exposed did not catch up to the weights of non-stressed control rats[81]. Stress activates the sympathetic nervous system, which stimulates the production of catecholamines that stimulate lipolysis and the release of fatty acids from adipose tissue in addition to glycogenolysis and gluconeogenesis in the liver[79].

When stressors are prolonged over a longer period of time, it is considered to be chronic and this type of stress leads to increased problems. In a persistent state of stress, the body tries to adapt; which in the short term is beneficial, however, over time this leads to maladaptive changes

to physiological responses in addition to the harm of the persistent stressor[78]. While chronic stress initially sees a body weight reduction similar to the acute condition, eventually weight gain starts to occur as the body makes metabolic adaptations to increase calorie efficiency[79]. In other words, a single calorie can provide more fuel to a chronically stressed individual than a non-stressed individual through the compensatory mechanisms the body uses to restore energy balance.

Chronic stress has been associated with perturbations in metabolic homeostasis, which can contribute to the presentation of visceral obesity, type 2 diabetes, atherosclerosis and metabolic syndrome[78]. In humans especially, it has been found that mild (non-traumatic) but chronic stressors increase body weight and preferences for palatable foods by activating pathways that increase the reward value of food[82]. Rising levels of stress in modern society are correlated with an increasing rate of obesity and metabolic syndrome; both of which have reached levels of epidemic proportion. Stress and these pathologies are interrelated and feed off each other. Chronic HPA activation favours visceral fat accumulation, which in turn causes increased stress on the body eventually leading to HPA axis dysfunction[78].

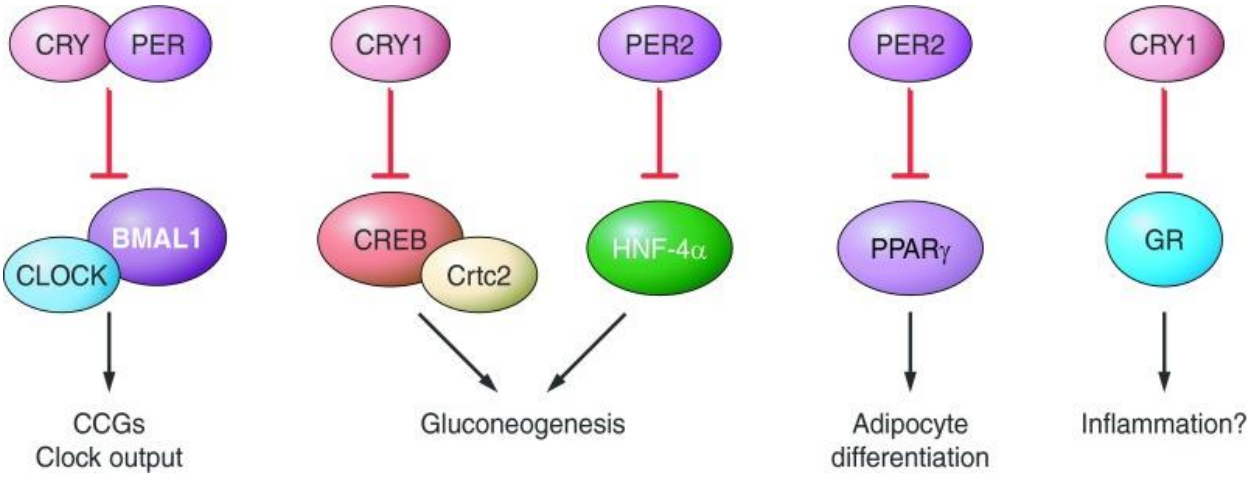

Figure 3. Additional functional roles of circadian clock proteins of the core clock machinery. The Clock-Bmal1 complex activates clock genes, but Cry1 and Per proteins can bind to nuclear receptors or other intracellular proteins to regulate some metabolic functions. Retrieved from Eckel-Mahan and Sassone-Corsi 2013[66].

1.8 Objectives/Hypothesis

1.8.1 Hypothesis

It has previously been found that prenatal stressors disrupt the circadian rhythm gene expression in the adrenal glands, which can further dysregulate the body through ill-timed GC release[52]. In this study, it is hypothesized that due to the interplay of the circadian rhythm clocks of the body and GCs, that prenatal GC exposure will result in dysregulated circadian rhythm gene expression in central and peripheral clocks, which can cause metabolic impairment in the adult offspring.

1.8.2 Objectives

The objectives of this study were:

Objective 1: Determine a mechanism of circadian rhythm dysregulation in the brains of GC exposed offspring and compare to the WKY/SHR genetic model of disease.

Objective 2: Assess circadian rhythm signaling and metabolic function in the livers of GC exposed offspring.

To elucidate the mechanism behind circadian rhythm dysregulation in GC exposed offspring, this investigation examined if this prenatal stressor can affect circadian rhythm gene expression in brain regions implicated in the HPA axis (see Figure 4). While the adrenal peripheral circadian clock can easily become uncoupled from the master clock located in the SCN, it is unclear if the adrenal gland dysfunction in the GC exposed offspring originates from a programmed dysregulation of the entire system going back to the SCN or if the dysfunction comes from a programmed uncoupling of the peripheral clock in the adrenal gland. While it is known that

cortisol and the central clock can affect the peripheral clocks, it is unclear whether cortisol or the peripheral clocks can affect the central clock.

Circadian rhythm gene expression in the SCN, amygdala, hippocampus, prefrontal cortex (PFC) and paraventricular nucleus (PVN) were investigated as they all play a role in the activation of the HPA axis and GC release. With the results from the circadian rhythm gene expression in the adrenal glands being compared to the brain regions, the mechanism behind circadian rhythm disruption caused by prenatal stress can be determined.

This investigation also examined at the mechanism of circadian rhythm dysregulation in the specific brain areas mentioned for the WKY/SHR genetic model of hypertension. It is known that circadian rhythm dysfunction poses an increased risk of hypertension, however, it is unknown if the pathology of hypertension itself can lead to a dysregulated circadian rhythm. Blood pressure has its own rhythm in the body and therefore we hypothesize that a disrupted blood pressure system will have an effect on circadian rhythm gene expression in these animals. Both the fetal programming and WKY/SHR models produce the same disease of hypertension, however, have markedly different etiologies. Through investigating the expression of core clock genes in the brain of both hypertensive animal models their circadian rhythm function could be compared.

The second aim of this project analyzed the liver from GC exposed animals. Given the link between circadian rhythms and metabolism, a goal of this study was to identify any metabolic dysregulations that could be associated with the impaired circadian rhythms in these animals. The liver was investigated due to its central role in all metabolic processes in the body. Using an untargeted metabolomic approach this study hoped to answer questions surrounding metabolism and circadian rhythms, such as: are they both being affected, is one impaired system the initiator of the dysregulation and is one system influencing the other or are they influencing each other.

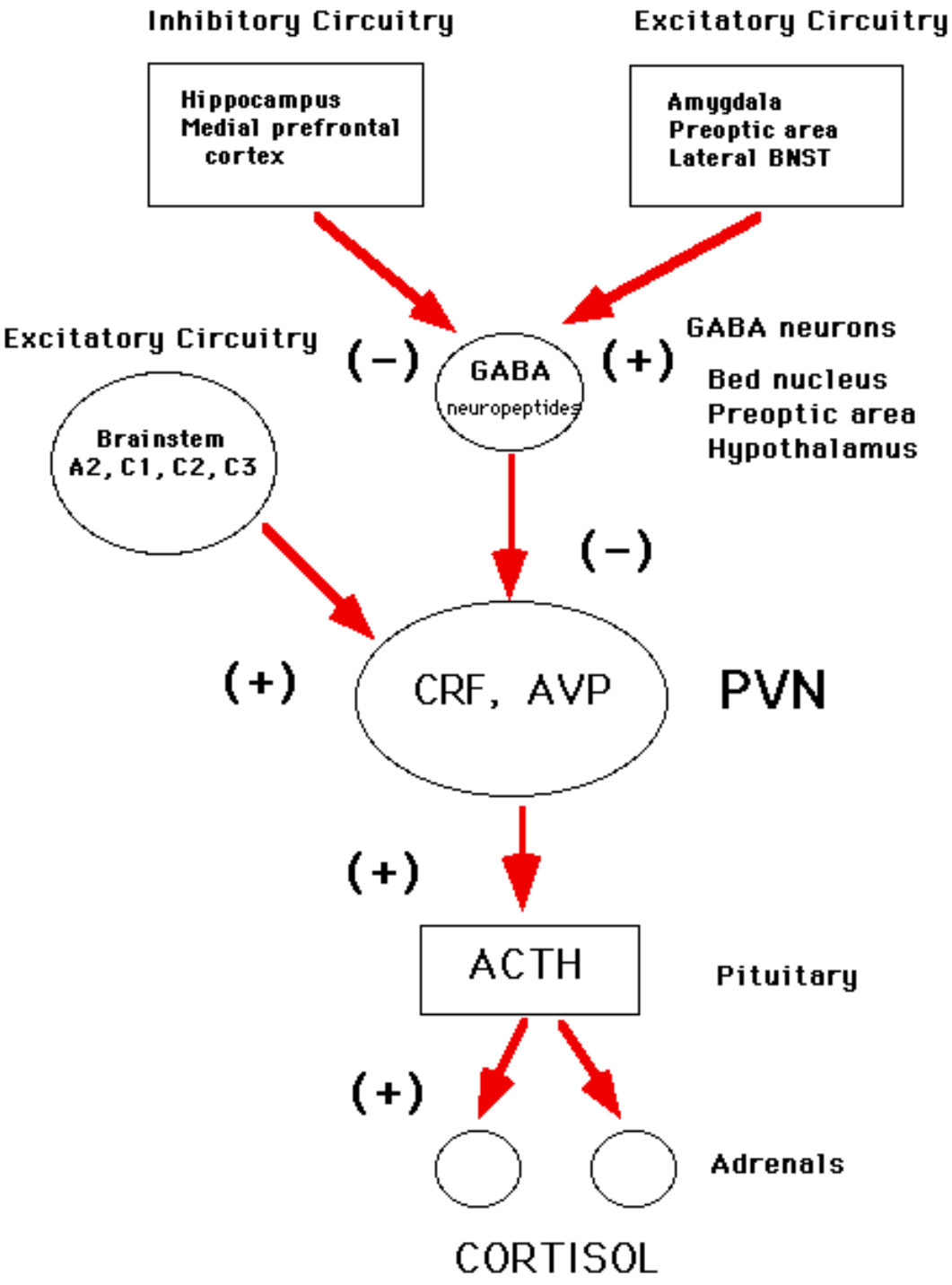

Figure 4. Brain circuitry of the HPA axis stimulation and interaction. Retrieved from McEwen, 2002 [83]

2. Materials and Methods

2.1 Tissue Collection

Brains, livers and plasma used for analysis were collected from previous animal studies involving the Dex-induced fetal programming model of hypertension as well as the WKY/SHR genetic model of hypertension. The animal care procedures were approved by Laurentian University's Animal Care Committee, in accordance with the Canadian Council on Animal Care. Protocols regarding animal handling from delivery to tissue collection were previously described[51,52]. Rats were exposed to a 12-hour light-dark cycle and food and water were provided ad libitum. Dex-induced fetal programming of WKY rats was previously shown[51,84]. Briefly, pregnant WKY females were administered subcutaneous injections of 100 μg/kg/day Dex in 0.9% NaCl with 4% ethanol or saline solution control throughout their third trimester (days 15-21). Resulting offspring were weaned at 3 weeks and housed at 2-3 rats per cage keeping sex consistent. At 19 weeks of age, male and female rats were anesthetized through intraperitoneal injection of 75 mg ketamine (CDMV Inc.) and 5 mg xylazine (Sigma) per kg of body weight. Brains, livers and plasma vials of each sex were collected from 19 week old WKY rats exposed *in utero* to 100 μg/kg/day Dex and saline (control), frozen on dry ice and stored at -80 °C until further use. Brains were also collected from 19 week old SHR and WKY rats that were purchased at 17 weeks and acclimatized without breeding or injection until 19 weeks when they were anesthetized. Anesthetizations and subsequent collection of tissue samples all occurred between 10 and 11 am.

2.2 RNA Extraction from Tissue

All brain areas were dissected using sectioning or a micro-punch technique as previously described[85]. Brains were mounted to a Cryostat blade (Leica) and thinly sliced. Each slice was then observed for neuroanatomical structures and brain areas of interest were punched out using a pipette tip[86]. Punches from each brain area were combined in 2 mL Eppendorf tubes and stored at -20 °C until time of extraction.

2.2.1 Phenol Extraction from Brain Micro-punches

To the 2 mL Eppendorf tubes containing the micro-punched tissue samples, 250 μL of "Solution D" was added (Solution D: 4 M guanidine thiocyanate, 25 mM sodium citrate, 0.5% sodium sarcosine, 0.1 M β-Mercaptoethanol in distilled water), along with a DEPC-water treated, autoclaved stainless steel bead. The tubes were then placed in the TissueLyser (QIAGEN; Newton, PA, USA) for 2 cycles of 1 minute at 30 Hz. The samples were spun down to condense the generated foam, 25 μL of a 3 M sodium acetate pH 4 solution was added. The tubes were placed back in the TissueLyser for 1 cycle of 1 minute at 30 Hz and spun down to condense foam. The samples were then transferred to fresh 1.5 mL microcentrifuge tubes and 300 μL of a mixed phenol/chloroform/isoamyl alcohol (25:24:1) solution (Fisher-Scientific) was added. Tubes were vortexed for 10-15 seconds and then incubated at room temperature for 10 minutes before being placed in the centrifuge at 12,000 x g for 20 minutes (Eppendorf).

After centrifuging, the tubes contained distinctly separated phases. The top, clear phase was carefully removed and placed in a new microcentrifuge tube taking care not to touch the white DNA interphase. To the separated aqueous phase, 1 mL of a 90% ethanol solution (Commercial

Alcohols) was added and gently pulsed to mix. The tubes were then placed in the -80 °C freezer for 4-5 days to allow for RNA precipitation.

Samples were then removed from the freezer and centrifuged at 12,000 x g for 20 minutes at 4 °C. Samples were removed from the centrifuge and 250 μL of a 70% ethanol solution (Commercial Alcohols) was added. Samples were gently inverted to mix and then placed back in the centrifuge at 12,000 x g for 20 minutes at 4 °C. A small pellet of RNA was present in the bottom of the tubes. Supernatant was carefully removed taking care not to disturb the pellet. Pellets were then air-dried for 10-15 minutes before being dissolved in 30 μL of DEPC water. These samples were then placed on a Thermomixer (Eppendorf) for 10 minutes at 37 °C and 1000 rpm to further dissolve. Dissolved RNA was then placed on ice for at least 20 minutes prior to spectrometry.

2.2.2 RNA Extraction from Tissue Sections

To the 2 mL Eppendorf tube containing the tissue section, TRI Reagent (Sigma-Aldrich) was added according to the manufacturer's instruction (1000 μL/50 g tissue) along with a stainless steel bead. The microfuge tube was then placed in a Tissuelyser (Qiagen) for 2 cycles at 30 Hz for 2 minutes to facilitate homogenization. The supernatant was mixed with 200 μL of chloroform per 1000 μL of TRI Reagent added (Fisher chemicals; Fisher Scientific; Toronto, ON, Canada) before vortexing for 10-15 seconds. Samples were then incubated at room temperature for 15 minutes before being centrifuged at 12,000 x g for 20 minutes at 4 °C (Eppendorf, Mississauga, ON, Canada).

After centrifugation, the tube contained three distinct layers. The aqueous phase, which appears colourless and sits as the topmost layer, was transferred to a fresh tube with care being taken not to disturb the other phases. In the fresh tube, 250 μL of isopropanol (per 1000 μL TRI Reagent) (Sigma-Aldrich) was added to the aqueous phase before being vortexed for 5-10 seconds. After vortexing, samples were incubated at room temperature for 10 minutes and then placed in the centrifuge at 12,000 x g for 8 minutes at 4 °C. After centrifuging, a pellet was present at the bottom of the tube. The supernatant was discarded and 1000 μL of a 70% ethanol solution (per 1000 μL TRI Reagent) (Commercial Alcohols; Brampton, ON, Canada) was added to wash away salt contamination of the pellet. These samples were then placed in the centrifuge at 7,600 x g for 5 minutes at 4 °C. After this, the ethanol was removed and the pellets were air-dried for 10-15 minutes. The RNA pellet was then dissolved in DEPC-treated water and placed on a thermomixer (Eppendorf) for 10 minutes at 37 °C and 1000 rpm to dissolve the pellet. Dissolved RNA was then placed on ice for at least 20 minutes prior to spectrometry.

2.3 Spectrometry

Using the NanoDrop One (Thermo-Scientific) spectrophotometer, the RNA setting was selected to complete the analysis. The pedestal was cleaned with water and wiped dry. 1 μL of DEPC-water was loaded onto the pedestal as the blank. Samples were mixed by pulsing and then 1 μL of each RNA sample was loaded and the concentration and relative purity was determined.

2.4 Reverse Transcription

To a labelled, autoclaved 0.2 mL PCR tube (Fisher Scientific), 2 μg of an RNA sample was added in addition to 2 μL of 10x DNAse Reaction Buffer (Sigma-Aldrich), 2 μL of Amplification Grade DNAse I (Sigma-Aldrich) at 1 U/μL and DEPC-treated water to a final volume of 20 μL. Tubes were then sealed, mixed, spun down and incubated at room temperature for 15 minutes. 2 μL of the DNAse Stop Solution (Sigma-Aldrich) was added. Tubes were sealed, mixed, and spun down before being placed in a Thermocycler (Bio-Rad, Mississauga, ON, Canada) and heated at 70 °C for 10 minutes with the lid set to 100 °C. Tubes were then removed and placed immediately on ice.

In the tubes with the DNAse-treated RNA, 1.0 μg (1 μL of a 1 μg/μL solution) of random primers (Roche; Mississauga, ON, Canada) was added. Tubes were sealed, mixed, and spun down before being heated in the Thermocycler at 70 °C for 5 minutes (lid at 100 °C). Samples were then immediately chilled on ice while the reverse transcriptase mastermix was prepared with a composition of 12.5 μL of DEPC water, 10 μL of 5x Reaction Buffer for Mu-MLV RT (Promega, Madison, WI, USA), 2.5 μL of dNTP mix (10 mM per each base; Froggabio; North York, ON, Canada) , and 2 μL of Mu-MLV RT (Promega) at 200 U/μL per experiment sample. This mastermix was then added to each sample, thoroughly mixed, and spun down before being incubated for 60 minutes at 37 °C in the Thermocycler. This freshly prepared cDNA with a concentration of 40 ng/μL was then stored at -20 °C until required.

2.5 Quantitative PCR

cDNA samples were diluted to a working concentration of 1.2 ng/μL using cDNA template and DEPC-water. Each well of the 96-well qPCR plate contained 6 ng of the cDNA template in a 5 μL volume. A mastermix was prepared for each primer used with 0.7 μL of DEPC-water, 0.9 μL of the 10 μM stocks of the forward and reverse primers (600 nM final concentration; Sigma-Aldrich) and 7.5 μL of 2X SYBR Green MasterMix (Thermo-Fisher Scientific) added per reaction. 10 μL of this mastermix was added to each well. The plate was then carefully sealed using an adhesive seal, mixed, and centrifuged at 500 x g for 5 minutes at room temperature.

The plate was then placed in the QuantStudio 5 Real Time PCR machine (Thermo-Fisher Scientific) and run with mixed cycling parameters for 40-45 cycles. The target genes for this study and their corresponding information can be found in Tables 1-4. Target genes for Aim 1 included Clock, Bmal1, Npas2, Per1, Per2, Per3, Cry1 and Cry2 (Table 1). All other target genes were utilized for Aim 2 of this study. All primers were designed using the primer-BLAST tool on NCBI to ensure specificity of amplification of target genes. Ct values obtained from experiment runs were normalized to housekeeping genes GAPDH, CycA and Ywhaz for the brain areas and GAPDH and Rpl32 for the livers.

Table 1. Primer sequences used for reverse transcription quantitative PCR (RT-qPCR) with amplicon sizes and annealing temperatures (Circadian Rhythm Gene Panel and Housekeeping Genes)

Gene Name and NCBI Accession Number	Forward Primer Sequence (5'-3')	Reverse Primer Sequence (5'-3')	Amplicon Size (bp)	Annealing Temperature (°C)
Clock NM_021856.2	AAGATGACACAGCGGAGGTC	ACTGTGACATGCCTTGTGGG	127	60
Bmal1 NM_024362.2	TGCCACTGACTACCAAGAAAGT	ATTTTGTCCCGACGCCTCTT	138	60
Per1 NM_001034125.1	CTCTCCGCAACCAGGATACC	GCTAGGAGCTCTGAGAAGCG	139	60
Per2 NM_031678.1	AAGTGACGGGTCGAGCAAAG	CATGTCGGGCTCTGGAATGA	71	60
Per3 NM_023978.2	CCACCCTCTCCAGGTCATGT	CGCCACTGAAACCAAAACCAA	125	60
Cry1 NM_198750.2	CCCACTAAAGCAAGGAAGAAGC	CCCGCATGCTTTCGTATCAGTT	134	60
Cry2 NM_133405.2	GGACTACATCCGGCGATACC	GCCAATGATGCACTTAGCGG	112	60
Npas2 NM_001108214.2	TCTTCTGAGAGGCAGCTTGAA	CAGGAGGGGCTAGGCACATT	85	60
Rev-ErbA NM_001113422.1	ATCTCGGTTGCCTCAGCATC	CTAGGCACCGAGCAGTAAGG	78	60
Mettl3 NM_001024794.1	ATGTGCAGCCCAACTGGATT	CTGTGCTTAAACCGGGCAAC	88	60
CSNK1D NM_139060.3	CACCTCACAGATTCCCGGTC	AAGGAGAGTTCTCATCGGTGC	72	60
CSNK1E NM_031617.1	CTCTGCAAAGGCTACCCCTC	CTCTGCAAAGGCTACCCCTC	125	60
FBXL3 NM_001100568.1	AGAGAAAGGAAGCTTTCCGCCC	TTCTCAGCAGTGCCTTCCTCA	102	60

GAPDH NM_017008.4	GTCATCCCAGAGCTGAACGG	ATACTTGGCAGGTTTCTCCAGG	108	60
Rpl32 NM_013226.2	GGTGGCTGCCATCTGTTTTG	GTTTCCGCCAGTTTCGCTTAAT	139	60
Ywhaz NM_013011.3	GGCAGAGCGATACGATGACA	AAGATGACCTACGGGCTCCT	131	60
CycA NM_017101.1	CAGACGCCGCTGTCTCTTTTC	CGTGATGTCGAAGAACACGGT	70	60
PPARA NM_013196.1	GTCCTCTGGTTGTCCCCTTG	TCAGTCTTGGCTCGCCTCTA	143	60
YTHDF2 NM_001047099.1	CAGGCAAGGCCGAATAATGC	TCTCCGTTGCTCAGTTGTCC	167	60

Table 2. Primer sequences used for reverse transcription quantitative PCR (RT-qPCR) with amplicon sizes and annealing temperatures (Glycerophospholipid and General Lipid Metabolism Gene Panel)

Gene Name and NCBI Accession Number	Forward Primer Sequence (5'-3')	Reverse Primer Sequence (5'-3')	Amplicon Size (bp)	Annealing Temperature (°C)
ACSL1 NM_012820.1	TGTGGGGTGGAAATCATCGG	TTGGGGTTGCCTGTAGTTCC	131	60
CRAT NM_001004085.2	CTGCCAGAACCGTGGTGAAA	GGTGGGCCTTAAATCGACCA	81	60
CPT1A NM_031559.2	GTGCAGAGCAATAGGTCCCC	AGGCAGATCTGTTTGAGGGC	125	60
CPT2 NM_012930.1	CTACATCTCAGGCCCCTGGT	GCCCTGGTAAGCTGGTCATT	126	60
ACADL NM_012819.1	TCCGCTTCCATGGCGAAATA	GCATCCACGTAGGCTTTTGC	125	60

ACADM NM_016986.2	GGCATATGGGTGTACAGGGG	ACGCAGTAGGCACACATCAT	144	60
ECH1 NM_022594.1	GATGCAGCAGCTGAGAGGTA	CTTCTCCGGCCGGTTTAGTT	184	60
HADH NM_057186.2	TCGTGAACCGTCTCTTGGTG	TCCTTAGATGCATCGCCTCG	73	60
ACAT1 NM_017075.2	AGTAACAGCTGCTAACGCCA	AGCAAATGCTGCGATTCGTG	118	60
PCCA NM_019330.1	TTGGCAGCAGAAGATGTCACT	CACAGGGTAGCCAATTTCCCT	183	60
PCCB NM_017030.2	TCACCAGGAAGGCCTATGGA	AAGATGATCTCCACGGCACC	130	60
MCEE NM_001106341.1	CCTGCCCACTCTCCTAGTTG	GAGAAAAGCCCTGTAGCGCC	117	58
MMUT XM_003754495.4	CAGCACAGCACATGCCAAAA	CGCGATGGTATAGGCCAGTT	101	60
ECI1 NM_017306.4	GGTTCACCATTCCGGACCAT	TCGCTGCTTGATCAGGTTGT	83	60
DECR1 NM_057197.2	GTGTGATCGCGAGCAGGAAT	AGGATGCCCTGCAACTTTGA	158	60
PLA1A NM_138882.1	ATCGCCCATCAAAACCCACA	CAGACCGTCTTCTTGCTGTCA	149	60
PLA2G2A NM_031598.3	GCCATACCACCATCCCATCC	GACCTGAATTGAGCCAAAGGC	92	56
PLCG1 NM_013187.1	CAGCAATCCTAGAGCCGGAG	TCAGGACGAATGGCGATCTG	109	60
PLD1 NM_030992.1	TGTAGGATAGCCAATTTCCCCC	GTAAAAACAGAGGGGCTGGG	131	60
GDE1 NM_032615.2	CCTGACGAAAGGATCCCCAC	AGAGCAGCAGAAGCCATATCT	110	60
PEMT NM_013003.1	CCCGCTGAGTTCATCACCAG	GAAGAGATCGGCCAGAACCA	87	60

Table 3. Primer sequences used for reverse transcription quantitative PCR (RT-qPCR) with amplicon sizes and annealing temperatures (Purine Metabolism Gene Panel)

Gene Name and NCBI Accession Number	Forward Primer Sequence (5'-3')	Reverse Primer Sequence (5'-3')	Amplicon Size (bp)	Annealing Temperature (°C)
NT5C2 XM_006223765.3	CCTGGAGTGACCGCTTACAG	CAAACACCCGGTGATAGGCT	99	60
ADA NM_130399.2	GCGAGAGGCTGTGGACATAC	GCATGCGTCGTTTTGGGATT	165	60
PNP NM_001106031.1	TGACCGGGATATGAGGCAGA	AAGTAGACAGAGCTCTCCGC	132	60
XDH NM_017154.1	AGCTTTTCCAAGAGGTGCCA	ACGTGATTTTAGCATGCGCC	183	60
UOX NM_053768.2	CGACTATGGAAAGAATGATGAAGTG	CTCAGAGTCAACTGCACCGA	138	60

Table 4. Primer sequences used for reverse transcription quantitative PCR (RT-qPCR) with amplicon sizes and annealing temperatures (Glutathione Metabolism Gene Panel)

Gene Name and NCBI Accession Number	Forward Primer Sequence (5'-3')	Reverse Primer Sequence (5'-3')	Amplicon Size (bp)	Annealing Temperature (°C)
GSR NM_053906.2	TCCAGATGTCGATTGCCTGC	GATCGCAACTGGGGTGAGAA	193	60
GPX1 NM_030826.4	GGACATCAGGAGAATGGCAAGA	GGCATTCCGCAGGAAGGTAA	153	60
GGT1 NM_053840.2	TACAGAGGTCACACCCGACT	TCCCCGCCTTTTCTGGAATC	96	64
SMS NM_001033899.1	CATCTTTCAGGAGCAGGGGAT	GGCAAAGCTGCCATTCTTGTTC	94	60
CAT NM_012520.2	GTGCATGCATGACAACCAGG	GAATGTCCGCACCTGAGTGA	163	60
SOD1 NM_017050.1	AAGAGAGGCATGTTGGAGACC	CGGCCAATGATGGAATGCTC	115	60
SOD2 NM_017051.2	ACGCGACCTACGTGAACAAT	TAACATCTCCCTTGGCCAGC	72	60

2.6 Metabolite Extraction

50 mg of liver tissue was harvested, placed in a 2 mL round bottom tube, and 1 mL of -20°C metabolite extraction buffer (0.1 M formic acid (Fisher) in methanol (Fisher): acetonitrile (Fisher): water [40:40:20]) was added, along with a stainless steel bead. The samples were placed in the TissueLyser (QIAGEN) for 2-3 cycles of 1 minute at 30 Hz with time taken in between cycles to cool the samples and ensure heating did not occur. Once the tissue was homogenized in the metabolite extraction buffer, the samples were placed at -20°C for 1 hour. Then, the samples were placed in the microcentrifuge at 4°C for 5 minutes at 16, 100 x g. The supernatant was transferred to a new 2 mL tube and stored at -20°C, while the pellet was resuspended in 300 μL of fresh -20°C extraction buffer. The resuspended pellet was placed at -20°C for another hour and the centrifugation, supernatant transfer and pellet resuspension steps were repeated once more, except this time the pellet was resuspended in 200 μL of fresh -20°C extraction buffer. After a third extraction step for 1 hour at -20°C, the supernatant was again transferred to the 2 mL tube stored at -20°C. The final 2 mL tube, therefore contained the supernatant from the three extractions. A total of 17 μL of concentrated ammonium hydroxide was added to each tube and mixed thoroughly to neutralize the supernatant. The samples were concentrated under a vacuum, while ensuring no heat was applied. The dried pellets were then stored at -80°C.

2.7 Untargeted Metabolomics

Ultra-high performance liquid chromatography (UHPLC) was performed on an UltiMate 3000 UHPLC system (ThermoFisher Scientific) and coupled to a Q Exactive Hybrid Quadrupole-Orbitrap Mass Spectrometer (ThermoFisher Scientific) at BioZone Mass Spectrometry facility (University of Toronto, Toronto, Ontario). Chromatographic separation was achieved using a

Hypersil Gold C_{18} column (50 mm x 2.1 mm x 1.9 μm) maintained at a temperature of 40°C. Chromatographic separation was prepared using a gradient method with a flow rate of 300 μL/min consisting of an aqueous solvent A that was 5 mM ammonium acetate, pH 6.0 in ddH_2O, and an organic solvent B that was 5 mM ammonium acetate, pH 6.0 in methanol. The injection volume for each sample was set to 10 μL. Prior to injection the samples were resuspended in water, vortexed to mix and spun at maximum speed in a microcentrifuge. The supernatants were collected and used for analysis. The gradient used for each UHPLC run were 0-1 min, 5% B; 1-7 min, linear gradient to 100% B; 7-10 min, 100% B, 10-11 min, linear gradient to 5% B; 11-15 min, 5% B.

The Q Exactive Mass Spectrometer was operated in the heated-electrospray mode using the heated-electrospray ionization probe (HESI-II; ThermoFisher Scientific) with the following parameters: sheath gas flow rate, 15; auxiliary gas, 5; spare gas, 2; electrospray voltage, 3.5 kV; capillary temperature, 320°C; S-Lens RF Level, 50. In full scan MS mode the spectra collected were scanned over a mass/charge (m/z) range of 100-1200 atomic mass units at a resolution of 70,000. The AGC target (the predefined value for the accumulation of ions) was set to $3e^6$, the maximum ion injection time (IT) was set to 100 ms. The full MS scan was run on both positive and negative ion modes. After the full scan was completed the setting was switched to data-dependent-MS2 where the top 5 most intense ions from the full MS scan were selected for further fragmentation. The parameters used for the data dependent-MS2 scan were as follows: a resolution of 17, 500; an AGC value of $1e^5$; a maximum IT of 50 ms; an isolation window of 1.0 m/z; and normalized collision energy (NCE) set to 30 eV.

2.7.1 Metabolite identification and pathway analysis

Metabolite identification was performed using the Chemspider database using the molecular weight and retention time from the mass spectrometry runs. Metabolic pathway analysis was performed using the Pathway Analysis feature on MetaboAnalyst 4.0 (Xia Lab, McGill University). Then, highlighted pathways were further investigated on the Kyoto Encyclopedia of Genes and Genomes (KEGG) database (Release 92.0) to identify target genes for further investigation.

2.8 Western Blotting

2.8.1 Protein Extraction

50 mg of liver tissue was harvested, placed in a 2 mL round bottom tube, and 1 mL of radioimmunoprecipitation assay (RIPA) lysis buffer was added to each tissue sample, along with a stainless steel bead. RIPA lysis buffer was prepared as follows: 25 mM Tris-HCl, pH 7.6, 150 mM NaCl (Fisher), 2 mM EDTA, 0.1% sodium dodecyl sulfate (SDS; Fisher), 1% sodium deoxycholate (Sigma-Aldrich), 1% NP-40 (Sigma-Aldrich), 0.5 mM phenylmethylsulphonyl fluoride (PMSF; Sigma-Aldrich) and 1 tablet of Complete Mini protease inhibitor cocktail tablet (per 10 mL; Roche). Samples were then placed in the TissueLyser (QIAGEN) for 2 cycles of 2 minutes at 30 Hz. The lysates were left on ice for 10 minutes and then centrifuged at 4°C for 20 minutes at 12, 000 x g. After centrifugation, the supernatant was transferred into a fresh Eppendorf tube and stored at -20°C.

2.8.2 Protein Quantification

Protein concentrations for whole protein extracts were determined using the Bradford assay procedure. Bradford assay standards were prepared with Immunoglobulin G (IgG; Sigma-Aldrich) and MilliQ water to prepare a standard curve ranging from 0-20 μg protein. Protein samples were added to a clear 96-well assay plate at a total volume of 20 μL and incubated for 5 minutes at room temperature with 250 μL of 1X Bradford reagent (BioRad). The samples and standards were then read at 595 nm using the PowerWave XS plate reader and Gen5 software (Biotek). Samples were stored at -20°C until the blotting procedure.

2.8.3 Sample Preparation

Whole protein samples were prepared by adding 25 μg of protein to a mixture of 2X loading dye (0.5 M Tris-HCl, pH 6.8, glycerol, 10% SDS, 0.5% Bromophenol Blue, β-mercaptoethanol (Sigma-Aldrich), and RIPA lysis buffer to a volume of 40 μL. Samples were mixed and placed on a block heater (VWR) at 95°C for 5 minutes to ensure denaturation.

2.8.4 Gel Casting

SDS-polyacrylamide gel electrophoresis (PAGE) was performed using the Mini-PROTEAN Tetra cell kit and manual from BioRad. All gels were made with 1.5 mm thick spacer plates. 10% resolving gels (4.9 mL H_2O, 2.5 mL 40% acrylamide/bis-acrylamide [19:1] solution (Fisher), 2.5 mL resolving buffer [1.5M Tris-HCl, pH 8.8], 100 μL 10% SDS, 50 μL 10% ammonium persulfate (APS, Fisher) and 5 μL tetramethylethylenediamine (TEMED, Fisher)) were overlaid with 1 mL of water saturated butanol and allowed to polymerize for at least 30 minutes. After polymerization, gels were thoroughly washed with distilled water to remove any

remaining butanol and 4% stacking gels (3.2 mL H_2O, 0.5 mL 40% acrylamide/bis-acrylamide [19:1] solution, 1.25 mL stacking buffer [0.5M Tris-HCl, pH 6.8], 100 μL 10% SDS, 25 μL 10% APS and 10 μL TEMED) were poured. 15-well combs were placed in the stacking gel and polymerization occurred for at least 15 minutes. After assembly of the gel apparatus, 1X running buffer (25 mM Tris, 192 mM glycine, 0.1% SDS) was added to the unit and samples were loaded into appropriate wells. 10 μL of the BLUeye Prestained Protein Ladder (GeneDirex, Inc.) was also loaded as a molecular weight reference. Using a BioRad PowerPac, electrophoresis through the stacking gel was completed at 75V. Due to a large molecular weight target protein, electrophoresis continued at 75V into the resolving gel for approximately 3 hours.

2.8.5 Protein Transfer

Proteins were transferred from the PAGE gel to polyvinylidene difluoride (PVDF) membrane using BioRad's Mini Trans-Blot Cell System. Transfer cassettes were immersed in a tank containing chilled 1X Transfer Buffer (48 mM Tris, 192 mM glycine, 20% methanol) and an ice pack. Polyacrylamide gels were equilibrated in cold transfer buffer for 10 minutes before transfer. A stir bar was added to the unit to even temperature and ion distribution during the transfer. The apparatus was surrounded with ice, placed on a magnetic stir plate (VWR) and transferred for 1 hour at 100V.

2.8.6 Blocking and Antibody Incubation

Post transfer, membranes were blocked with 5% milk in tris buffered saline with Tween-20 (TBS-T, 2% 1M Tris-HCl, pH 7.4, 0.5 mM NaCl, 0.1% Tween-20) for at least 30 minutes at room temperature on a Belly Dancer at medium speed. Prior to primary incubation, membranes

were washed four times for 5 minutes each with TBS-T on the Belly Dancer at high speed. Primary antibodies were diluted in blocking buffer using the conditions provided in Table 5. Membranes were placed in 2 mL of primary antibody mixture and left on a rocker at 4°C overnight on a gentle speed. Following the overnight incubation, the membranes were washed four times for 10 minutes each with TBS-T and then incubated with 2mL of the appropriate horseradish peroxidase (HRP) conjugated secondary antibody diluted in blocking buffer (Table 5) for 1 hour at room temperature on a rocker. After the secondary antibody incubation, membranes were again washed four times for 10 minutes on a Belly Dancer with TBS-T.

2.8.7 Enhanced Chemiluminescence and Imaging

Following the final washing procedure with TBS-T, the protein of interest was detected by enhanced chemiluminescence (ECL) using Clarity or Clarity Max ECL Western Blotting Substrates (BioRad) in a 1:1 ratio. The ECL mixture was applied to each blot for 2 minutes and then blotted to remove excess. The membranes were placed in intensifying screens before being imaged on the ChemiDoc (BioRad) using the auto optimal or auto rapid exposure settings. Densitometry of bands were quantified using ImageJ software and protein bands were normalized to glyceraldehyde 3-phosphate dehydrogenase (GAPDH).

Table 5. Antibody specifications and appropriate conditions used for western blotting

Antibody Specificity	Antibody Type	Host Animal	Dilution	Vendor and Catalogue Number	Molecular Weight
CPT1A	Primary	Mouse	1:1000	Abcam; ab128568 Lot # GR3293083-10	89 kDa
GAPDH	Primary	Mouse	1:10 000	Abcam; ab8245 Lot # GR232949-3	40 kDa
Anti-Mouse	Secondary HRP-conjugated	Goat	1:2000	Pierce; 1858413 Lot # IA110692	N/A

2.9 Triglyceride Extraction

Approximately 100 mg of tissue was harvested from the livers of eight male and female animals in the Saline and Dex treatment conditions. The tissue was washed with cold PBS before resuspending in 1 mL of 5% NP-40 in ddH_2O (Sigma Aldrich) in a 2 mL round bottom tube. An autoclaved stainless steel bead was added to each tube and homogenized using the TissueLyser (QIAGEN) for 2 cycles of 1 minute at 20 Hz. After homogenization had been completed samples were slowly heated to 90°C in a water bath for 5 minutes (when the NP-40 solution became cloudy). The samples were removed from the water bath and allowed to cool to room temperature. This heating and cooling step was repeated once more to solubilize all triglycerides and then the lysates were centrifuged for 2 minutes at 16,100 x g. The supernatant was transferred into a fresh tube and the samples were diluted 10-fold with ddH_2O.

2.10 Triglyceride (TG) Assay

Triglyceride concentrations were determined using the Triglyceride Quantification Assay Kit from Abcam (ab65336; Lot: GR3347939-1). TG standards were prepared from a 1mM standard included in the kit. Using an intermediate standard of 0.2 mM TG diluted in the Assay

Buffer, 6 standards were prepared to create a standard curve ranging from 0-10 nmol. Plasma and liver samples were assayed prior to sample runs to ensure readings would be in range of the standard curve. Samples and standards were added to a clear 96-well assay plate at a total volume of 50 μL adjusted with Triglyceride Assay Buffer. Then, 2 μL of Lipase was added to each well, the plate was gently agitated to mix and incubated for 20 minutes at room temperature to convert triglycerides to glycerol and fatty acids. A reaction mix of assay buffer, probe and enzyme mix was prepared as per the manufacturer's instructions and 50 μL of this mix was added to each well. The plate was gently agitated to mix and incubated at room temperature for 60 minutes in the dark before being measured using the PowerWave XS spectrophotometer and Gen5 software from Biotek at 570 nm.

2.11 Statistical Analysis

All statistical analyses were performed using GraphPad Prism software (La Jolla, CA, USA). All data are presented as the mean ± SEM. Interquartile range (IQR) was calculated for all treatment groups and outliers were determined when measurements were lower than the first quartile or higher than the third quartile by magnitudes greater than 1.5 x IQR. Statistical significance between two groups (i.e saline and Dex animals as well as between WKY and SHR animals) was determined by an unpaired t-test. Statistical significance between greater than two treatment groups was determined by one-way analysis of variance (ANOVA), followed by post-hoc Tukey's multiple comparison test. Values of $p \leq 0.05$ (confidence interval 95%) were considered statistically significant.

3. Results

3.1 Mechanism of circadian rhythm dysregulation in glucocorticoid exposed offspring

In order to determine circadian rhythm gene expression in brain regions implicated in the circadian clocks and the HPA axis, the brains of fetal-programmed WKY rat offspring were dissected using a micro-punch technique and mRNA expression levels of the circadian genes of interest were detected using RT-qPCR.

3.1.1 Circadian Rhythms in the SCN

Results from the RT-qPCR analysis of circadian rhythm genes found in the SCN of male and female GC exposed offspring show a dysregulated pattern when compared to their saline controls. In the female offspring the Clock gene was found to be downregulated by 3.5-fold ($p < 0.05$) (Figure 5A), while the other selected circadian genes analyzed showed no statistically significant changes. Male offspring, however, showed statistically significant differences in five of the eight selected circadian rhythm genes, displaying a much greater dysregulation than the females. Per1 and Cry2 were significantly upregulated with Per1 displaying a 3.5-fold increase ($p < 0.05$) and Cry2 a 5-fold increase ($p < 0.01$) (Figure 5B). The mRNA levels of Per2, Per3 and Cry1 were found to be significantly downregulated in the SCN of GC exposed male offspring with 2-fold ($p < 0.05$), 4-fold ($p < 0.05$) and 3.5-fold ($p < 0.01$) decreases respectively (Figure 5B). It should also be noted that the males tended to display mostly downregulation of these circadian genes.

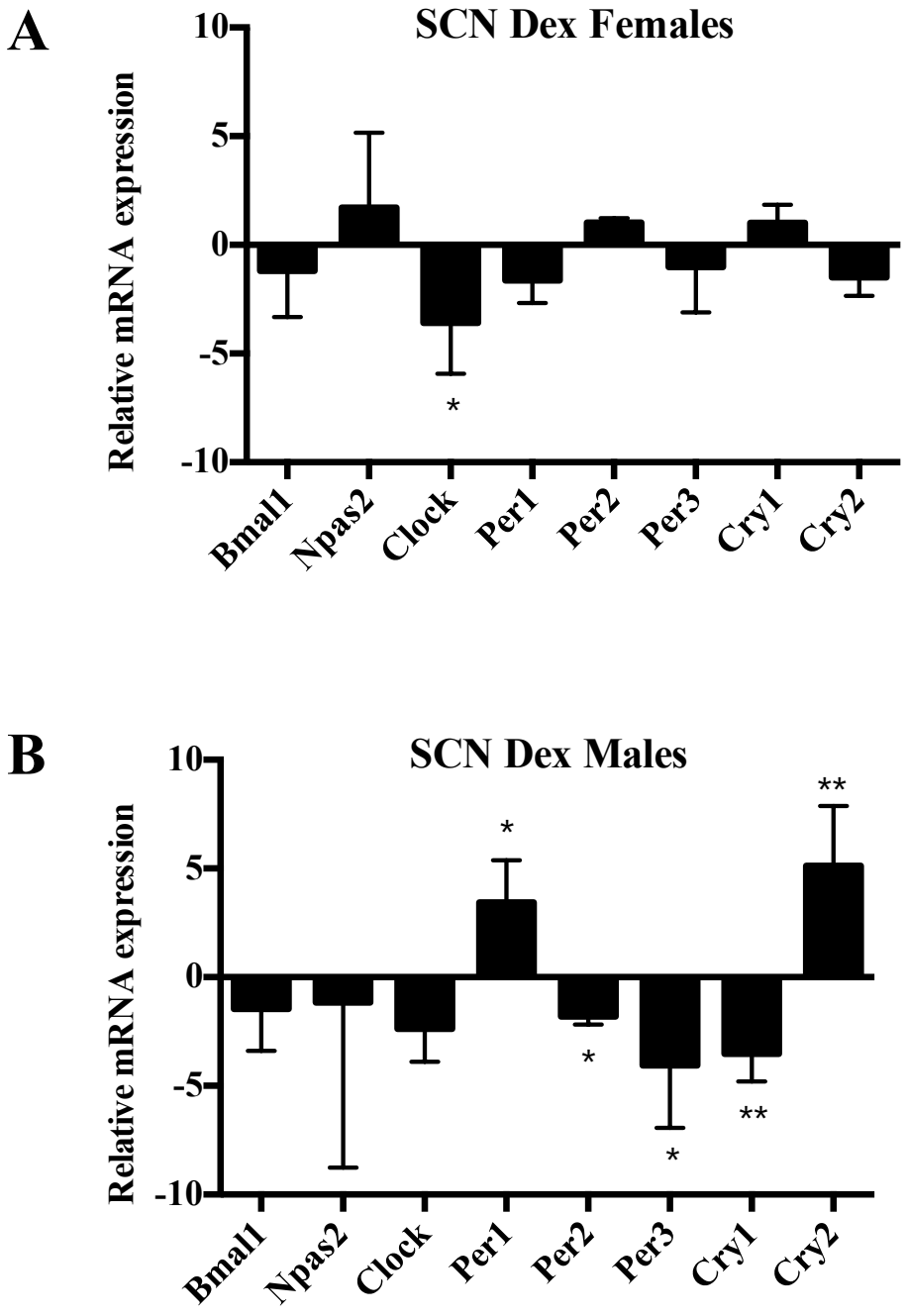

Figure 5. mRNA levels of circadian rhythm genes in suprachiasmatic nucleus of 19 week old prenatally DEX-exposed offspring relative to saline control. Fold changes in mRNA levels of Bmal1, Npas2, Clock, Per1, Per2, Per3, Cry1 and Cry2 in female (A) and male (B) offspring. Fold changes in gene expression were calculated by relative quantification (ΔΔCt) of RT-qPCR threshold cycles (Ct) as per Livak and Schmittgen[87] using mean Ct values of housekeeping genes GAPDH, Ywhaz and CycA. Data is expressed as mean fold change of Dex relative to the saline group ± SEM (n = 8). Statistical significance between saline and DEX-treated groups is shown by: * $p < 0.05$, ** $p < 0.01$.

3.1.2 Circadian Rhythms in the Hippocampus

The RT-qPCR analysis of the circadian gene panel in hippocampi of GC exposed offspring showed dysregulation when compared to the saline control, however, this pattern is unlike that seen in the SCN. Female offspring showed statistically significant changes across three circadian rhythm genes with Npas2 showing a downregulation of 4.5-fold ($p < 0.001$), Clock showing a 9-fold increase ($p < 0.01$), and Cry1 showing an upregulation of 3.5-fold ($p < 0.05$) (Figure 6A). Male offspring also showed statistically significant changes in three circadian genes, however, the dysregulated genes were all different from those in the females. The males showed significant downregulation of Per1 by 5.5-fold ($p < 0.01$), as well as a 2-fold increase in Per2 ($p < 0.05$) and a 9-fold increase in Cry2 ($p < 0.01$) (Figure 6B).

3.1.3 Circadian Rhythms in the Amygdala

Results from RT-qPCR analysis of the amygdala of GC exposed offspring show significant changes in selected circadian rhythm genes relative to their saline controls. Again, these changes are different from the dysregulation patterns seen in both the SCN and the hippocampus. Female offspring showed statistically significant changes in two of the eight circadian genes measured, with Clock and Per1 both shown to be upregulated by 5.5-fold ($p < 0.05$ and $p < 0.01$ respectively) (Figure 7A). Male offspring also showed statistically significant changes in two circadian genes, however, the dysregulated genes were different from those in the females. Males showed significant downregulation of Per2 by 8.5-fold ($p < 0.05$), as well as a 5.5-fold decrease ($p < 0.05$) in Cry2 (Figure 7B). It should also be noted that females have the majority of the selected genes showing an upregulation, while the males showed a downregulation in all circadian genes tested.

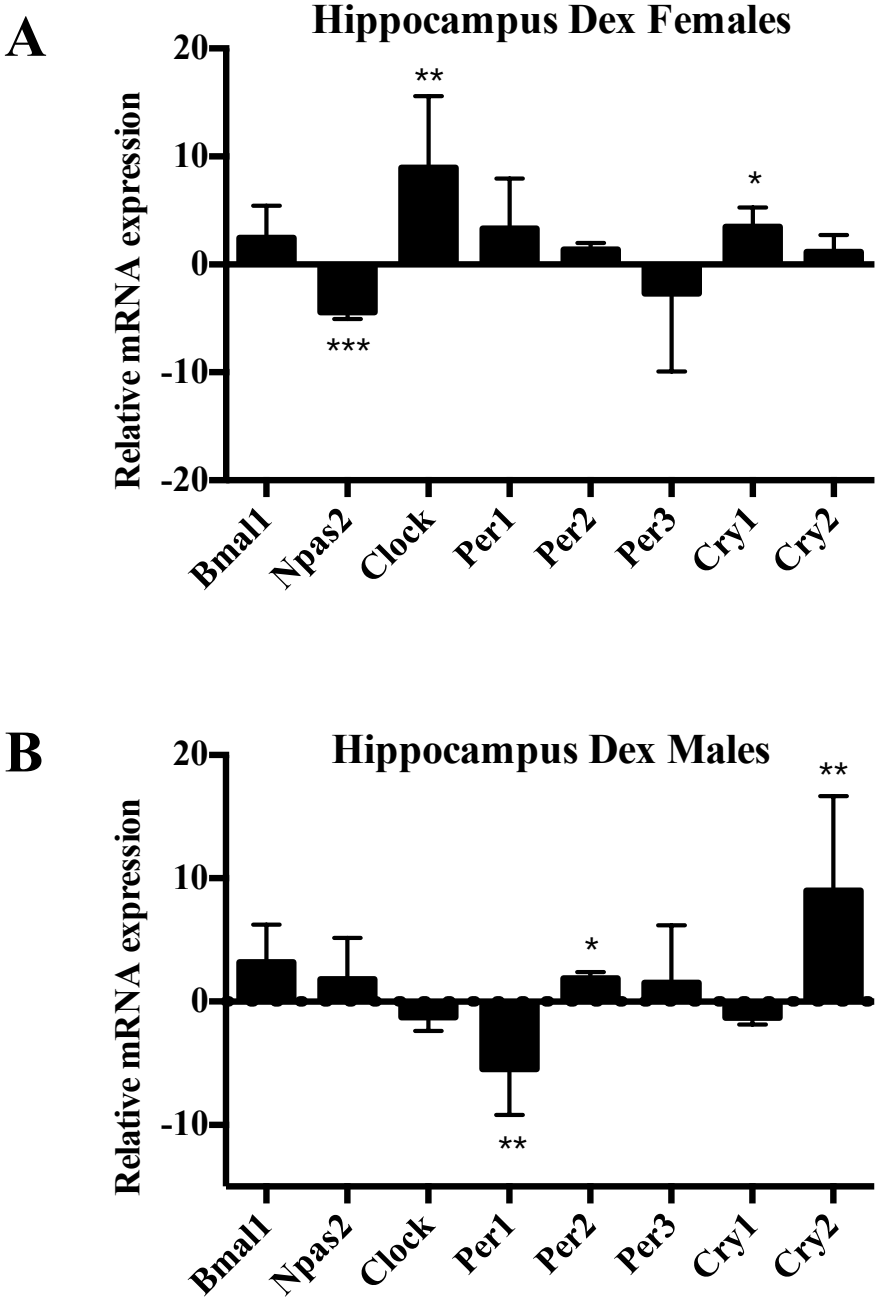

Figure 6. mRNA levels of circadian rhythm genes in hippocampus of 19 week old prenatally DEX-exposed offspring relative to saline control. Fold changes in mRNA levels of Bmal1, Npas2, Clock, Per1, Per2, Per3, Cry1 and Cry2 in female (A) and male (B) offspring. Fold changes in gene expression were calculated by relative quantification (ΔΔCt) of RT-qPCR threshold cycles (Ct) as per Livak and Schmittgen[87] using mean Ct values of housekeeping genes GAPDH, Ywhaz and CycA. Data is expressed as mean fold change of Dex relative to the saline group ± SEM (n = 8). Statistical significance between saline and DEX-treated groups is shown by: * $p < 0.05$, ** $p < 0.01$, *** $p < 0.001$

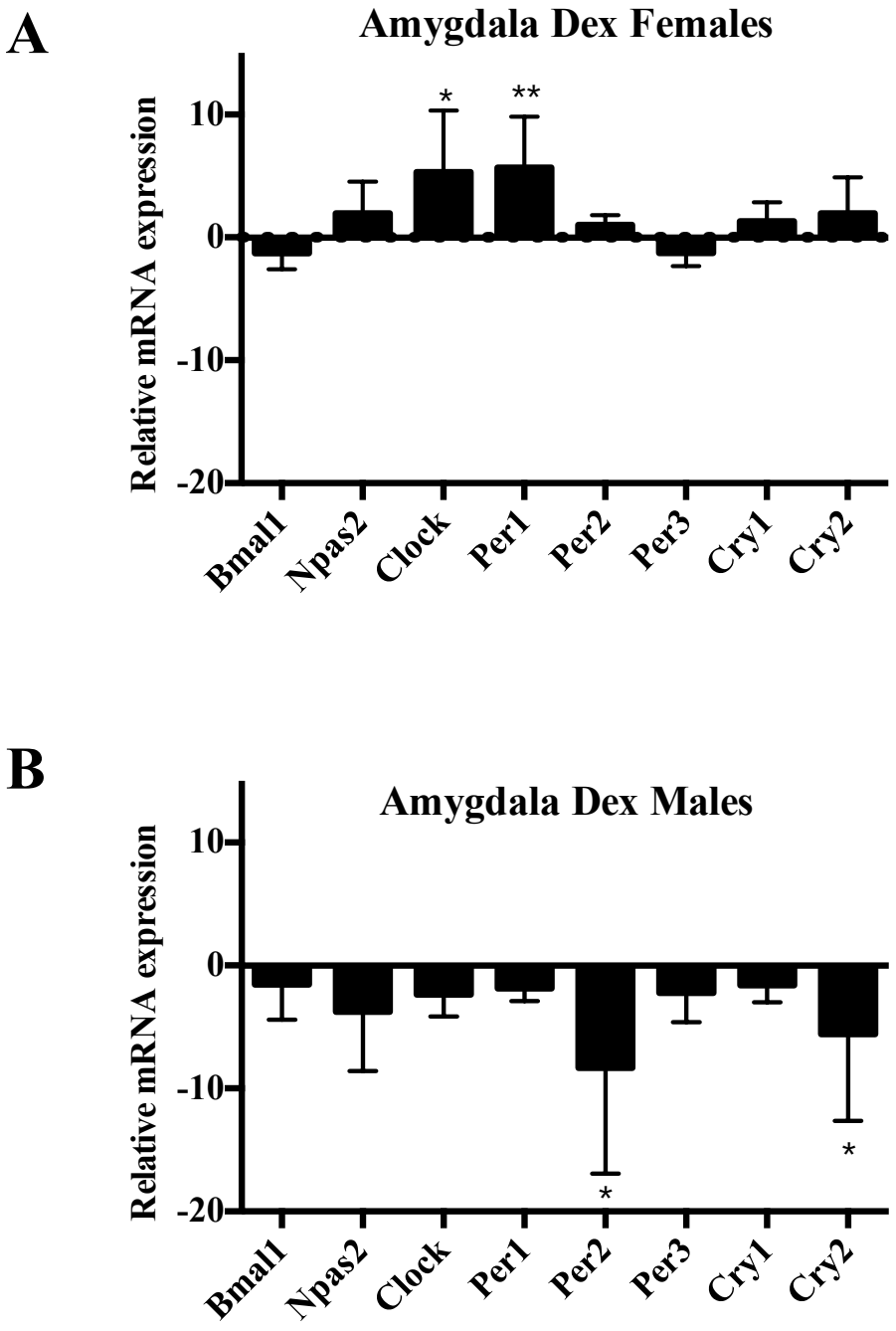

Figure 7. mRNA levels of circadian rhythm genes in amygdala of 19 week old prenatally DEX-exposed offspring relative to saline control. Fold changes in mRNA levels of Bmal1, Npas2, Clock, Per1, Per2, Per3, Cry1 and Cry2 in female (A) and male (B) offspring. Fold changes in gene expression were calculated by relative quantification (ΔΔCt) of RT-qPCR threshold cycles (Ct) as per Livak and Schmittgen[87] using mean Ct values of housekeeping genes GAPDH, Ywhaz and CycA. Data is expressed as mean fold change of Dex relative to the saline group ± SEM (n = 8). Statistical significance between saline and DEX-treated groups is shown by: * $p < 0.05$, ** $p < 0.01$.

3.1.4 Circadian Rhythms in the PVN

Results from RT-qPCR analysis of the paraventricular nucleus of GC exposed offspring show significant changes in the circadian rhythm gene panel relative to their saline controls. These changes are different from the dysregulation patterns seen in the three other brain areas above, however, the pattern in the female PVN is similar to the pattern seen in the female hippocampus. Female offspring showed no statistically significant changes in the circadian genes measured (Figure 8A). Male offspring, however, showed statistically significant changes in two circadian genes with significant upregulations of Bmal1 (9-fold; $p < 0.05$) and Per2 (6-fold; $p < 0.05$).

3.1.5 Circadian Rhythms in the PFC

The results from the RT-qPCR analysis of circadian rhythm genes found in the prefrontal cortex of male and female GC exposed offspring show a dysregulated pattern when compared to their saline controls. Expression levels in the PFC in both males and females were much more similar to their saline controls than any other brain area tested. Female offspring showed no statistically significant changes across the selected circadian genes (Figure 9A). Male offspring, however, showed statistically significant differences in one of the eight selected circadian rhythm genes with Per2 being significantly upregulated 1.3-fold ($p < 0.05$) (Figure 9B).

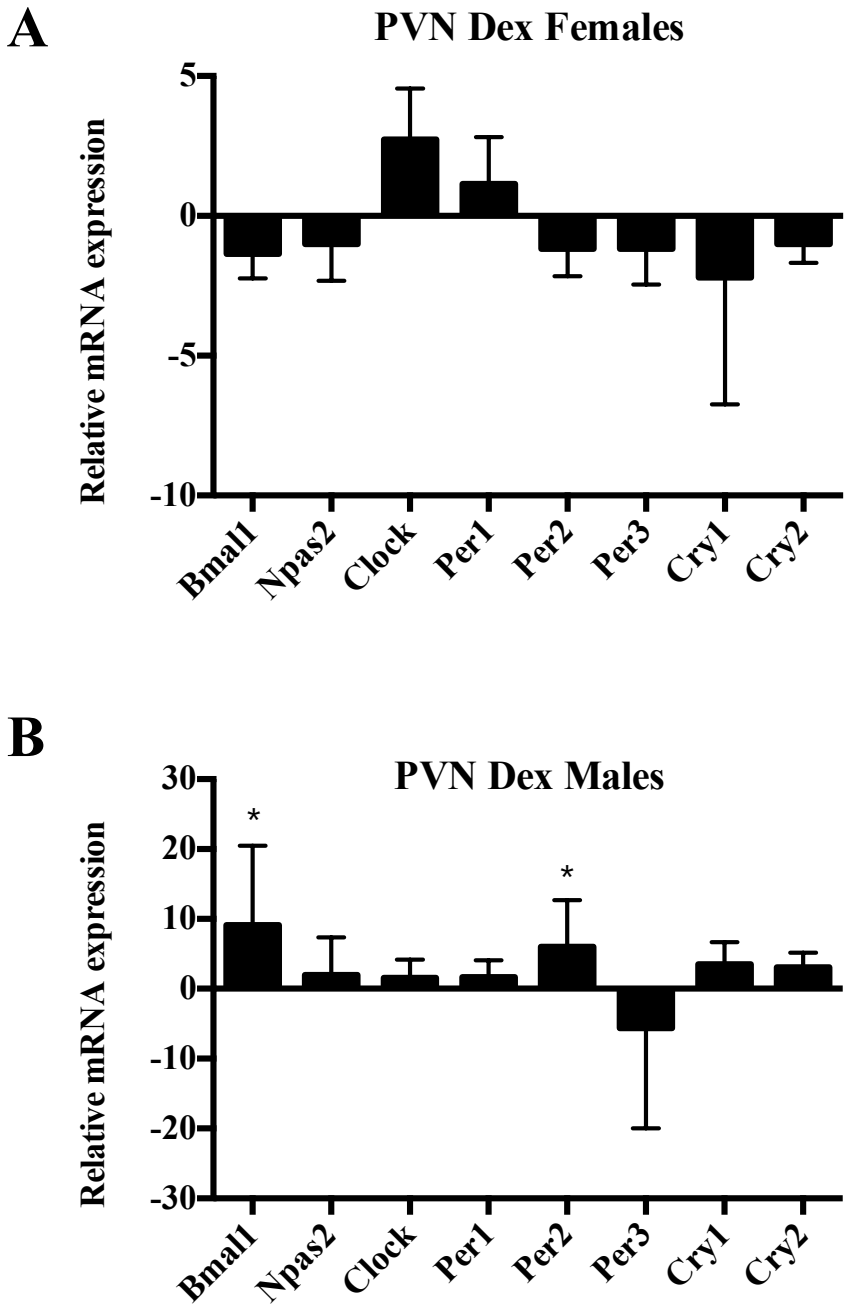

Figure 8. mRNA levels of circadian rhythm genes in the paraventricular nuclei of 19 week old prenatally DEX-exposed offspring relative to saline control. Fold changes in mRNA levels of Bmal1, Npas2, Clock, Per1, Per2, Per3, Cry1 and Cry2 in female (A) and male (B) offspring. Fold changes in gene expression were calculated by relative quantification ($\Delta\Delta$Ct) of RT-qPCR threshold cycles (Ct) as per Livak and Schmittgen[87] using mean Ct values of housekeeping genes GAPDH, Ywhaz and CycA. Data is expressed as mean fold change of Dex relative to the saline group ± SEM (n = 8). Statistical significance between saline and DEX-treated groups is shown by: * $p < 0.05$.

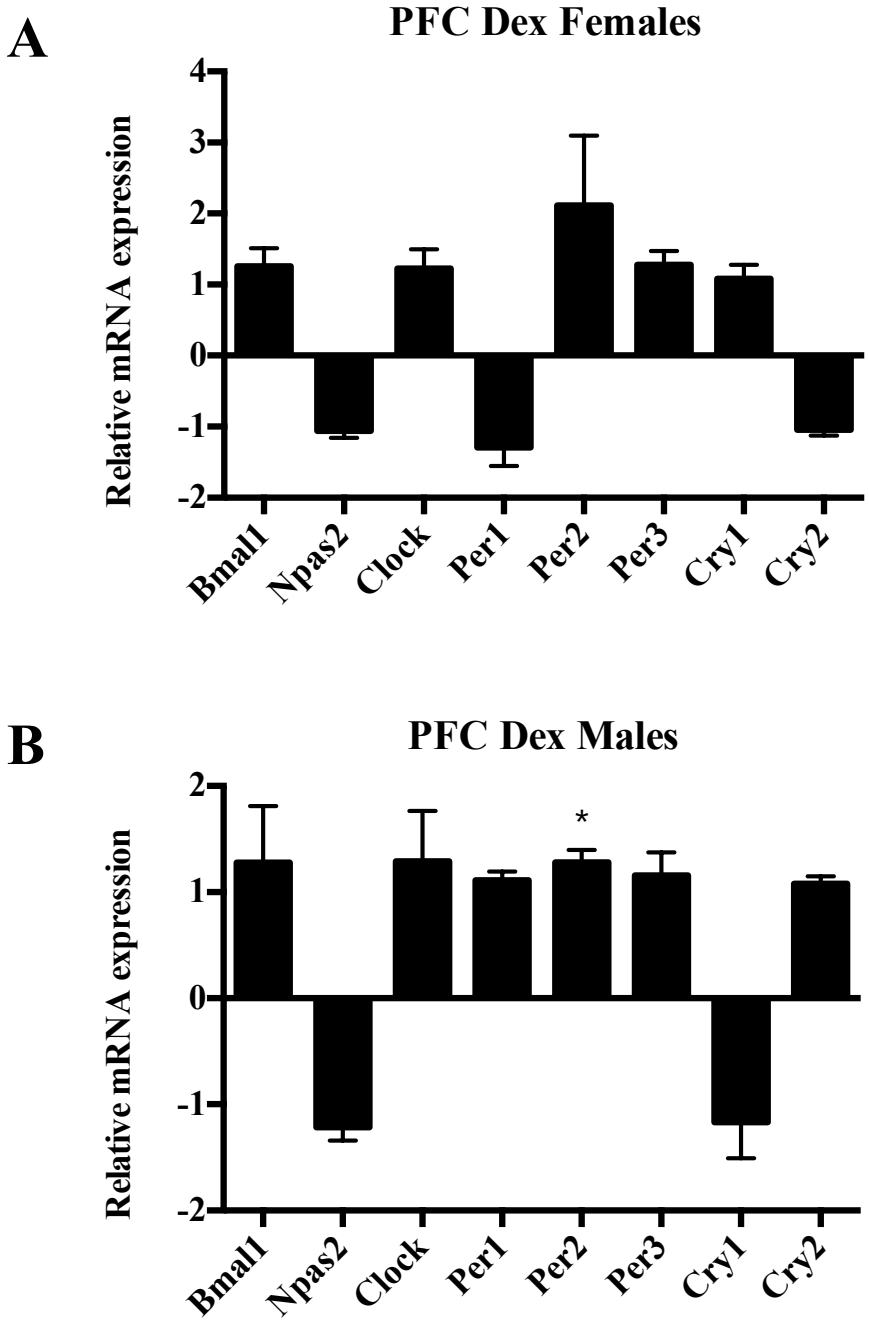

Figure 9. mRNA levels of circadian rhythm genes in the prefrontal cortex of 19 week old prenatally DEX-exposed offspring relative to saline control. Fold changes in mRNA levels of Bmal1, Npas2, Clock, Per1, Per2, Per3, Cry1 and Cry2 in female (A) and male (B) offspring. Fold changes in gene expression were calculated by relative quantification (ΔΔCt) of RT-qPCR threshold cycles (Ct) as per Livak and Schmittgen[87] using mean Ct values of housekeeping genes GAPDH, Ywhaz and CycA. Data is expressed as mean fold change of Dex relative to the saline group ± SEM (n = 8). Statistical significance between saline and DEX-treated groups is shown by: * $p < 0.05$.

3.2 Mechanism of circadian rhythm dysregulation in the spontaneously hypertensive rat

In order to determine circadian rhythm gene expression in brain regions implicated in circadian clocks and the HPA axis, the brains of SHR rats were dissected using a micro-punch technique and mRNA expression levels of the circadian genes of interest were detected using RT-qPCR.

3.2.1 Circadian Rhythms in the SCN

Results from the RT-qPCR analysis of circadian rhythm genes found in the SCN of male and female SHR rats showed a dysregulated pattern when compared to their WKY controls. This was especially relevant in the females where three of eight circadian genes examined were dysregulated. The female SHR rats showed downregulation in Bmal1 (7.5-fold; $p < 0.05$) and upregulations in both Npas2 (18-fold; $p < 0.05$) and Per2 (3-fold; $p < 0.05$) (Figure 10A). Male offspring, however, showed no statistically significant differences in the circadian rhythm gene panel, however, had a trending upregulation in Npas2 and a trending downregulation in Clock (Figure 10B). Expression levels of Per3 were extremely low, therefore its relative expression was unable to be detected in the SCN of the male SHR brains.

3.2.2 Circadian Rhythms in the Hippocampus

RT-qPCR analysis on the hippocampus of male and female SHR rats show dysregulated circadian rhythm genes compared to WKY controls. The pattern of dysregulation was much different to that seen in the SCN of these animals. The females showed statistically significant changes in two circadian genes with downregulations in both Per1 (13.5-fold; $p < 0.05$) and Cry2 (11-fold; $p < 0.05$) and trending downregulations in both Clock and Cry1 as well (Figure 11A). The males showed a much greater amount of

dysregulation than the females with five of eight genes being statistically downregulated. These downregulations occurred in Clock (26-fold; $p < 0.0001$), Per1 (126.5-fold; $p < 0.001$), Per2 (2.4-fold; $p < 0.05$), Cry1 (5.8-fold; $p < 0.05$) and Cry2 (7-fold; $p < 0.01$) (Figure 11B). In this brain area the male and female dysregulation patterns were quite similar with each gene showing a similar trend in fold change, however, the males had a much greater degree of expression level differences when compared to the females.

3.2.3 Circadian Rhythms in the Amygdala

Analysis of circadian rhythm genes in the amygdala of male and female SHR rats by RT-qPCR show a great deal of dysregulation when compared to their WKY controls. The pattern of dysregulation was markedly different than those seen in the SCN and hippocampus. Females especially showed a large amount of dysregulation with five of eight circadian genes analyzed showing differences. Female SHR rats showed an upregulation in Bmal1 (26-fold; $p < 0.01$), Npas2 (21-fold; $p < 0.001$), Clock (15-fold; $p < 0.01$), Per1 (16.5-fold; $p < 0.01$) and Per2 (11-fold; $p < 0.001$) (Figure 12A). Females had an overall trend of upregulation in the circadian panel tested. Males also showed dysregulation compared to their WKY counterparts, however a different pattern of dysregulation compared to the females was observed. They showed significant changes in two of the eight genes with Per1 being significantly upregulated (6.6-fold; $p < 0.01$) and Cry2 being significantly downregulated at a fold change of 507 ($p < 0.001$) (Figure 12B).

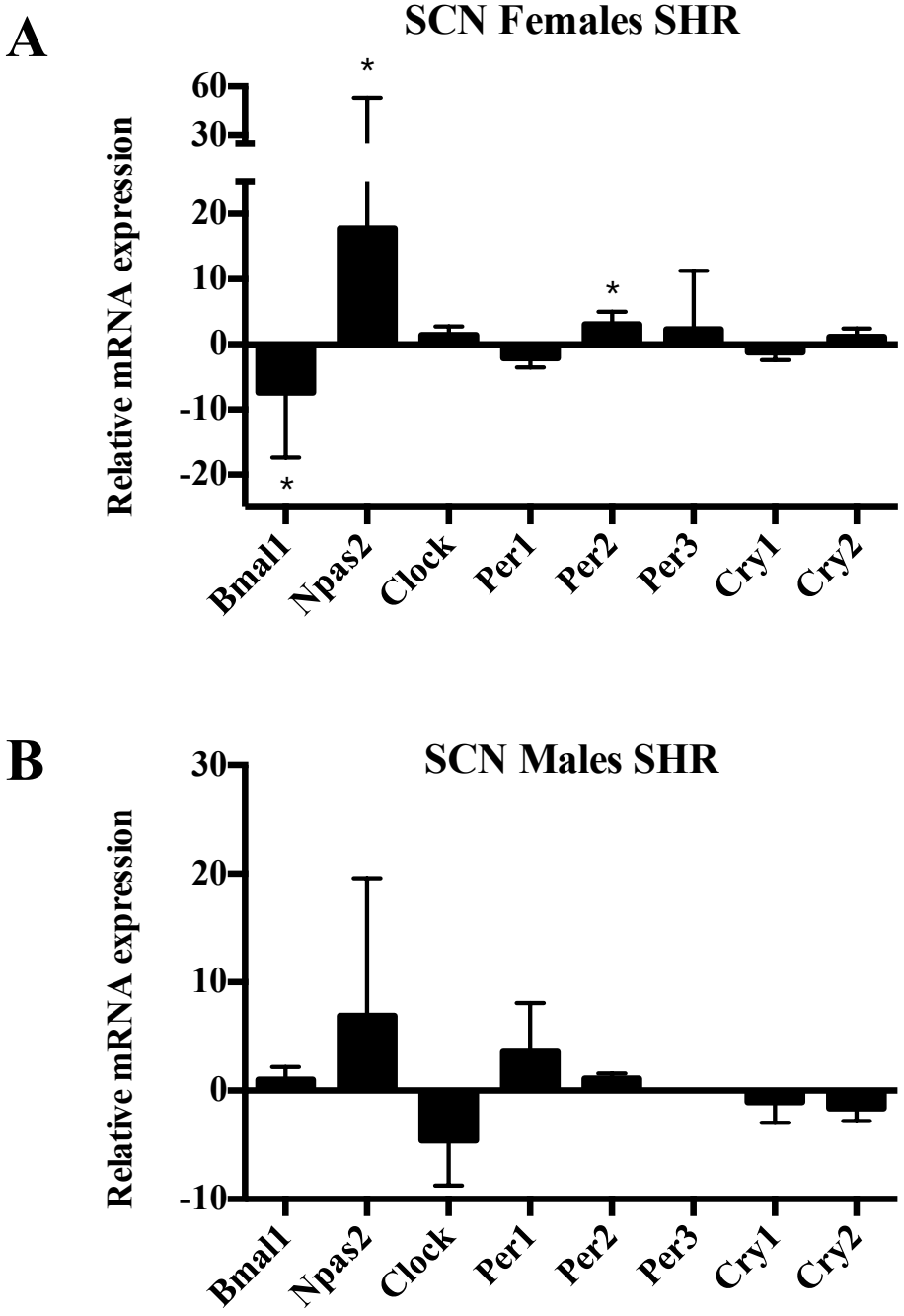

Figure 10. mRNA levels of circadian rhythm genes in the suprachiasmatic nucleus of 19 week old SHR rats relative to WKY control. Fold changes in mRNA levels of Bmal1, Npas2, Clock, Per1, Per2, Per3, Cry1 and Cry2 in female (A) and male (B) rats. Fold changes in gene expression were calculated by relative quantification (ΔΔCt) of RT-qPCR threshold cycles (Ct) as per Livak and Schmittgen[87] using mean Ct values of housekeeping genes GAPDH, Ywhaz and CycA. Data is expressed as mean fold change of SHR relative to the WKY group ± SEM (n = 8). Statistical significance between WKY and SHR groups is shown by: * $p < 0.05$.

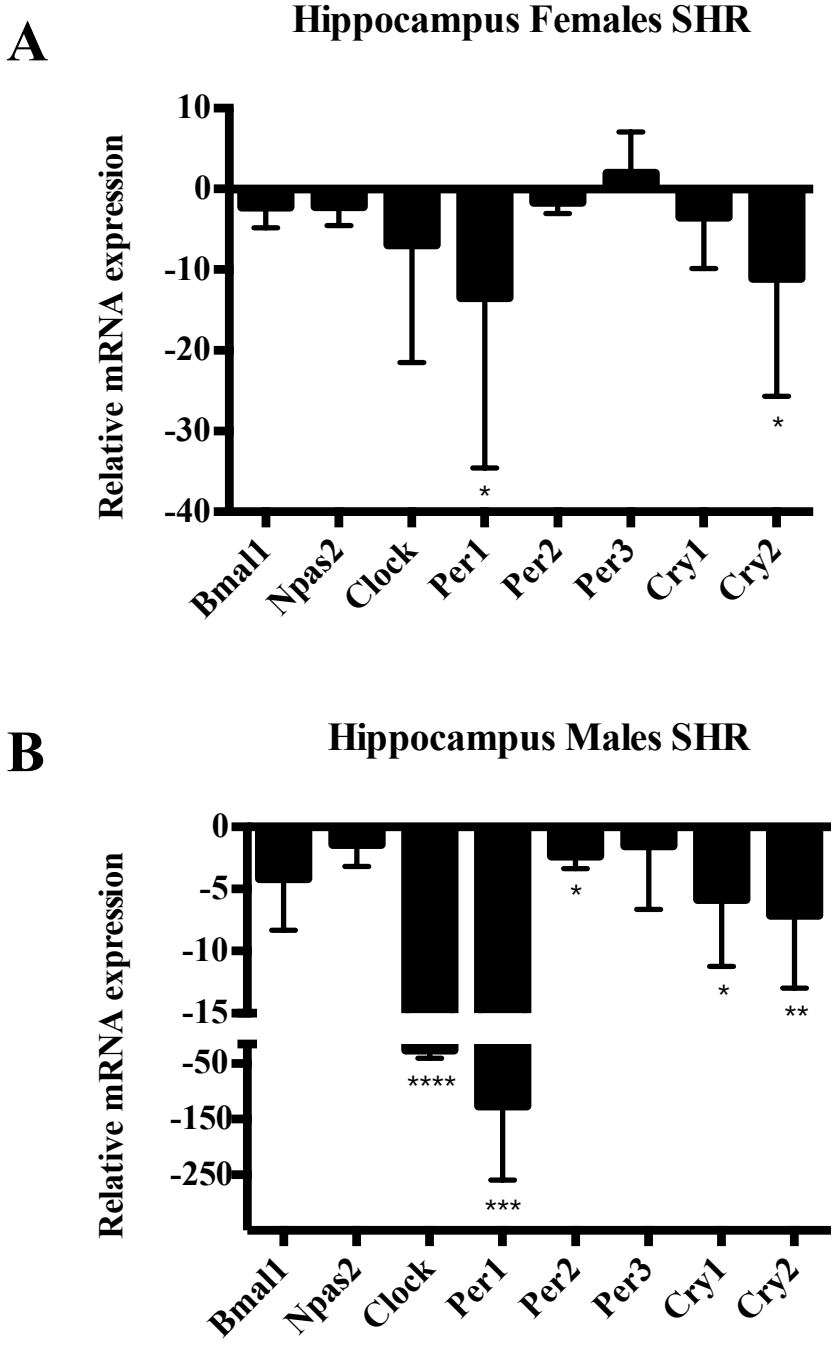

Figure 11. mRNA levels of circadian rhythm genes in the hippocampus of 19 week old SHR rats relative to WKY control. Fold changes in mRNA levels of Bmal1, Npas2, Clock, Per1, Per2, Per3, Cry1 and Cry2 in female (A) and male (B) rats. Fold changes in gene expression were calculated by relative quantification (ΔΔCt) of RT-qPCR threshold cycles (Ct) as per Livak and Schmittgen[87] using mean Ct values of housekeeping genes GAPDH, Ywhaz and CycA. Data is expressed as mean fold change of SHR relative to the WKY group ± SEM (n = 8). Statistical significance between WKY and SHR groups is shown by: * $p < 0.05$, ** $p < 0.01$, *** $p < 0.001$, **** $p < 0.0001$.

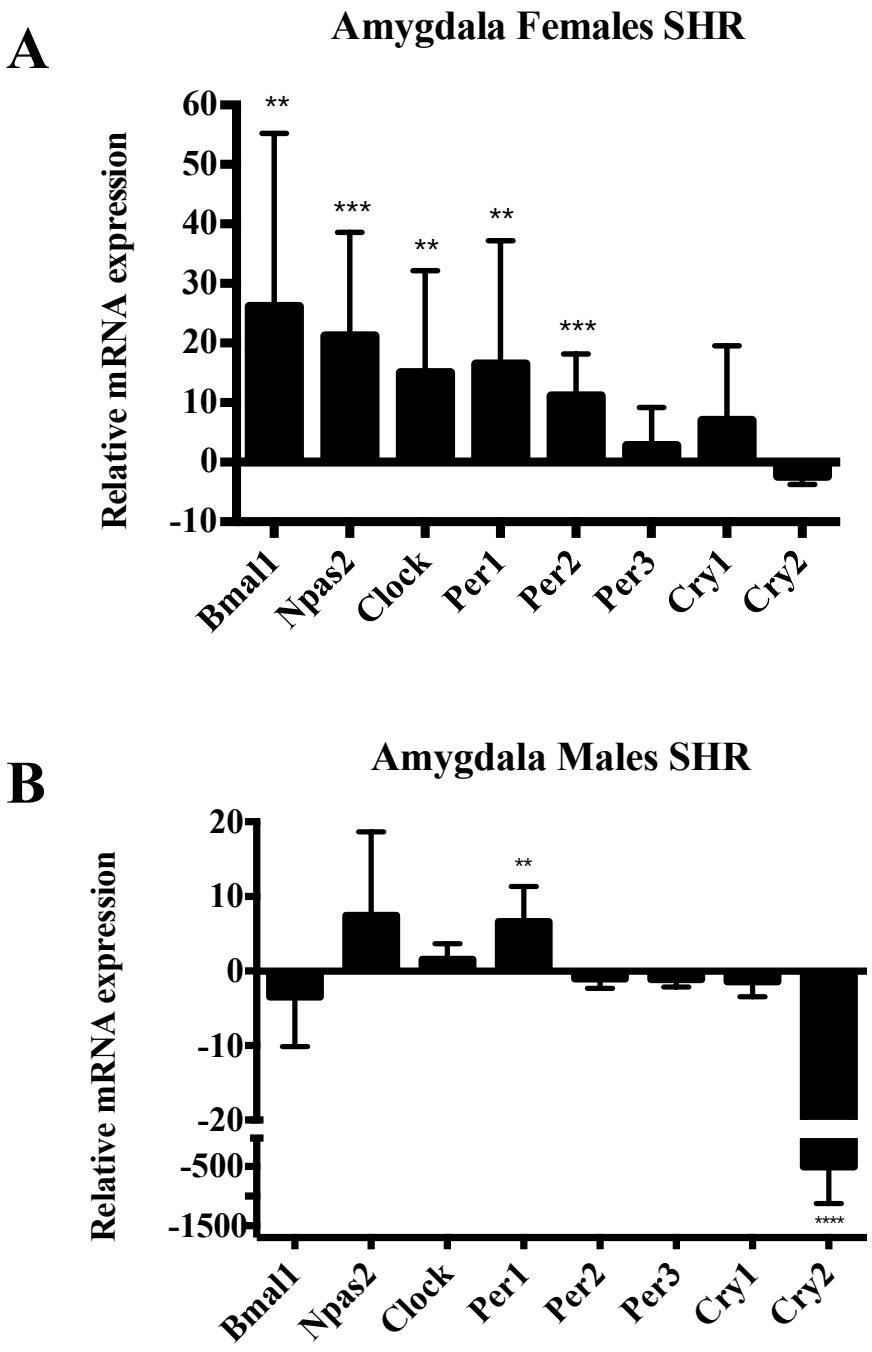

Figure 12. mRNA levels of circadian rhythm genes in the amygdala of 19 week old SHR rats relative to WKY control. Fold changes in mRNA levels of Bmal1, Npas2, Clock, Per1, Per2, Per3, Cry1 and Cry2 in female (A) and male (B) rats. Fold changes in gene expression were calculated by relative quantification (ΔΔCt) of RT-qPCR threshold cycles (Ct) as per Livak and Schmittgen[87] using mean Ct values of housekeeping genes GAPDH, Ywhaz and CycA. Data is expressed as mean fold change of SHR relative to the WKY group ± SEM (n = 8). Statistical significance between WKY and SHR groups is shown by: * $p < 0.05$, ** $p < 0.01$, *** $p < 0.001$.

3.2.4 Circadian Rhythms in the PVN

Results from RT-qPCR analysis of the paraventricular nucleus of SHR brains showed significant changes in the circadian rhythm gene panel relative to their WKY controls. These changes are different from the dysregulation patterns seen in the three other brain areas above, however, the pattern in the female PVN is similar to the pattern seen in the female amygdala with regard to trends. Female offspring showed a great deal of statistically significant changes in the circadian genes analyzed with five out of eight being significantly upregulated. Females showed upregulations in Bmal1 (5-fold; $p < 0.05$), Clock (98-fold; $p < 0.0001$), Per1 (7-fold; $p < 0.01$), Per2 (3.5-fold; $p < 0.05$) and Cry1 (5.5-fold; $p < 0.05$) (Figure 13A). It should be noted that expression levels of Per3 were so extremely low that its relative expression was unable to be detected in the PVN of female SHR brains. Male offspring showed statistically significant upregulations in six of eight circadian genes examined, however, these changes were different from those seen in the females. The males saw significant upregulations of Bmal1 (29-fold; $p < 0.001$), Npas2 (8-fold; $p < 0.05$), Clock (11.7-fold; $p < 0.05$), Per2 (15.4-fold; $p < 0.001$), Cry1 (9.2-fold; $p < 0.05$) and Cry2 (15.2-fold; $p < 0.01$) (Figure 13B).

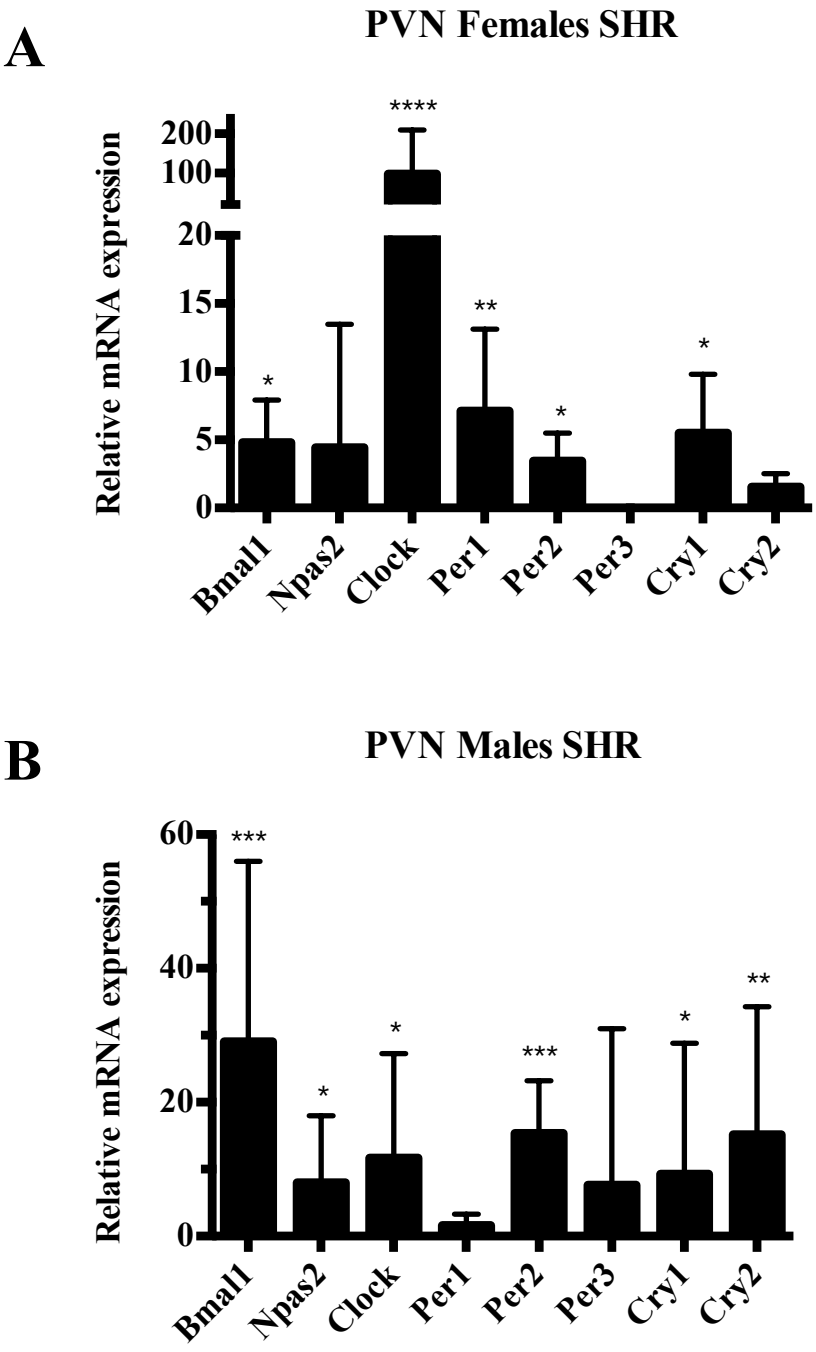

Figure 13. mRNA levels of circadian rhythm genes in the paraventricular nucleus of 19 week old SHR rats relative to WKY control. Fold changes in mRNA levels of Bmal1, Npas2, Clock, Per1, Per2, Per3, Cry1 and Cry2 in female (A) and male (B) rats. Fold changes in gene expression were calculated by relative quantification (ΔΔCt) of RT-qPCR threshold cycles (Ct) as per Livak and Schmittgen[87] using mean Ct values of housekeeping genes GAPDH, Ywhaz and CycA. Data is expressed as mean fold change of SHR relative to the WKY group ± SEM (n = 8). Statistical significance between WKY and SHR groups is shown by: * $p < 0.05$, ** $p < 0.01$, *** $p < 0.001$, **** $p < 0.0001$.

3.2.5 Circadian Rhythms in the PFC

The results from the RT-qPCR analysis of circadian rhythm genes found in the prefrontal cortex of male and female SHR animals show a dysregulated pattern when compared to their WKY controls. These dysregulation patterns were quite different from those seen in all other brain areas. Female offspring showed five statistically significant changes across the selected circadian genes. The results show upregulations in Npas2 (3.3-fold; $p < 0.0001$), Per1 (2.2-fold; $p < 0.001$), Per3 (2.4-fold; $p < 0.001$), Cry1 (1.5-fold; $p < 0.05$) and Cry2 (2.7-fold; $p < 0.0001$) (Figure 14A). Male offspring also showed five statistically significant changes in the circadian gene panel with similar genes that were dysregulated in females. Upregulations in Npas2 (4.1-fold; $p < 0.0001$), Per1 (2.3-fold; $p < 0.0001$), Per3 (2.4-fold; $p < 0.0001$), Cry2 (2.3-fold; $p < 0.0001$) and a downregulation in Per2 (1.3-fold; $p < 0.01$) (Figure 14B) were observed in males. In this brain area the male and female dysregulation patterns were quite similar with most genes showing a similar trend in fold change.

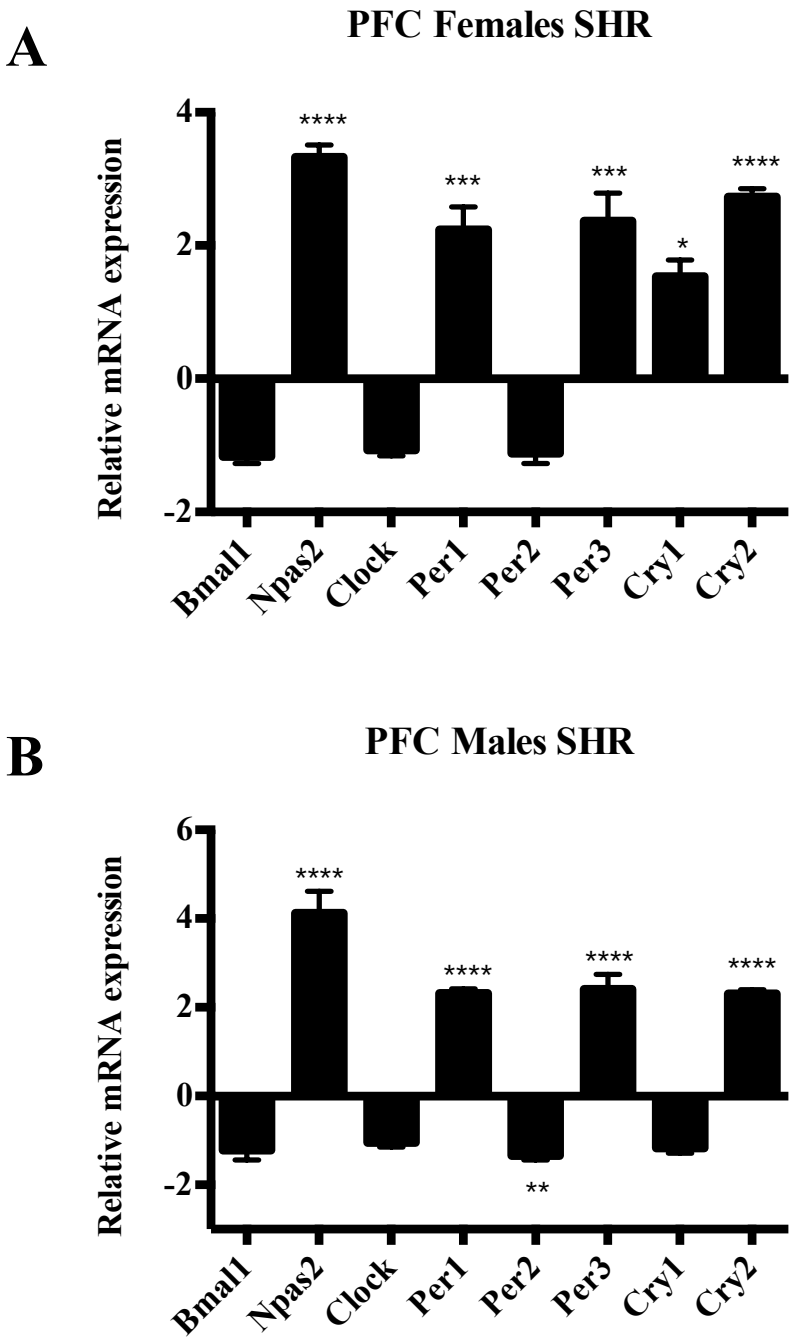

Figure 14. mRNA levels of circadian rhythm genes in the prefrontal cortex of 19 week old SHR rats relative to WKY control. Fold changes in mRNA levels of Bmal1, Npas2, Clock, Per1, Per2, Per3, Cry1 and Cry2 in female (A) and male (B) rats. Fold changes in gene expression were calculated by relative quantification (ΔΔCt) of RT-qPCR threshold cycles (Ct) as per Livak and Schmittgen[87] using mean Ct values of housekeeping genes GAPDH, Ywhaz and CycA. Data is expressed as mean fold change of SHR relative to the WKY group ± SEM (n = 8). Statistical significance between WKY and SHR groups is shown by: * $p < 0.05$, ** $p < 0.01$, *** $p < 0.001$, **** $p < 0.0001$.

3.3 Untargeted Metabolomics based screen through LC/MS

In order to determine a potential link between disrupted circadian rhythms and metabolism in the GC exposed offspring, a liquid chromatography-mass spectrometry based untargeted metabolomic screen was performed using the livers of eight male and female offspring of saline or Dex exposed WKY dams. A total of 704 compounds were identified during the chromatographic separation and their molecular weight was determined using mass spectrometry. Using the ChemSpider database 460 of the 704 compounds were positively identified. Metabolite data of prenatal Dex exposed male offspring compared with saline-treated controls showed 12 significantly dysregulated metabolites ($p < 0.05$) that could be identified with the ChemSpider database with 8 of these also meeting the secondary cut-off (fold change > 2 or < 0.5) (Table 6). Of the 8 metabolites that met both cut-offs, 7 were downregulated while only 1 was upregulated. Metabolite data of prenatal Dex exposed females offspring compared with their saline-treated controls showed 18 significantly dysregulated metabolites ($p < 0.05$) that were identified on ChemSpider with 7 of those also meeting the secondary fold-change cut-off. Of the 7 metabolites meeting the 2 cut-offs, 3 showed an upregulation while 4 showed a downregulation (Table 7). Further information from the metabolomic results for males and females, such as molecular weight and retention time can be found in Appendixes 1 and 2 respectively.

Brief analysis was performed to determine baseline differences between males and females by sorting metabolites by significance. Utilizing the ChemSpider database, 84 metabolites were identified to be significantly dysregulated ($p < 0.05$), of which 61 met the secondary cut-off of a fold change > 2 or < 0.5. Metabolic results for the baseline sex data can be found in Appendix 3.

Table 6. Significant results from the untargeted metabolomic screen in male Dex exposed offspring compared to their saline controls. Rows with a white background indicated metabolites that reached the two cut-off criteria ($p < 0.05$ and fold change > 2 or < 0.5) while rows with a grey shaded background indicate metabolites that reach the $p < 0.05$ criteria. Upregulations are presented first in descending order while downregulations follow.

Name	Fold Change	p value	Description	Pathway(s)
Vanillin 4-sulfate	3.004	0.0035	Polyphenol metabolite	
L-Carnitine tetradecanoyl ester	0.203	0.0329	Carnitine with a fatty acid attached; beta oxidation of long chain fatty acids	Lipid metabolism
Alpha-aminoadipic acid	0.212	0.0472	Intermediate of metabolism of lysine	Lysine biosynthesis and degradation
PC(18:1(9Z)/22:6(4Z,7Z,10Z,13Z,16Z,19Z))	0.265	5.42E-04	A type of phosphatidylcholine; a glycerophospholipid	Glycerophospholipid/ lipid metabolism
LysoPC(18:3(9Z,12Z,15Z))	0.355	0.0417	Monoglycerol phospholipid, formed by hydrolysis of phosphatidylcholine by phospholipase A2	Phospholipid metabolism, lipid transport, lipid metabolism, fatty acid metabolism
Eicosapentanoic acid	0.430	0.0486	Important polyunsaturated fatty acid found in fish oils	Alpha linolenic acid and linoleic acid metabolism; lipid metabolism pathway
Uracil	0.464	0.0405	Help carry out synthesis of many enzymes necessary for cell function	Pyrimidine metabolism; beta-alanine metabolism
DL-Carnitine	0.487	0.0106	Conditionally essential metabolite; transports fat into mitochondria of muscle cells	Thermogenesis; bile secretion; fatty acid metabolism; beta oxidation
Xanthine	0.623	0.0124	Intermediate of degradation of AMP to uric acid	Purine metabolism
DL-Tyrosine	0.630	0.0113	Essential amino acid; more needed under stress; rapidly metabolized	Cathecholamine biosynthesis; Phe and Tyr metabolism
Hypoxanthin	0.717	0.0406	Purine derivative; present in anticodon of tRNA	Purine metabolism
DL-Tryptophan	0.770	0.0291	Essential amino acid; precursor for melatonin and serotonin	Transcription/translation

Table 7. Significant results from the untargeted metabolomic screen in female Dex exposed offspring compared to their saline controls. Rows with a white background indicated metabolites that reached the two cut-off criteria ($p < 0.05$ and fold change > 2 or < 0.5) while rows with a grey shaded background indicate metabolites that reach the $p < 0.05$ criteria. Upregulations are presented first in descending order with downregulations follow.

Name	Fold Change	p value	Description	Pathway(s)
2,3,4,5-Tetrahydroxypentanal	6.228	1.31E-07	Heterosaccharide	Upstream of glycerol metabolism
Ophthalmic acid	4.303	3.55E-04	Oligopeptide; L-glutamine derivative; analogue of glutathione	Cysteine and methionine metabolism
Propionylcarnitine	2.059	0.0269	Acylcarnitine; a fatty ester lipid molecule	Lipid/ fatty acid metabolism; lipid transport, oxidation of branched chain fatty acids
Adenosine	1.970	0.0047	Component of DNA and RNA; neurotransmitter and potent vasodilator	Purine metabolism; cAMP signaling pathway; cGMP-PKG signaling; sphingolipid signaling
Adenine	1.911	0.0109	Purine nucleobase; pre-sugar attached version	Purine metabolism
Creatinine	1.905	0.0012	Breakdown product of creatine phosphate by loss of water; metabolized in liver	Arginine and proline metabolism
Spermidine	1.869	8.44E-05	Polyamine found in almost all tissues in association with nucleic acids; helps stabilize membranes and nucleic acid structures	Arginine and proline metabolism; beta-alanine metabolism; glutathione metabolism; bile secretion
Glutathione disulfide	1.775	0.0416	Enzyme for glutathione peroxidase production	Glutathione metabolism
Choline	1.683	0.0221	Precursor of acetylcholine; plays a role in lipid metabolism	Many pathways
L-(-)-methionine	1.667	0.0493	Essential amino acid	Cysteine and methionine metabolism
Hypoxanthin	1.634	0.0354	Purine derivative	Purine metabolism
L-(+)-Ergothioneine	1.558	0.0385	Metabolite of histidine that has antioxidant properties	Histidine metabolism
3-hydroxyisovaleryl carnitine	1.486	0.0186	Intermediate of fatty acid oxidation	Lipid/fatty acid metabolism; lipid transport
Nicotinamide	1.464	0.0433	Pyridine derivative; form of vitamin B3;	Nicotinate and Nicotinamide metabolism

			precursor for NAD+/NADH and NADP+/NADPH molecules	
Phosphatidylethanolamine (18:2/18:2)	0.006	6.18E-05	Phosphatidylethanol-amine lipid	Glycerophospholipid/ lipid metabolism; lipid transport
Lactosylceramide (d18:1/12:0)	0.216	0.0018	Important ceramide molecule; assists in stabilizing plasma membrane	Lipid/fatty acid metabolism; lipid transport phospholipid/ sphingolipid metabolism
Linolenelaidic acid	0.308	0.0116	Polyunsaturated omega-6 long chain fatty acid	Lipid metabolism; lipid transport; fatty acid metabolism
Phosphatidylserine (14:0/14:1)	0.491	0.0012	Phosphatidylserine lipid	Glycerophospholipid metabolism; lipid metabolism; lipid transport

3.4 Metabolic Pathway Analysis

In order to understand the relevance of the dysregulated metabolites in regards to specific biological processes, a metabolic pathway analysis was performed using the online tool MetaboAnalyst 2.0. For this analysis, all metabolites that reached the $p < 0.05$ significance cut-off were utilized due to the small amount of dysregulated metabolites in each sex. From the pathway analysis there were 16 metabolic pathways highlighted for the male dataset and 12 pathways highlighted for the female data. Using the MetaboAnalyst pathway tool, the males had significance in four of these pathways, including Glycerophospholipid metabolism (match status 2/36 metabolites in the pathway; $p = 0.0221$), Phenylalanine, tyrosine and tryptophan biosynthesis (match status 1/4; $p = 0.0263$), Linoleic acid metabolism (match status 1/5; $p = 0.0327$) and Aminoacyl-tRNA biosynthesis (match status 2/48); $p = 0.0379$). For the females 3 of the highlighted pathways showed significance with MetaboAnalyst. These pathways were purine metabolism (match status 3/66; $p = 0.0206$), Glutathione metabolism (match status 2/28; $p = 0.0263$) and Glycerophospholipid metabolism (match status 2/36; $p = 0.0421$).

3.4.1 Selection of metabolic pathways and creation of gene panels

Three metabolic pathways were selected to undergo further investigation from the metabolomic screen as these showed the greatest significance and had matching metabolites from the metabolomic screen. These included glycerophospholipid metabolism, purine metabolism and glutathione metabolism. Metabolites from these pathways that showed dysregulation in the metabolomics experiment were located in their metabolic pathway on the KEGG database and genes/enzymes that appeared up and downstream of them were selected and placed into gene panels. The glycerophospholipid metabolism gene panel consisted of 20 genes that play an essential role in both phospholipid and general lipid metabolism. The purine metabolism gene panel was created with 5 genes pertaining specifically to the purines that showed up in our screen. The glutathione metabolism panel was created with 7 genes related to general and specific antioxidant responses.

3.5 RT-qPCR analysis of gene panels

In order to get a better understanding of the results from the metabolomic screen, gene panels from top dysregulated metabolic pathways were analyzed using RT-qPCR. Across all four gene panels of glycerophospholipid metabolism and general lipid metabolism (Table 8), purine metabolism (Table 9), glutathione metabolism (Table 10) and circadian rhythms (Table 11), females had 17 significantly dysregulated genes in offspring prenatally exposed to Dex compared to their saline counterparts. Broken down into categories, 11/15 lipid metabolism genes, 2/6 phospholipid metabolism genes, 2/5 purine metabolism genes, 2/7 glutathione metabolism genes, and 0/14 circadian rhythm signalling genes were affected. All 11 dysregulated genes in the lipid metabolism category were upregulated. Genes affected were carnitine palmitoyltransferase 1 (CPT1A; 2.54-fold), carnitine palmitoyltransferase 2 (CPT2;

1.44-fold), acyl-CoA dehydrogenase long chain (ACADL; 1.21-fold); enoyl-CoA hydratase (ECH1; 1.66-fold), L-hydroxyacyl-CoA dehydrogenase (HADH; 1.23-fold), thiolase (ACAT1; 1.15-fold), propionyl-CoA carboxylase A (PCCA; 1.23-fold), propionyl-CoA carboxylase B (PCCB; 1.18-fold), methylmalonyl-CoA racemase (MCEE; 1.26-fold), methylmalonyl-CoA mutase (MMUT; 1.30-fold), and 2, 4-dienoyl-CoA reductase (DECR1; 1.27-fold). The two dysregulated genes in phospholipid metabolism were also both upregulated with phospholipase A1 (PLA1A) showing a fold change of 1.41 and glycerophosphodiester phosphodiesterase (GDE1) showing a fold change of 1.45. The two significantly dysregulated purine metabolism gene both showed a downregulation: adenosine deaminase (ADA) with a fold change of 0.79 and uricase (UOX) with a fold change of 0.89. Finally, the two significantly dysregulated glutathione metabolism genes were glutathione reductase (GSR) with a 1.40-fold upregulation and superoxide dismutase 1 (SOD1) with a 0.73-fold downregulation.

The male offspring showed a different pattern with only 3 dysregulated genes compared to their saline controls across the four gene panels. Broken down into categories, 0/15 selected lipid metabolism genes, 0/6 phospholipid metabolism genes, 2/5 purine metabolism genes, 0/7 glutathione metabolism genes, and 1/14 circadian rhythm signalling genes were affected. The two significantly dysregulated purine metabolism genes were adenosine deaminase (ADA) with a 0.76-fold downregulation and xanthine oxidase/dehydrogenase (XDH) with a 1.18-fold upregulation. The significantly dysregulated gene in the circadian rhythm signaling panel was Period 2 (PER2) with a 1.56-fold upregulation.

Table 8. Glycerophospholipid Metabolism and General Lipid Metabolism gene panel RT-qPCR results. mRNA levels in the livers of 19 week old prenatally DEX-exposed offspring relative to saline control. Fold changes in gene expression were calculated by relative quantification (ΔΔCt) of RT-qPCR threshold cycles (Ct) as per Livak and Schmittgen[87] using mean Ct values of housekeeping genes GAPDH and Rpl32. Data is expressed as mean fold change of Dex relative to the saline group ± SEM (n = 8). Unpaired t-test: Statistical significance between groups is shown by: * $p < 0.05$, ** $p < 0.01$, *** $p < 0.001$.

Gene	Sex	Fold Change + SEM
ACSL1	Male Female	0.93 ± 0.14 1.24 ± 0.16
CRAT	Male Female	0.82 ± 0.13 1.17 ± 0.26
CPT1A	Male Female	1.18 ± 0.36 **2.54 ± 0.28 *** **
CPT2	Male Female	0.91 ± 0.14 **1.44 ± 0.19 ***
ACADL	Male Female	0.89 ± 0.15 **1.21 ± 0.08 ***
ACADM	Male Female	0.96 ± 0.12 1.10 ± 0.10
ECH1	Male Female	1.07 ± 0.14 **1.66 ± 0.19 ****
HADH	Male Female	0.98 ± 0.08 **1.23 ± 0.12 ***
ACAT1	Male Female	0.94 ± 0.15 **1.15 ± 0.08 ***
PCCA	Male Female	0.92 ± 0.05 **1.23 ± 0.12 ***
PCCB	Male Female	0.99 ± 0.09 **1.18 ± 0.08 ***
MCEE	Male Female	1.14 ± 0.12 **1.26 ± 0.14 ***
MMUT	Male Female	1.01 ± 0.10 **1.30 ± 0.12 ****
ECI1	Male Female	0.99 ± 0.27 1.21 ± 0.27
DECR1	Male Female	1.00 ± 0.19 **1.27 ± 0.14 ***
PLA1A	Male Female	0.97 ± 0.16 **1.41 ± 0.18 ***
PLA2G2A	Male Female	1.05 ± 0.07 1.21 ± 0.16

PLCG1	Male Female	1.10 ± 0.14 1.11 ± 0.12
PLD1	Male Female	1.09 ± 0.34 1.26 ± 0.34
GDE1	Male Female	0.96 ± 0.15 **1.45 ± 0.16 ****
PEMT	Male Female	1.02 ± 0.11 0.97 ± 0.16

Table 9. Purine Metabolism gene panel RT-qPCR results. mRNA levels in the livers of 19 week old prenatally Dex-exposed offspring relative to saline control. Fold changes in gene expression were calculated by relative quantification (ΔΔCt) of RT-qPCR threshold cycles (Ct) as per Livak and Schmittgen[87] using mean Ct values of housekeeping genes GAPDH and Rpl32. Data is expressed as mean fold change of Dex relative to the saline group ± SEM (n = 8). Unpaired t-test: Statistical significance between groups is shown by: * $p < 0.05$, ** $p < 0.01$.

Gene	Sex	Fold Change + SEM
NT5C2	Male Female	0.96 ± 0.13 1.19 ± 0.12
ADA	Male Female	**0.76 ± 0.11 **** **0.79 ± 0.11 ****
PNP	Male Female	1.02 ± 0.08 1.08 ± 0.10
XDH	Male Female	**1.18 ± 0.09 *** 1.09 ± 0.13
UOX	Male Female	1.00 ± 0.09 **0.89 ± 0.05 ***

Table 10. Glutathione Metabolism gene panel RT-qPCR results. mRNA levels in the livers of 19 week old prenatally Dex-exposed offspring relative to saline control. Fold changes in gene expression were calculated by relative quantification (ΔΔCt) of RT-qPCR threshold cycles (Ct) as per Livak and Schmittgen[87] using mean Ct values of housekeeping genes GAPDH and Rpl32. Data is expressed as mean fold change of Dex relative to the saline group ± SEM (n = 8). Unpaired t-test: Statistical significance between groups is shown by: * $p < 0.05$.

Gene	Sex	Fold Change + SEM
GSR	Male	1.19 ± 0.30
	Female	**1.40 ± 0.22 ***
GPX1	Male	0.98 ± 0.21
	Female	0.97 ± 0.18
GGT1	Male	1.25 ± 0.18
	Female	0.63 ± 0.31
SMS	Male	0.96 ± 0.10
	Female	1.02 ± 0.12
CAT	Male	0.99 ± 0.07
	Female	1.08 ± 0.08
SOD1	Male	1.05 ± 0.23
	Female	**0.73 ± 0.20 ***
SOD2	Male	1.05 ± 0.18
	Female	0.84 ± 0.14

Table 11. Circadian Rhythm gene panel RT-qPCR results. mRNA levels in the livers of 19 week old prenatally Dex-exposed offspring relative to saline control. Fold changes in gene expression were calculated by relative quantification (ΔΔCt) of RT-qPCR threshold cycles (Ct) as per Livak and Schmittgen[87] using mean Ct values of housekeeping genes GAPDH and Rpl32. Data is expressed as mean fold change of Dex relative to the saline group ± SEM (n = 8). Unpaired t-test: Statistical significance between groups is shown by: * $p < 0.05$.

Gene	Sex	Fold Change + SEM
CLOCK	Male	0.88 ± 0.10
	Female	0.94 ± 0.19
BMAL1	Male	0.65 ± 0.42
	Female	0.66 ± 0.65
NPAS2	Male	0.75 ± 0.49
	Female	0.83 ± 0.56
PER1	Male	0.95 ± 0.38
	Female	1.59 ± 0.43
PER2	Male	**1.56 ± 0.21 ***
	Female	0.93 ± 0.51
PER3	Male	1.28 ± 0.79
	Female	1.23 ± 1.00
CRY1	Male	0.83 ± 0.46
	Female	1.26 ± 0.26
CRY2	Male	1.09 ± 0.15
	Female	1.12 ± 0.23
REV	Male	0.70 ± 1.05
	Female	0.66 ± 0.78
METTL3	Male	1.10 ± 0.14
	Female	0.80 ± 0.17
FBXL3	Male	1.04 ± 0.16
	Female	0.92 ± 0.19
CSNK1D	Male	1.01 ± 0.10
	Female	0.92 ± 0.11
CSNK1E	Male	0.78 ± 0.20
	Female	1.12 ± 0.44
PPARA	Male	0.87 ± 0.31
	Female	1.31 ± 0.33
YTHDF2	Male	0.91 ± 0.12
	Female	1.10 ± 0.09

3.6 Carnitine palmitoyltransferase 1 protein expression

CPT1A showed the highest dysregulation of any gene in the RT-qPCR analysis for gene expression. Carnitine and some carnitine derivatives were highly dysregulated in the metabolomic screen (DL-Carnitine and L-Carnitine tetradecanoyl ester in the males and propionylcarnitine in the females). This made CPT1A a good target to undergo further investigation. Western blot analysis was completed on the liver tissue of male and female Dex exposed offspring and their saline counterparts (Figure 15). From this analysis it showed that males have a higher baseline expression of CPT1A compared to their female counterparts. Both male and female Dex exposed animals show a slight reduction in CPT1A protein expression compared to their saline controls, however, no significance was detected between treatment groups.

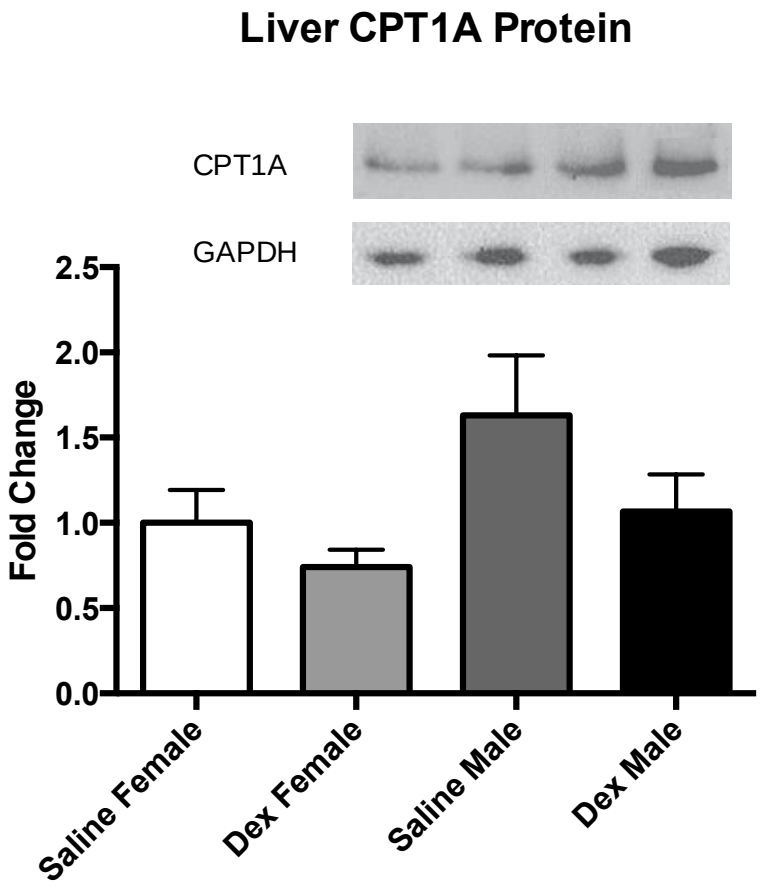

Figure 15. Protein expression of carnitine palmitoyltranferase 1 (CPT1A) in the liver of 19 week old prenatally Dex-exposed offspring relative to saline control. Protein bands of interest were normalized to GAPDH protein. Fold changes relative to the saline female group are presented graphically. One way ANOVA with post-hoc Tukey test was used to determine significance. Images shown are representative gel bands of each group measured. Data are represented at mean ± SEM (n = 8).

3.7 Triglyceride (TG) Assay

Since lipid metabolism was strongly implicated in the metabolomic screen and especially dysregulated in the female gene expression analysis, a triglyceride assay was performed on both liver tissue and plasma of the Dex-exposed offspring and their saline controls. This assay quantified the amount of triglycerides present in the livers of the Dex-exposed offspring by comparing the absorbance of the colorimetric assay to the TG standard curve completed from a range of 0-10 nm and then normalizing to the weight of tissue used for the analysis. In the liver (Figure 16-A), saline females had a triglyceride content of 1.83 ± 0.12 mM, Dex females a TG content of 2.87 ± 0.21 mM, saline males a content of 3.11 ± 0.24 mM and Dex males had 3.07 ± 0.15 mM TGs. When compared to saline females, Dex females, saline males and Dex males all had significantly elevated levels of TGs. Males showed no difference between saline and Dex groups, while the female Dex livers showed similar levels of triglycerides to their male counterparts.

For the triglyceride analysis in the plasma (Figure 16-B), samples were assayed directly by comparing the absorbance values of the colorimetric assay to the standard curve. No normalization was needed as the same volume of plasma was used for all samples. In the plasma, saline females had a TG content of 1.06 ± 0.09 mM, Dex females 0.91 ± 0.16 mM, saline males 1.40 ± 0.14 mM and Dex males 1.35 ± 0.10 mM. Compared to the liver, a different trend was seen with saline and Dex groups of the same sex having very similar levels of TGs. The plasma samples also had much lower levels of TGs, hovering around 1 mM compared to the liver which showed 2-3 mM TG concentrations.

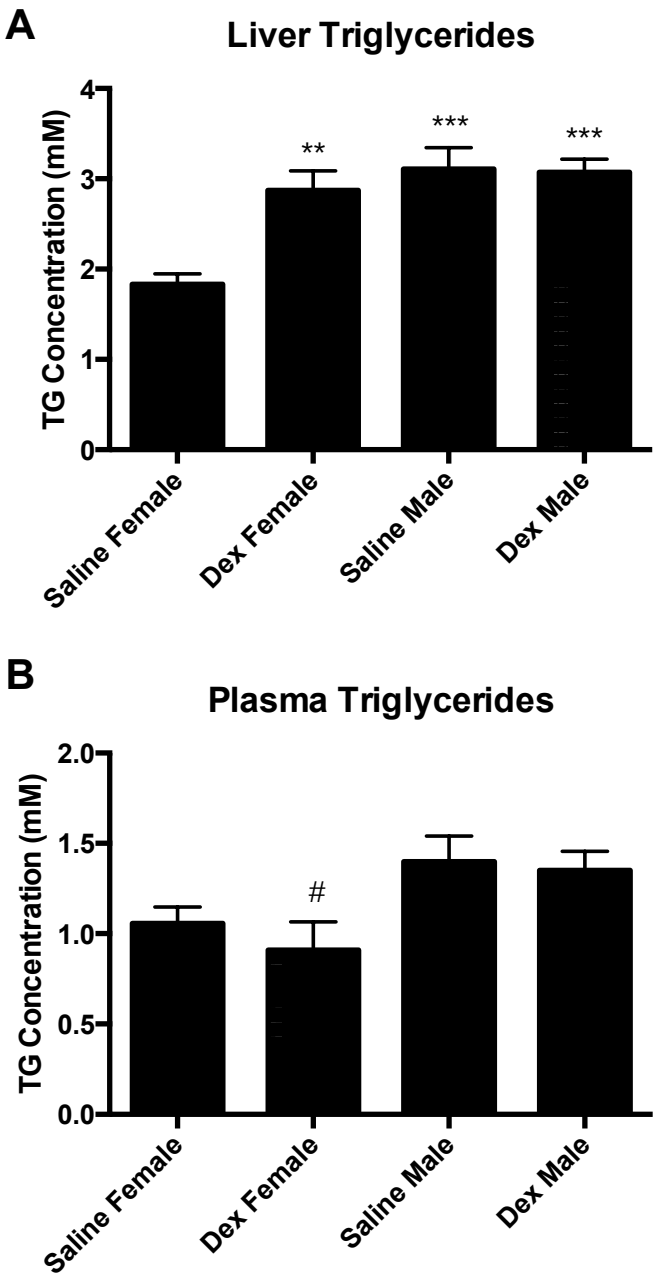

Figure 16. Triglyceride concentrations in the liver and plasma of saline and Dex exposed offspring. Levels of triglycerides were measured in the liver (A) and plasma (B) by the Triglyceride Quantification Assay (Abcam) in a colorimetric assay at 570nm. For the livers, the triglyceride concentration was normalized to the weight of the tissue used for the analysis. The triglyceride concentrations are represented graphically. Statistical significance between saline and Dex groups and sex was determined by one-way ANOVA with a post-hoc Tukey test. Data are presented as mean ± SEM (n = 8). Statistical significance between groups is shown by: * $p < 0.05$, ** $p < 0.01$, *** $p < 0.001$. The * indicates significance when compared to saline female group and the # indicates significance when compared to saline male group.

3.8 Body Weights

Body weight data from offspring of saline or Dex-exposed mothers is shown in Figure 17. Animals were weighed weekly between 4 and 17 weeks of age. Offspring that were exposed to Dex *in utero* had significantly lower body weights than their saline controls starting at week 7 in the males (Figure 17-A) and week 8 in the females (Figure 17-B). It can also be seen that males weighed significantly more than their female counterparts with an average body weight around 300 g for saline and 280 g for Dex at week 17 while females had an average body weight around 190 g for the saline condition and 180 g for the Dex at week 17.

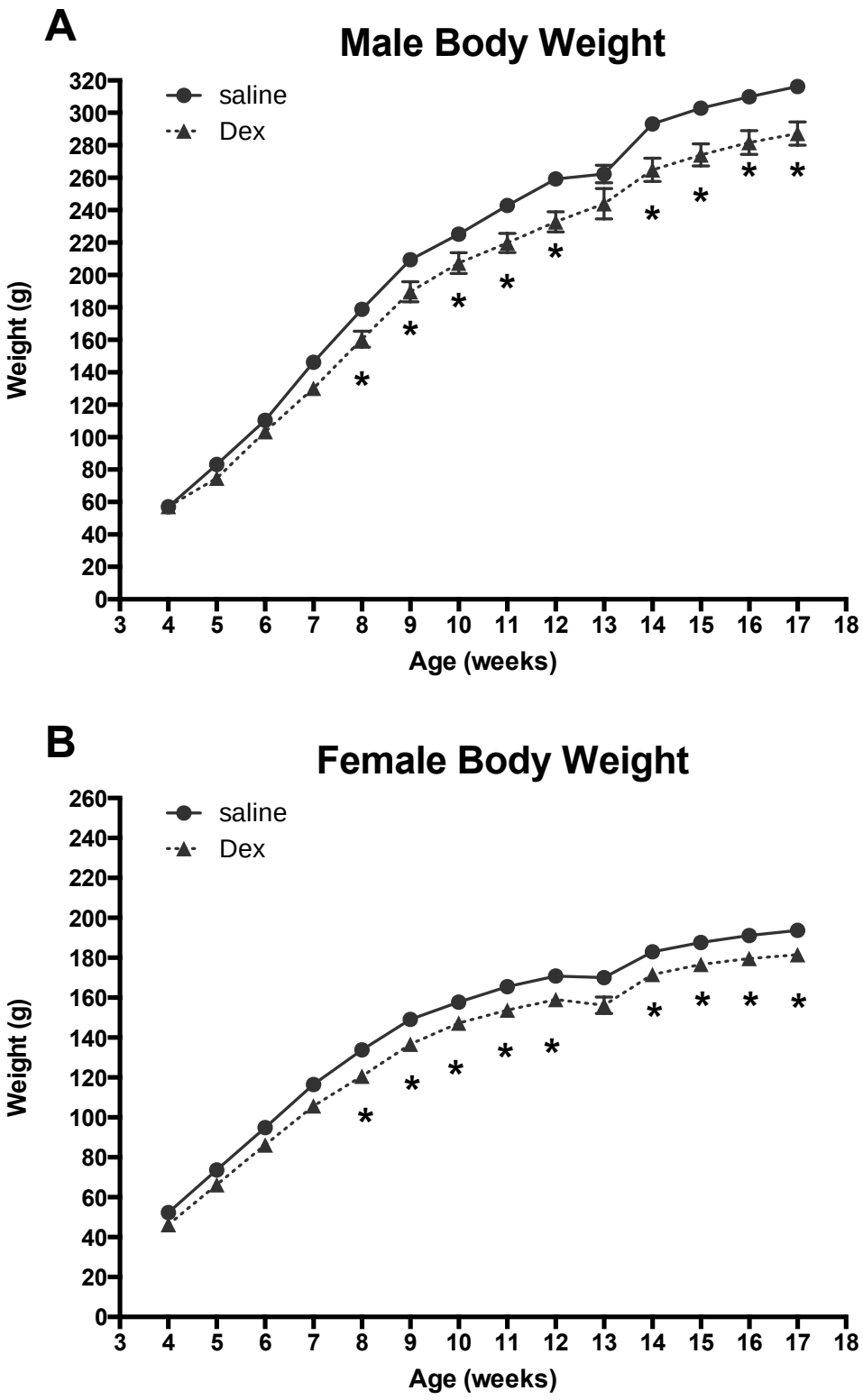

Figure 17. Body weight of male (A) and female (B) offspring born to saline or Dex-treated Wistar-Kyoto dams. Data is reported at mean ± SEM. Significant difference between groups indicates * $p < 0.05$.

4. Discussion

4.1 Circadian rhythm genes show sex and tissue specific expression in multiple brain areas of fetal programmed animals

This investigation examined the effect of prenatal exposure to Dex on central and peripheral circadian clocks in WKY rat offspring. From the results, it was found that all circadian genes analyzed demonstrated sex specific expression and that dysregulation of the circadian rhythm genes varied between brain areas. The circadian rhythm genes analyzed with RT-qPCR (see Table 1) were selected due to their inter-related roles of the main circadian oscillator[16,18] as well as due to many of these genes being dysregulated in our previous study in the adrenal glands[52].

In the SCN, the core circadian oscillator, it was shown that the females had much less dysregulation in their circadian functioning than in the males (Figure 5). Only Clock showed a significant dysregulation; where it was downregulated (Figure 5A). Due to Clock having such an integral role in circadian rhythm functioning and its close association with Bmal1, this downregulation was surprising. It has been shown, however, that under Clock deficient conditions the gene Npas2 can be expressed to compensate and act as a substitute for Clock in the SCN[88]. While not statistically significant, it is seen that Npas2 is slightly upregulated in the SCN of the female animals, and may be used to form the heterodimer with Bmal1.

Gene expression in the SCN of the male animals showed significantly greater dysregulation than the females indicating that males exhibit a greater susceptibility to the effects of fetal programming than females. This effect is also seen in the blood pressure phenotype of Dex exposed offspring with males having a more pronounced effect than females[84]. It has been shown that circulating estrogen has a protective role in maintaining daily

rhythms in females[89]. In the absence of the protective effects of estrogen, the male animals likely exhibited a different and more dysregulated pattern of effect. Unlike the females, males had normal expression levels in the positive limb of the oscillator with Bmal1 and Clock showing similar expression levels, while Npas2 was extremely lowly expressed (very high Ct values lead to the large amount of error present). As previously mentioned, Npas2 expression in the SCN is largely driven by the lack of the Clock transcript. As Bmal1 and Clock are expressed at similar levels, there is little need for the expression of Npas2. On the negative limb of the oscillator, however, significant dysregulation could be seen. Significant upregulation in the expression of Per1 and Cry2 occur alongside downregulation in the expression of Per2, Per3 and Cry1. It is hypothesized that due to the redundancy of the Per and Cry genes[90], Per1 and Cry2 are almost solely being transcribed to drive the negative limb of the circadian oscillator while Per2, Per3 and Cry1 play a lesser role.

In the hippocampus, a brain structure in the limbic system involved in learning and memory[33], sex specific effects could also be seen in circadian rhythm function (Figure 6). In the females, the greatest dysregulation occurred at the positive limb of the oscillator where Npas2 was significantly downregulated and Clock was significantly upregulated (Figure 6A). While it was previously thought that Npas2 had a SCN-specific role, it has been shown that peripheral circadian clocks are fundamentally similar and therefore share this Npas2/Clock compensation mechanism[88]. Since Clock is significantly upregulated, a downregulation in Npas2 would be expected; and is what is shown. Females also showed a significant upregulation in Cry1. While no other significance is seen in the Per and Cry genes, Per1 does show a slight upregulation and Per3 a slight downregulation, which may be correlated to the increase in Cry1 which is seen.

In the males, a different pattern of dysregulation could be seen (Figure 6B). Similar to the SCN results, the males did not show any significant changes to the genes of the positive limb of the oscillator but instead showed dysregulation in the negative limb. Per1 expression was downregulated while Per2 and Cry2 were both upregulated. The hippocampus region of the brain is extremely dense with GRs[91]. It has been shown that Cry1 and Cry2 are capable of interacting with GR and altering the transcriptional response to GCs[92]. This can result in high levels of circulating GCs and suppression of the HPA axis[92] through the damage of nerve cells and compromise hippocampal function[93]. In the GC exposed animals, this large increase in the expression of Cry2 may play a protective role in trying to inhibit the activation of GR. The large dysregulation in Per1 may follow from the effect of Cry2 on GR, as GR will no longer be activated and capable of translocating to the nucleus where it can interact with GREs present in the promoter of the Per1 gene and transcription will occur at a slower rate[35].

In the amygdala, a brain structure in the limbic system involved in fear and emotions[32], sex specific effects were once again seen with extremely different patterns in dysregulation occurring in the two sexes (Figure 7). In the females (Figure 7A), dysregulation was seen with significant upregulation in the genes Clock and Per1. On the positive limb, this dysregulation may be accounted for by a transcription factor which affects the transcription of Clock but not Bmal1. The positive limb of the oscillator has evolved to activate simultaneously as they need to form a heterodimer for the activation of circadian rhythm driven genes. This typically occurs through the cAMP/Ca^{2+} response element binding (CREB) protein-binding protein (CBP)[94]. Since a surprising difference in expression was observed within the positive limb, a possible transcription factor may have been driving the overexpression of Clock in this dysregulated system. Since the levels of Clock are generally reduced by the presence of Bmal1 (due to the degradation of the complex), it is also possible an imbalance in Bmal1 is driving

this increased expression of Bmal1. Expression of Clock is described to be nearly constitutive[95] and that it contains histone acetyltransferase activity, which can participate in chromatin remodelling to drive circadian rhythmicity[96]. The increase in Per1 that was seen may be accounted for by an increase in expression caused by the binding of GR to the GREs located in the promoter region[35].

Similar to the other brain areas, the males showed a greater degree of dysregulation than the females and in the amygdala the males showed downregulation of all circadian genes, particularly Per2 and Cry2 (Figure 7B). This significantly dysregulated system with all genes being downregulated speaks to a decrease in protection related to the conservation of rhythms in males when compared to the females[89]. It is proposed that the significant decrease in Per2 and Cry2 in these animals correlates to a lowered expression of these genes and they are therefore not used in the loop compared to the other Pers and Cry1. Redundancy in the Pers and Crys ensures a narrow range of entrainment of the circadian clocks (ensures cycle is tied to light/dark cycles); Per2/Cry2 mutants have been shown to be less sensitive to rhythmicity and have a wider range of entrainment[90]. The lowered expression of Per2 and Cry2 may be acting in a similar manner to compensate for the dysregulation seen in the amygdala of these animals.

In the paraventricular nucleus, an important region in the hypothalamus for autonomic control[97], a sex specific pattern of dysregulation could be seen. Females showed no significantly dysregulated genes while males showed an upregulation in both Bmal1 and Per2 (Figure 8). This result is interesting as it shows upregulations in both the positive and negative limbs of the oscillator. This is quite similar to the pattern seen in the female amygdala and may share a similar explanation. It has been reported that circadian rhythm expression profiles of various clock genes are similar between the SCN and PVN in male Wistar rats[98]. This is

anticipated as the PVN acts as a relay between the SCN and the HPA axis. In this system, however, the pattern of circadian gene expression is extremely different in the PVN compared to the SCN. This points to either a delay in rhythm between the SCN and PVN or a neural miscommunication between these closely connected brain areas.

The prefrontal cortex, the brain region that regulates thoughts, actions, emotions and other higher order cognition[99] showed the least amount of change compared to the saline controls. The males had one dysregulated gene (Per2), which was slightly upregulated. When looking at the other circadian genes (Figure 9) while not significant the fold changes are similar to infer this slight rise in Per2 may be normal oscillation in the PFC.

Examining the five brain areas that were analyzed as well as the adrenal glands of male offspring[52] a few trends can be seen. Significant gene expression changes for each tissue are summarized in Table 12. Overall, the data trend shows that female offspring are more protected from circadian rhythm dysregulation. Across all brain regions the females had much less dysregulation of the core clock genes than males. Notably, the female animals tend to display more dysregulation in the positive limb of the oscillator while in the males, a disruption of the negative limb is seen. Interestingly, while the females saw the most dysregulation in the positive limb, Bmal1 was never effected. In the males, Bmal1 was the only gene in the positive limb to be dysregulated. Based on clinical SNP data on Bmal1, it is possible that Bmal1 in these animals is mutated and produces a less functional protein. In fact, strong associations have been found between Bmal1 SNPs that confer reduced transcriptional efficiency and increased susceptibility to type 2 diabetes and hypertension[61]. If the Bmal1 protein was dysfunctional this could be causing downstream effects on the entire circadian loop, which may contribute to the hypertensive phenotype that is seen in both this model as well as Bmal1 knockouts[71].

As well, when comparing the male brain areas to the adrenal glands, it is clear that a more significant dysregulation has occurred in the adrenal glands. While the male adrenal glands show a clear pattern of dysregulation that implies a shift in phase from the saline controls, the patterns in the brain tend to be much more erratic with no clear dysregulation mechanism. This also holds true within the different brain areas. Due to their proximity to each other and the SCN it would seem that they would have similar circadian rhythm action, however, this is not true. While sex-specific effects are seen on the positive and negative limbs of the oscillator, these effects are not consistent. This points to an uncoupling of circadian rhythm in the peripheral clocks such as the adrenal gland and other brain structures from the central clock in the SCN, which was what was hypothesized. Since the offspring was exposed to high levels of GCs *in utero* it is possible that these mistimed cues of GCs permanently uncoupled the peripheral clocks from the central clock through GR activation and subsequent signalling[34].

The brain regions all show a different pattern of dysregulation and the expected reciprocal expression of genes in the positive and negative limbs of the oscillator are not seen. This suggests that these brain regions do not have a properly cycling circadian system. While we and others have shown that peripheral clocks can be uncoupled from the SCN and still maintain an independent circadian rhythm[41,52], the expression seen in the brain regions suggest they are not maintaining a cycling circadian rhythm in general. At this point it is unclear which clock system (central or peripheral) was the initiator of this widespread dysregulation or whether this programmed dysregulation occurred simultaneously across all clocks.

Table 12. Summary of circadian rhythm gene expression changes in Dex exposed offspring. Expression represented as fold change (± SEM) relative to saline control. Statistically significant ($p < 0.05$) changes compared to saline are represented as bolded red text (upregulation) and blue text (downregulation).

Sex	Gene	SCN	Hippocampus	Amygdala	PVN	PFC
Male	Bmal1	0.69 ± 0.66	3.19 ± 2.31	0.65 ± 0.81	**9.13 ± 8.21**	1.28 ± 0.45
	Npas2	0.87 ± 3.25	1.81 ± 2.27	0.26 ± 0.24	1.95 ± 3.42	0.82 ± 0.08
	Clock	0.42 ± 0.22	0.79 ± 0.54	0.43 ± 0.25	1.56 ± 1.81	1.29 ± 0.41
	Per1	**3.44 ± 1.58**	**0.18 ± 0.10**	0.53 ± 0.24	1.67 ± 1.71	1.11 ± 0.08
	Per2	**0.55 ± 0.10**	**1.87 ± 0.47**	**0.12 ± 0.09**	**6.00 ± 4.92**	**1.28 ± 0.11**
	Per3	**0.25 ± 0.14**	1.53 ± 2.91	0.45 ± 0.36	0.18 ± 0.29	1.16 ± 0.20
	Cry1	**0.28 ± 0.09**	0.77 ± 0.29	0.62 ± 0.40	3.53 ± 2.41	0.86 ± 0.22
	Cry2	**5.13 ± 2.28**	**9.00 ± 5.90**	**0.18 ± 0.16**	3.09 ± 1.67	1.08 ± 0.07
Female	Bmal1	0.84 ± 1.02	2.45 ± 2.17	0.78 ± 0.50	0.74 ± 0.38	1.26 ± 0.23
	Npas2	1.71 ± 2.30	**0.23 ± 0.03**	1.93 ± 1.86	0.99 ± 0.93	0.94 ± 0.08
	Clock	**0.28 ± 0.15**	**8.94 ± 5.22**	**5.29 ± 3.81**	2.73 ± 1.46	1.23 ± 0.24
	Per1	0.61 ± 0.31	3.31 ± 3.28	**5.67 ± 3.27**	1.15 ± 1.17	0.78 ± 0.14
	Per2	1.02 ± 0.19	1.39 ± 0.50	1.01 ± 0.62	0.84 ± 0.54	2.11 ± 0.83
	Per3	0.97 ± 1.31	0.37 ± 0.64	0.79 ± 0.52	0.84 ± 0.67	1.27 ± 0.18
	Cry1	1.01 ± 0.64	**3.50 ± 1.49**	1.32 ± 1.12	0.45 ± 0.62	1.08 ± 0.18
	Cry2	0.67 ± 0.31	1.16 ± 1.12	1.96 ± 2.05	1.00 ± 0.54	0.96 ± 0.07

4.2 Circadian rhythm genes show sex and tissue specific expression in multiple brain areas of the spontaneously hypertensive rat

Circadian rhythm function in central and peripheral clocks was also investigated in the WKY/SHR genetic model of hypertension. These results also showed that all circadian genes examined demonstrated sex specific expression, varied between brain areas and had dysregulation patterns which were markedly different that those seen in the Dex animals.

In the SCN, SHR males showed no dysregulation, while SHR females showed a downregulation of Bmal1, an upregulation in Npas2 and an upregulation in Per2 (Figure 10). No observed dysregulation in the males is an interesting, given what was observed in the Dex model. It appears that the central clock in the male SHR animals is fully functional. In the females, a non-coordinated effect between the genes of the positive limb of the oscillator was

seen. It is known that there is a SNP in the Bmal1 gene of SHR animals[61]. While this could account for the decrease in Bmal1 expression, it is unclear why Npas2 is so strongly upregulated, especially under conditions where Clock is normally expressed.

In the hippocampus, SHR males showed a significant dysregulation in the positive limb with a downregulation in Clock and also in the negative limb with downregulations of Per1, Per2, Cry1 and Cry2 (Figure 11B). Since both Npas2 and Bmal1 are unaffected, they may be driving the positive limb and this 26-fold downregulation in Clock may not affect the complex with Bmal1. What is interesting, however, is the downregulation in the negative limb of the oscillator; in particular the 126-fold downregulation of Per1. While Npas2 and Clock have been found to have similar circadian roles[88], it is unclear how far the similarity goes. It may be the case that the Clock-Bmal1 complex can activate compounds that the Npas2-Bmal1 complex cannot and vice versa. For example, the transcription factor DBP, which is regulated by Clock-Bmal1, can cooperatively activate Per1 with the Clock-Bmal1 complex by directly binding to its promoter region[100]. Perhaps DBP was not activated in the system due to the downregulation of Clock, which in turn resulted in the downregulation of Per1.

In the hippocampus of the female SHR, there was a downregulation of nearly all circadian genes with statistical significance in both Per1 and Cry2 (Figure 11A). Aside from the significantly downregulated genes in the hippocampus of the male SHR discussed above, a downregulation of all circadian genes was seen also. The visual pattern of dysregulation is very similar between the males and females, even though the fold changes are larger in the males. This was a pattern that was not seen in the Dex model animals; however, this is a very similar pattern of dysregulation to what was seen in the male amygdala of the Dex model. It seems that the circadian machinery in the hippocampus of SHR are repressed compared to their WKY counterparts. A study investigating the effects of circadian rhythm disorder (CRD)

on the hippocampus of SHR and WKY rats found that CRD and hypertension reduced memory performance, caused changed in hippocampal plasticity by decreasing the number of neurons and astrocytes and reduced blood flow in the brain[101]. It appears that the hippocampus is particularly vulnerable to the effects of CRD and hypertension, which could be why we see such a high level of dysregulation in that brain structure.

In the amygdala of female SHR, nearly all circadian genes showed an upregulation with significance in Bmal1, Npas2, Clock, Per1 and Per2 (Figure 12A). This is the opposite effect of what was seen in the hippocampus of these animals. It seems in the amygdala the circadian clock is activated compared to female WKY. Given the amygdala's role in fear and the fight or flight response, it is possible that an overactive amygdala is contributing to the hypertensive phenotype of female SHR. It is known that the amygdala normally reinforces emotionally induced defensive reactions and when amygdala of SHR rats are lesioned, blood pressure is significantly attentuated[102]. It is thought that the amygdala may play an important role in aggravating hypertension in SHR animals by reinforcing maladaptive reactions to stressful situations[102].

In the amygdala of male SHR animals, there was a significant upregulation of Per1 and downregulation of Cry2 (Figure 12B). Due to the redundant nature of the Per and Cry genes[90], it is possible that the dysregulation seen in this brain region is the result of Per1 and Cry2 not being used in the loop compared to the other Pers and Cry1. Perhaps the downregulation of these two redundant genes are acting to compensate for the dysregulation that is seen in the other brain regions as well as the adrenal glands.

In the PVN of both male and female SHR all circadian genes were upregulated to some extent (Figure 13). In the females, a significant dysregulation of Bmal1, Npas2, Clock, Per1, Per2 and Cry1 was seen, while in the males Bmal1, Npas2, Clock, Per2, Cry1 and Cry2 were

significantly upregulated. This is opposite of the trend that was seen in the hippocampus in the SHR model and presents another brain region where the male and female data are paralleled. In the female PVN the Per3 transcript was not picked up as it was very lowly expressed and the large error bar on the male PVN Per3 expression presents a similar trend. Like in the female amygdala, it appears that the circadian clock machinery are activated compared to their WKY counterparts. It has been suggested that the PVN participates in blood pressure regulation and through lesioning of the PVN in SHR and WKY rats it has been shown that the PVN contributes to the development of spontaneous hypertension[103]. The activation of the core circadian rhythm genes in the PVN may be contributing to the blood pressure phenotype seen in SHR animals.

Finally, in the PFC of the male and female SHR a similar pattern of dysregulation was seen again. In the females Npas2, Per1, Per3, Cry1 and Cry2 were all significantly upregulated (Figure 14A), while in the males Npas2, Per1, Per3 and Cry2 were all significantly upregulated while Per2 was significantly downregulated (Figure 14B). Both male and females showed an almost 4-fold increase in Npas2. Variations in Npas2 has been shown to be linked to hypertension in humans[53]. Variations in the Pers and Crys could be related to an altered timing compared to the WKYs. As discussed in our previous work, SHR animals have a phase advance with regard to circadian rhythms[52]. Perhaps the upregulation of the negative limb and downward trend in the positive limb are accounting for this alteration in circadian signaling.

Significant gene expression changes for each tissue are summarized in Table 13. Looking across all five brain areas in addition to the adrenals glands of the male offspring[52] it is difficult to pick out a clear trend. Male and female SHR appeared to have similar amounts of dysregulation across the brain areas and the patterns of dysregulation in the hippocampus,

PVN and PFC were very similar in the two sexes. The dysregulation was widespread across the circadian oscillator and no clear mechanism could be seen to link the brain areas together. Over-activation of the circadian in the PVN of these animals may have a link to the hypertensive phenotype but more information is needed to make a true connection. When comparing the male brain areas to the adrenal gland data, while the adrenal glands show a clear shift from their WKY counterparts, the brain areas appear to be more dysregulated overall. Given that the adrenal glands are indicative of a phase shift from the WKY controls, perhaps the brain areas are also part of a shift in rhythm but one different from that in the adrenal gland. In conclusion, we saw a notable tissue specific effect across the five brain regions and a sex-specific effect in only two brain regions.

Table 13. Summary of circadian rhythm gene expression changes in the spontaneously hypertensive rat. Expression represented as fold change (± SEM) relative to WKY control. Statistically significant ($p < 0.05$) changes compared to WKY are represented as bolded red text (upregulation) and blue text (downregulation).

Sex	Gene	SCN	Hippocampus	Amygdala	PVN	PFC
Male	Bmal1	1.01 ± 0.87	0.24 ± 0.18	0.29 ± 0.37	**29.04 ± 20.47**	0.82 ± 0.13
	Npas2	6.87 ± 8.58	0.70 ± 0.62	7.46 ± 7.84	**7.96 ± 7.24**	**4.12 ± 0.47**
	Clock	0.22 ± 0.15	**0.04 ± 0.02**	1.55 ± 1.50	**11.69 ± 11.13**	0.95 ± 0.09
	Per1	3.58 ± 3.24	**0.01 ± 0.01**	**6.62 ± 3.72**	1.62 ± 1.24	**2.31 ± 0.11**
	Per2	1.11 ± 0.42	**0.43 ± 0.15**	0.94 ± 0.83	**15.35 ± 6.52**	**0.75 ± 0.05**
	Per3	Not detected	0.65 ± 1.35	0.87 ± 0.58	7.63 ± 14.56	**2.40 ± 0.32**
	Cry1	0.96 ± 1.21	**0.19 ± 0.14**	0.70 ± 0.69	**9.24 ± 12.93**	0.85 ± 0.08
	Cry2	0.62 ± 0.36	**0.14 ± 0.09**	**0.002 ± 0.002**	**15.18 ± 13.77**	**2.31 ± 0.09**
Female	Bmal1	**0.14 ± 0.13**	0.45 ± 0.37	**26.15 ± 21.43**	**4.78 ± 2.51**	0.86 ± 0.08
	Npas2	**17.77 ± 23.53**	0.45 ± 0.35	**21.23 ± 13.44**	**4.42 ± 6.00**	**3.33 ± 0.18**
	Clock	1.40 ± 1.01	0.14 ± 0.20	**15.09 ± 12.57**	**97.99 ± 81.85**	0.94 ± 0.08
	Per1	0.48 ± 0.26	**0.07 ± 0.08**	**16.53 ± 14.94**	**7.11 ± 4.64**	**2.23 ± 0.32**
	Per2	**3.06 ± 1.54**	0.61 ± 0.40	**11.14 ± 5.68**	**3.45 ± 1.65**	0.89 ± 0.12
	Per3	2.28 ± 5.39	1.94 ± 3.27	2.80 ± 4.17	Not detected	**2.37 ± 0.39**
	Cry1	0.80 ± 0.58	0.28 ± 0.35	7.02 ± 8.53	**5.49 ± 3.37**	**1.53 ± 0.23**
	Cry2	1.11 ± 0.96	**0.09 ± 0.09**	0.43 ± 0.21	1.53 ± 0.78	**2.73 ± 0.12**

4.3 General Discussion of Circadian Rhythms in the Brain Across Models

The main conclusion that can be drawn from this investigation is that circadian rhythm dysregulation occurs in both male and female GC-exposed offspring as well as in SHR animals in all tissue types tested; however, the dysregulation occurs in a sex and tissue specific manner. These findings truly speak to the complexity of circadian rhythms and their variability across tissue types. Even within animals not subjected to any treatment, differences in expression levels of circadian rhythm genes between sex and tissue is seen[104] and therefore it is not surprising that this high degree of variability was seen in this investigation on fetal programmed offspring and a genetic model of disease.

Differences in circadian rhythms between males and females have been noted in the literature. As previously mentioned in the discussion of the differences between males and females in the SCN, estrogen has been shown to have a protective role in maintaining the circadian rhythms of females[89]. This protective effect may be more necessary in maintaining the normal circadian rhythm functioning in females, as circadian rhythm disruption leads to more detrimental outcomes in females compared to males[104]. Female circadian rhythms are less likely to be shifted from normal cycling patterns, however, when they are shifted they produce a much greater effect and can lead to significant mental health disorders[104]. In a study involving the human cerebral cortex, it was found the circadian cycles in men and women run differently with rhythms in men showing a slight delay in comparison to females[105]. It has also been shown that the absence of the Per1 gene elicits a different response between the sexes. In male mice, the lack of Per1 disrupted circadian blood pressure rhythms, however, they were maintained in female mice[106]. Finally, women tend to have less circadian disruption overall[89], and this is in accordance with what was found in this investigation; particularly in the Dex model. These results show how truly important a role biology plays in physiology;

while both male and female offspring were subjected to the same conditions *in utero*, the future effects seen were extremely different.

Very few studies have been performed linking prenatal stress with circadian rhythm entrainment, however, of those completed they have mainly focused on phenotypic outcomes rather than mechanistic effects on a molecular level. It is widely known that the circadian rhythm system is established during a critical period of perinatal life and that genetics and the environment both play a role in determining its functional responses later in life[107]. As such, while circadian rhythms and fetal programming are not often linked, there has been evidence suggesting a programming of the circadian system *in utero*, by changing gene expression through epigenetic mechanisms[107]. It has been shown previously that male rats whose mothers were subjected to circadian rhythm phase disruption had altered daily physiological rhythms such as blood pressure and corticosterone, however, presented normal rhythms in Bmal1 and Per2 gene rhythms in the SCN[108]. While these results are different than what was seen in this investigation, this could be because a different prenatal stressor was used. The GC exposure model of prenatal stress, while producing a similar phenotypic effect, likely programs the circadian clock system differently than circadian disruption as a stressor does.

It has previously been documented that SHRs exhibit abnormal circadian rhythms, however, there have not been many studies and they did not focus on the expression of core clock genes. It has been shown that the mRNA expression of vasoactive intestinal peptide, which plays an important role in circadian entrainment, is upregulated in the SCN of SHRs compared to WKYs[109]. This same study found significant changes to the circadian rhythm of locomotor activity in SHR animals such as phase advances in wheel running behaviour under a consistent 24 hour light-dark cycle, in addition to shortened free-running period while under constant light or darkness[109]. SHRs have also been shown to differ from WKYs in their

response to period-altering effects of light intensity and were altogether more active than WKYs[110]. Alterations in sleep have also been seen in the SHR model with these rats exhibiting more frequent sleep interruptions than WKYs[111]. Interestingly, the SHR model is also used as a model for Attention Deficit Hyperactivity Disorder (ADHD). Individuals with ADHD often have sleep disturbances and those with circadian rhythm sleep disorders often have ADHD symptoms[112]. Genome wide association studies have identified several polymorphisms in core clock genes in individuals with ADHD[112]. The SHR model is thus a complex model bringing together behaviour, cellular mechanisms and physiology and proving just how interconnected all bodily processes are.

Next steps for this investigation will be to optimize RT-qPCR more effectively in each tissue type. The measured expression of the circadian genes in some brain areas was low compared to the adrenal using RT-qPCR, which may have been due to the low RNA yield that could be extracted from these extremely small micropunches of tissue. Possible ways to reduce error in extremely lowly expressed transcripts such as Npas2 or Per3 include using more sensitive gene expression assays including Digital Droplet PCR or Targeted Next-Generation Sequencing of the PCR amplicons. Future work may also look to harvest tissues at different times of day, and also to determine whether these changes in transcript levels are reflected at the protein level. Due to the rhythmic nature of these genes, the levels of expression depend on the time of day and it would be important to link transcript, protein and physiological functioning to gain a better understanding of the system. One of the major limitations of this study was that harvesting at multiple time points was not considered, due to the retrospective findings with regard to circadian rhythms. Future work should also focus on analyzing adrenal glands from female animals will be analyzed and compared to the results of the males, and the sex-matched brain areas. Further studies can then be undertaken to try

and rescue these animals exposed to prenatal stress, with the aim of reversing the effects of circadian rhythm dysregulation. This may be accomplished through the use of circadian driven hormones such as melatonin, which have previously been shown to resynchronize circadian rhythms[113].

4.4 Circadian rhythm signaling and metabolic function in the livers of glucocorticoid exposed offspring

Given the strong link between circadian rhythm and metabolism[66] and the monumental role of the liver in metabolism we wanted to examine if Dex exposed animals experienced any changes in liver metabolism. Using an LC/MS based untargeted metabolomics screen many dysregulated metabolites in both male and female livers were identified. Across male (Table 6) and female (Table 7) results, lipids, fatty acids, carnitine and carnitine intermediates, as well as purine derivatives were common dysregulated metabolites. Even though there were commonalities between male and female metabolites, the only specific metabolite that was dysregulated in both sexes was the purine derivative hypoxanthin. The dysregulation of this compound, however, was not the same in both sexes with males showing a 0.717-fold downregulation while females showed a 1.634-fold upregulation. This trend in fold-change was actually seen across the significant hits between sexes. With the exception of one metabolite, males displayed a downregulation in all significantly dysregulated metabolites. Females on the other hand showed more of a mix in behaviour. Metabolites involved in lipid metabolism, with the exception of carnitine derivatives, were downregulated but all other metabolites showed an upregulation.

Metabolic pathway analysis was performed with the online tool MetaboAnalyst 4.0 using dysregulated metabolites from each sex and unsurprisingly the glycerophospholipid

metabolism pathway was highlighted in both males and females. Purine metabolism was the top dysregulated pathway found in females and appeared as the sixth highest dysregulated pathway in males. As such, both of these pathways were selected to undergo further analysis. We also selected glutathione metabolism to investigate as it was one of the top dysregulated pathways in the females and higher levels of oxidative stress have been shown to result from fetal programming through GC exposure[114]. Gene panels were created by locating dysregulated metabolites within selected pathways and selecting genes that appeared up and downstream of them.

From the RT-qPCR analysis performed using the selected gene panels in liver tissue, it was clear that females were more metabolically affected than the males. Males only showed 3 dysregulated genes while females displayed dysregulation in 17. In the males there was no dysregulation in lipid metabolism or phospholipid metabolism (Table 8). This was actually quite surprising given that 5/7 significantly dysregulated metabolites were involved in lipid metabolism and that glycerophospholipid metabolism was the top dysregulated pathway from the pathway analysis. Given that metabolites are intermediates or end products of metabolic reactions it is possible that the timing of our analysis occurred just as the levels of metabolites began to fall but gene transcription had not yet been activated to account for this reduction in metabolite concentration. It is also possible that the Dex exposed males have adapted to become more metabolically efficient than their saline controls and are able metabolize a greater number of lipid molecules while maintaining the same level of transcription and translation. This is actually indicative of what occurs to chronically stressed individuals[78,79]. When the body is in a persistent state of stress it tries to adapt and in regard to metabolism it adapts to increase calorie efficiency[79].

Males exhibited 2 dysregulated genes in purine metabolism which were adenosine deaminase (ADA; 0.76-fold downregulated) and xanthine oxidase/dehydrogenase (XDH) 1.18-fold upregulated) (Table 9). ADA and XDH are both enzymes in the purine metabolism converting AMP to the end product of uric acid with ADA being separated from XDH with the enzyme PNP[115]. With both enzymes in the same pathway it is curious that they exhibit opposite effects in expression. In the male metabolomics it was seen that xanthine and hypoxanthin were slightly downregulated. Perhaps the upregulation seen in XDH expression is indicating increased metabolism of this pathway, which would result in the decreased amount of metabolites. For ADA, neither AMP or adenosine were dysregulated in the metabolomic screen but as indicated above, xanthine and hypoxanthin were. Since xanthine is an intermediate of the degradation of AMP to uric acid this downregulation in ADA may be negative feedback as the pathway concentrates toward the end product of uric acid. High levels of uric acid, also known as hyperuricemia is implicated in the initiation and progression of many manifestations of metabolic syndrome including hypertension[116]. It has been suggested that uric acid can penetrate vascular smooth muscle fibres and results in a rise of arterial pressure, vascular smooth muscle cell hypertrophy and hypertension[117]. It is also interesting to note that in our previous transcriptome study of the adrenal glands of male offspring, purine metabolism was a top signaling pathway that was dysregulated[52].

The last gene dysregulated in the males was the circadian rhythm gene Per2. This was the only circadian gene significantly altered and was upregulated 1.56-fold (Table 11). Interestingly, Per2 is a circadian clock protein that has been shown to have intracellular roles apart from the core circadian oscillator in the liver (Figure 3). Per2 can bind to the nuclear receptors PPARα, PPARγ and Rev-Erbα and plays a role in controlling white adipose and

liver tissue metabolism[74,75]. Further analysis of both PPARα and Rev-Erbα showed no changes in gene expression, but seeing that Per2 binds to the receptors and has not been shown to influence transcription, it is possible that Per2 is acting with these receptors in the liver to help control metabolic perturbations caused by fetal programming.

As previously mentioned, females showed a total of 17 dysregulated genes across all gene panels. The greatest amount of dysregulation came from the lipid metabolism panel with 11 genes affected and the phospholipid metabolism with 2 genes affected. Interestingly all dysregulated genes in lipid and phospholipid metabolism were upregulated. The largest upregulation came from carnitine palmitoyltransferase 1 (CPT1A) with a 2.54-fold increase and CPT2 was also upregulated albeit not as strongly at 1.44-fold. CPT1A and CPT2 are involved in the formation of acyl carnitines to allow for transport of lipids from the cytosol to the mitochondria and the product of this reaction is usually palmitoylcarnitine[118]. In the female metabolomics it was seen that propionylcarnitine, an acylcarnitine, was increased by 2.069-fold. An intermediate of fatty acid oxidation, 3-hydroxyisovalerylcarnitine was also upregulated by 1.486-fold. The dysregulation in these metabolites matches with the increase in CPT1A and CPT2 gene expression. Since these carnitine intermediates are involved in the metabolic reaction but not consumed it makes sense there are matching increases in enzyme activity. The remaining 9 dysregulated genes in the lipid metabolism panel participate in fatty acid β-oxidation and include ACADL, ECH1, HADH, ACAT1, PCCA, PCCB, MCEE, MMUT and DECR1. In the female metabolomics, the following lipids were found to be dysregulated: phosphatidylethanolamine (18:2/18:2) (downregulated 167-fold), phosphatidylserine (14:0/14:1) (downregulated 2-fold), lactosylceramide (d18:1/12:0) (downregulated 4.5-fold), and linolenelaidic acid, a polyunsaturated fatty acid (downregulated

3-fold). This widespread upregulation seen across the 9 genes involved in β-oxidation indicates that an increased metabolism of lipids is occurring and matches the decreased lipid levels that were seen in the metabolomic screen. The two dysregulated genes involved in phospholipid metabolism were PLA1A, which hydrolyzes fatty acids at the sn-1 position of phosphatidylserine and GDE1, which hydrolyzes glycerophospholipids in general. In the metabolomics results, a phosphatidylethanolamine and phosphatidylserine were each shown to be downregulated and similarly to the lipid metabolism discussed above, the upregulation in phospholipid metabolism genes indicates there is an increased metabolism of phospholipids and matches the metabolomics data.

Like the males, females also exhibited 2 genes dysregulated in purine metabolism; adenosine deaminase (ADA; 0.79-fold downregulated), which converts AMP to Adenosine, and uricase (UOX; 0.89-fold downregulated) which converts uric acid to allantoin[115] (Table 9). With both enzymes located in the same pathway it makes sense that they exhibit similar effects in expression. In the female metabolomics it was seen that adenosine and adenine were upregulated about 2-fold. The downregulation in ADA indicates a decreased rate of metabolism of purine intermediates and matches the increased levels that were seen in the metabolomic screen. The metabolomics also indicated that hypoxanthin was upregulated 1.6-fold. As hypoxanthin is an upstream metabolite of the UOX reaction, this gives greater evidence to the slowing of the purine metabolism pathway. It is curious, however, that XDH or PNP, the other enzymes in this pathway, did not also experience dysregulation.

Lastly, the females had 2 genes dysregulated in the glutathione metabolism pathway (Table 10). Glutathione reductase (GSR), the enzyme responsible for reducing oxidized glutathione disulfide to glutathione which is an important cellular antioxidant[119], was

upregulated. This matches the metabolite data where females showed a 1.8-fold upregulation in glutathione disulfide. This upregulation in GSR activity could possibly be reacting to an increased amount of reactive oxygen species (ROS) within the liver in order to regenerate the antioxidant activity of glutathione. Superoxide dismutase 1 (SOD1) was also affected in this pathway with a downregulation. SOD1 is the cytoplasmic variant of superoxide dismutase, SOD2 is the mitochondrial form and SOD3 an extracellular form but all share a similar role of destroying superoxide radicals and provide an antioxidant response[120]. This investigation examined both SOD1 and SOD2 and showed that there is a decrease in cytoplasmic antioxidant activity compared to the mitochondrial in Dex exposed female offspring. Superoxide anions are dismutated by SOD to form hydrogen peroxide, which is then catalyzed to water by enzymes such as glutathione peroxidase or catalase[120]. With GSR and glutathione disulfide being elevated while SOD1 levels are lowered, it is possible that the antioxidant pathway had just been activated, which effectively turned off transcription of SOD1, oxidized glutathione to glutathione disulfide and increased transcription for GSR to reduce glutathione disulfide back to glutathione. It has been shown that the transcription of SOD1 is particularly susceptible to changes in methylation status in female Dex-exposed offspring[121]. Therefore it is also possible that the decrease in SOD1 expression is the product of a programmed hypermethylation event in female offspring of prenatal stress.

CPT1A protein analysis did not show significance with regard to programming or sex (Figure 15). This was especially interesting in females where the CPT1A gene and carnitine intermediates were found to be upregulated. It is possible that this upregulation at the gene level is accounting for this discrepancy at the protein level. As the entire fatty acid metabolism pathway is activated, it is possible the CPT1A enzyme is being consumed rapidly as it prepares lipids for transport to the mitochondria and this is why CPT1A has the highest fold-change of

the genes analyzed: to replenish the amount of CPT1A protein and continue metabolizing lipids at a faster rate.

As lipids and their metabolism were strongly implicated in this investigation, the concentration of triglycerides (TGs) was determined in both the liver and plasma of Dex-exposed offspring. Measuring the concentration of TGs in the liver and plasma of male and female offspring showed that the amount of TGs in the liver of Dex females is significantly upregulated from their saline counterparts and appears to match the concentration of TGs found in both saline and Dex males (Figure 16). Plasma TG levels were unaffected across all groups. It is interesting that the concentration of TGs in Dex females match TG concentrations in the males. Moreover, when RT-qPCR analysis was being performed it was noted that Ct values of Dex females were similar to their male counterparts as well (data not shown). Again, results show that females are more affected than the males; something that is not common in fetal programming. It is possible that this dysregulation in females is serving a potentially protective role. We then investigated if there was a link between the body weights of these animals and metabolic rate. When examining the body weight data (Figure 17), we see that both male and female Dex offspring show a decrease in their body weight compared to the saline control up to 17 weeks. By week 19, however, we have shown that the body weights of females subjected to the 100 Dex condition were more similar to the saline control[84]. It is possible an increased metabolism could be beneficial in this balancing out of body weight.

The liver TG data for females makes sense given what was already known of the system. The increased concentration of liver TGs could be driving the activation of lipid metabolism seen through the gene panel of that pathway. This increase in metabolism through increased fatty acid β-oxidation and activation of mitochondria (the site of the metabolism) is

likely driving the increase in glutathione metabolism and its subsequent antioxidant effects as tissues with increased lipid metabolism are at greater risk of oxidative stress[114] (see Figure 18 for hypothesized model of metabolic disruption).

In summary, in the liver females showed an increase in lipid metabolism and glutathione metabolism, a slight decrease in purine metabolism, an increase in the concentration of TGs and an overall decreased body weight. The males showed a different response in the liver with slightly increased purine metabolism, decreased body weight and a possible adaption for increasing the efficiency of lipid metabolism. This provides evidence of a programming of liver metabolism as reflected by permanent changes in the metabolic pathways investigated. This study adds further evidence to the idea that hepatic metabolism can be programmed by events during early life and also that these programming events are sex specific.

Due to the lack of circadian rhythm disruption in the liver, it appears as though the hepatic circadian clock was not affected during the programming, however, metabolism was. It is possible, however, that the disrupted circadian rhythms in these animals are still playing a role in this dysregulated metabolism possibly through ill-timed GC release by the adrenal glands, which show an altered circadian rhythm[52] or by mistimed signals from the brain areas, such as the hypothalamus, which drives feeding responses.

Next steps for this investigation will further explore the protein expression of key dysregulated genes in the highlighted metabolic pathways, such as ADA, XDH, GSR and dysregulated lipid metabolism genes to get a better understanding of the metabolic system from gene expression through to metabolite levels. As mentioned in previous sections, it may be appropriate in future animal studies to further investigate with an experimental plan where liver and plasma samples are harvested at different times of day to see fluctuations in response

to events such as sleeping, feeding, or presence of a stressor. A major limitation of this study was that it examined only one timepoint, which provided a snapshot in time of an everchanging system like metabolism. After that, further studies may be completed to try to reverse these effects, possibly by supplementing animals' postnatal diet. It has been shown that programmed hyperlipidemia and hypertension can be mediated by a postnatal diet supplemented with ω-3 fatty acids[122]. It is possible this supplementation or other diets could be beneficial in reducing the harm of prenatal stress seen in offspring.

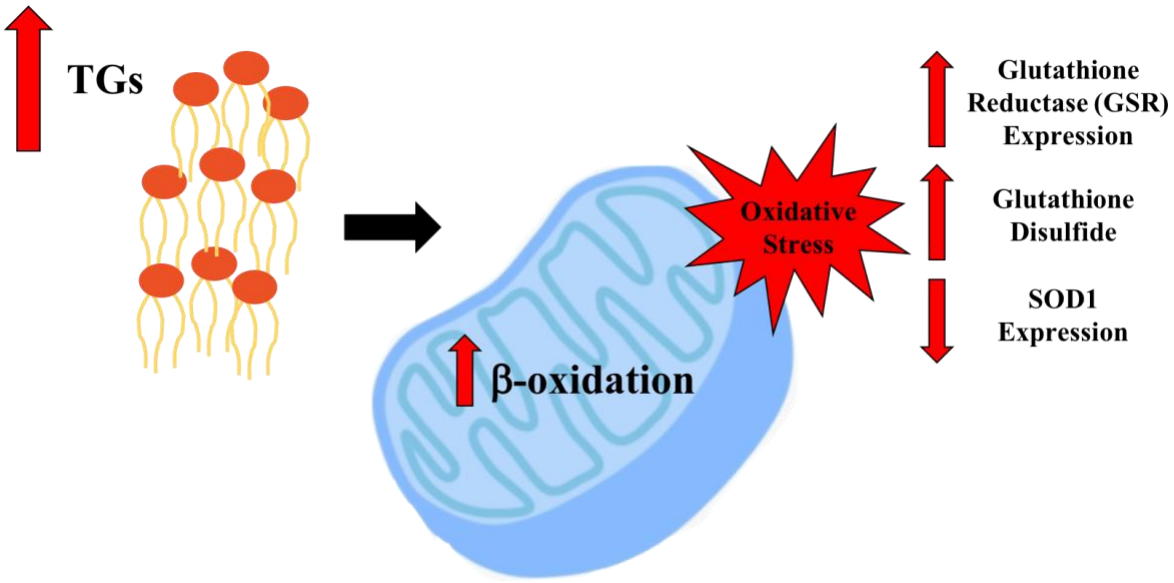

Figure 18. Exposure to Dex *in utero* causes disruption of lipid storage and metabolism in female offspring. Proposed model in which an increased level of triglycerides in the liver regulates lipid metabolism through the activation of β-oxidation, which leads to increased oxidative stress and subsequent activation of glutathione disulfide reduction through increased GSR activity.

5. Conclusion

Through an investigation into circadian rhythm gene expression in the SCN, amygdala hippocampus, PVN and PFC of GC exposed offspring, it was determined that prenatal stress in the form of GC exposure causes significant dysregulation in the expression of the circadian rhythm genes Bmal1, Clock, Npas2 as well as the Pers and Crys in both a sex and tissue specific manner. This study is the first to examine the molecular mechanism of circadian rhythm dysregulation in the brains of fetal programmed offspring. The widespread dysregulation that was shown to be both sex and tissue specific points to one of the initially hypothesized mechanisms whereby the peripheral clock dysfunction seen in the adrenal glands arises from a programmed dysregulation of the entire circadian system beginning at the master clock in the SCN. This investigation also examined circadian rhythm gene expression in the same five brain areas in SHR animals and again we saw widespread dysregulation. In this animal model dysregulation was tissue specific but not sex specific with the hippocampus, PVN and PFC all showing similar patterns between the sexes. This study is the first to examine all core circadian clock genes across these regions of the brain in SHRs. It is possible that over-activation in the PVN may be linked to the hypertensive phenotype seen. We also determined metabolic profiles in the livers of GC exposed offspring where we saw sex specific effects as the result of fetal programming. Females displayed increased lipid and glutathione metabolism, increased levels of liver TGs and decreased purine metabolism, while males showed increased purine metabolism and a hypothesized increase in lipid metabolism efficiency. These findings provide a link between fetal programming, circadian rhythms and metabolism in the brain, adrenal gland and liver and prove how interrelated physiology truly is.

References

1. Czeizel, A. E. Ten years of experience in periconceptional care. *Eur. J. Obstet. Gynecol. Reprod. Biol.* **84**, 43–49 (1999).
2. Barker, D. J. P. The fetal and infant origins of adult disease: The womb may be more important than the home. *BMJ* **301**, 1111 (1990).
3. Hales, C.N., Barker, D.J.P., Clark, P.M.S., Cox, J., Fall, C., Oxmond, C., and Winter, P. D. Fetal and infant growth and impaired glucose tolerance at age 64. *BMJ* **303**, 1019–1022 (1991).
4. Barker, D. J. P. Fetal origins of coronary heart disease. *BMJ* **311**, 171–174 (1995).
5. Godfrey, K. M. & Barker, D. J. P. Fetal programming and adult health. *Public Health Nutr.* **4**, 611–624 (2001).
6. Godfrey, K. M. & Barker, D. J. P. Fetal nutrition and adult disease. *Am. J. Clin. Nutr.* **71**, 1344S-1352S (2000).
7. Barker, D. J. P. The fetal and infant origins of disease. *Eur. J. Clin. Invest.* **25**, 457–463 (1995).
8. Lau, C., Rogers, J. M., Desai, M. & Ross, M. G. Fetal programming of adult disease: Implications for prenatal care. *Obstet. Gynecol.* **117**, 978–985 (2011).
9. Reppert, S. M. & Schwartz, W. J. Maternal suprachiasmatic nuclei are necessary for maternal coordination of the developing circadian system. *J. Neurosci.* **6**, 2724–2729 (1986).
10. McGraw, K., Hoffmann, R., Harker, C. & Herman, J. H. The development of circadian rhythms in a human infant. *Sleep* **22**, 303–310 (1999).
11. Serón-Ferré, M. *et al.* Circadian rhythms in the fetus. *Mol. Cell. Endocrinol.* **349**, 68–

75 (2012).

12. Seron-Ferre, M., Valenzuela, G. J. & Torres-Farfan, C. Circadian clocks during embryonic and fetal development. *Birth Defects Res. (Part C)* **81**, 204–214 (2007).

13. Jud, C. & Albrecht, U. Circadian rhythms in murine pups develop in absence of a functional maternal circadian clock. *J. Biol. Rhythms* **21**, 149–154 (2006).

14. Koch, C. E., Leinweber, B., Drengberg, B. C., Blaum, C. & Oster, H. Interaction between circadian rhythms and stress. *Neurobiol. Stress* **6**, 57–67 (2017).

15. Zelinski, E. L., Deibel, S. H. & McDonald, R. J. The trouble with circadian clock dysfunction: Multiple deleterious effects on the brain and body. *Neurosci. Biobehav. Rev.* **40**, 80–101 (2014).

16. Nakao, A., Nakamura, Y. & Shibata, S. The circadian clock functions as a potent regulator of allergic reaction. *Allergy Eur. J. Allergy Clin. Immunol.* **70**, 467–473 (2015).

17. Xie, Y. *et al.* New insights into the circadian rhythm and its related diseases. *Front. Physiol.* **10**, (2019).

18. Nader, N., Chrousos, G. P. & Kino, T. Interactions of the circadian CLOCK system and the HPA axis. *Trends Endocrinol. Metab.* **21**, 277–286 (2010).

19. Lange, T., Dimitrov, S. & Born, J. Effects of sleep and circadian rhythm on the human immune system. *Ann. N. Y. Acad. Sci.* **1193**, 48–59 (2010).

20. Nicolaides, N. C., Charmandari, E., Chrousos, G. P. & Kino, T. Circadian endocrine rhythms: the hypothalamic-pituary-adrenal axis and its actions. *Ann. N. Y. Acad. Sci.* **1318**, 71–80 (2014).

21. Zhang, R., Lahens, N. F., Ballance, H. I., Hughes, M. E. & Hogenesch, J. B. A circadian gene expression atlas in mammals: Implications for biology and medicine.

Proc. Natl. Acad. Sci. **111**, 16219–16224 (2014).

22. Karlsson, B., Knutsson, A. & Lindahl, B. Is there an association between shift work and having a metabolic syndrome? Results from a population based study of 27,485 people. *Occup. Environ. Med.* **58**, 747–52 (2001).
23. Vegiopoulos, A. & Herzig, S. Glucocorticoids, metabolism and metabolic diseases. *Mol. Cell. Endocrinol.* **275**, 43–61 (2007).
24. Stevens, R. G. Circadian disruption and breast cancer: From melatonin to clock genes. *Epidemiology* **16**, 254–258 (2005).
25. Shi, S., Ansari, T. S., Mcguinness, O. P., Wasserman, D. H. & Johnson, C. H. Circadian Disruption Leads to Insulin Resistance and Obesity. *Curr. Biol.* **23**, 372–381 (2013).
26. Huang, W. *et al.* Circadian rhythms, sleep, and metabolism. **121**, 2133–2141 (2011).
27. McGinnis, G. R. & Young, M. E. Circadian regulation of metabolic homeostasis : causes and consequences. *Nat. Sci. Sleep* **8**, 163–180 (2016).
28. Zhao, M., Xing, H., Chen, M., Dong, D. & Wu, B. Circadian clock-controlled drug metabolism and transport. *Xenobiotica* **50**, 495–505 (2020).
29. Rosenwasser, A. M. Alcohol, antidepressants, and circadian rhythms: Human and animal models. *Alcohol Res. Heal.* **25**, 126–135 (2001).
30. Salvatore, P., Indic, P., Murray, G. & Baldessarini, R. J. Biological rhythms and mood disorders. *Dialogues Clin. Neurosci.* **14**, 369–379 (2012).
31. McEwen, B. S. *et al.* Mechanism of stress in the brain. *Nat. Neurosci.* **18**, 1353–1363 (2016).
32. Drake, A. J., Tang, J. I. & Nyirenda, M. J. Mechanisms underlying the role of glucocorticoids in the early life programming of adult disease. *Clin. Sci.* **113**, 219–232

(2007).

33. Garabedian, M. J., Harris, C. A. & Jeanneteau, F. Glucocorticoid receptor action in metabolic and neuronal function. *F1000Research* **6**, 1208 (2017).

34. Dickmeis, T. Glucocorticoids and the circadian clock. *J. Endocrinol.* **200**, 3–22 (2009).

35. Yan, J., Wang, H., Liu, Y. & Shao, C. Analysis of gene regulatory networks in the mammalian circadian rhythm. *PLoS Comput. Biol.* **4**, e1000193 (2008).

36. Nader, N., Chrousos, G. P. & Kino, T. Circadian rhythm transcription factor CLOCK regulates the transcriptional activity of the glucocorticoid receptor by acetylating its hinge region lysine cluster: potential physiological implications. *FASEB J.* **23**, 1572–1583 (2009).

37. Balsalobre, A. *et al.* Resetting of circadian time in peripheral tissues by glucocorticoid signaling. *Science (80-.).* **289**, 2344–2347 (2000).

38. Bell-Pedersen, D. *et al.* Circadian rhythms from multiple oscillators: Lessons from diverse organisms. *Nat. Rev. Genet.* **5**, 544–556 (2005).

39. Son, G. H., Chung, S. & Kim, K. The adrenal peripheral clock: Glucocorticoid and the circadian timing system. *Front. Neuroendocrinol.* **32**, 451–465 (2011).

40. Chung, S., Son, G. H. & Kim, K. Circadian rhythm of adrenal glucocorticoid: Its regulation and clinical implications. *Biochim. Biophys. Acta - Mol. Basis Dis.* **1812**, 581–591 (2011).

41. Yoo, S.-H. *et al.* PERIOD2::LUCIFERASE real-time reporting of circadian dynamics reveals persistent circadian oscillations in mouse peripheral tissues. *Proc. Natl. Acad. Sci.* **101**, 5339–5346 (2004).

42. Hill, M. A. Hypothalamus - Pituitary - Adrenal Endocrine Axis. *UNSW Embryology*

(2012). Available at: https://embryology.med.unsw.edu.au/embryology/index.php%3Ftitle%3DFile:HPA_axis.jpg&rct.

43. Kapoor, A., Dunn, E., Kostaki, A., Andrews, M. H. & Matthews, S. G. Fetal programming of hypothalamo pituitary adrenal function: prenatal stress and glucocorticoids. *J. Physiol.* **572**, 31–44 (2006).

44. Mirmiran, M., Maas, Y. G. H. & Ariagno, R. L. Development of fetal and neonatal sleep and circadian rhythms. *Sleep Med. Rev.* **7**, 321–334 (2003).

45. Iqbal, M., Moisiadis, V. G., Kostaki, A. & Matthews, S. G. Transgenerational effects of prenatal synthetic glucocorticoids on hypothalamic-pituitary-adrenal function. *Endocrinology* **153**, 3295–3307 (2012).

46. Drake, A. J., Walker, B. R. & Seckl, J. R. Intergenerational consequences of fetal programming by in utero exposure to glucocorticoids in rats. *Am. J. Physiol. Integr. Comp. Physiol.* **288**, R34–R38 (2004).

47. Bol, V., Desjardins, F., Reusens, B., Balligand, J. L. & Remacle, C. Does early mismatched nutrition predispose to hypertension and atherosclerosis, in male mice? *PLoS One* **5**, e12656 (2010).

48. Adair, L. S. & Cole, T. J. Rapid child growth raises blood pressure in adolescent boys who were thin at birth. *Hypertension* **41**, 451–456 (2003).

49. Grgic, G., Fatusic, Z. & Bogdanovic, G. Stimulation of fetal lung maturation with dexamethasone in unexpected premature labor. *Med Arh* **57**, 291–294 (2003).

50. Williamson, C. R., Khurana, S., Nguyen, P., Byrne, C. J. & Tai, T. C. Comparative Analysis of Renin-Angiotensin System (RAS)-Related Gene Expression Between Hypertensive and Normotensive Rats. *Med. Sci. Monit. Basic Res.* **23**, 20–24 (2017).

51. Nguyen, P. *et al.* Prenatal glucocorticoid exposure programs adrenal PNMT expression and adult hypertension. *J. Endocrinol.* **227**, 117–127 (2015).

52. Tharmalingam, S., Khurana, S., Murray, A., Lamothe, J. & Tai, T. C. Whole transcriptome analysis of adrenal glands from prenatal glucocorticoid programmed hypertensive rodents. *Sci. Rep.* **10**, (2020).

53. Englund, A. *et al.* NPAS2 and PER2 are linked to risk factors of the metabolic syndrome. *J. Circadian Rhythms* **7**, 1–9 (2009).

54. Edelmann, M. N., Sandman, C. A., Glynn, L. M., Wing, D. A. & Davis, E. P. Antenatal glucocorticoid treatment is associated with diurnal cortisol regulation in term-born children. *Psychoneuroendocrinology* **72**, 106–112 (2016).

55. Douma, L. G. & Gumz, M. L. Circadian clock-mediated regulation of blood pressure. *Free Radic. Biol. Med.* **119**, 108–114 (2018).

56. Rudic, R. D. & Fulton, D. J. Pressed for time: the circadian clock and hypertension. *J. Appl. Physiol.* **107**, 1328–1338 (2009).

57. Diaz, A. I. G. *et al.* New Wistar Kyoto and spontaneously hypertensive rat transgenic models with ubiquitous expression of green fluorescent protein. *DMM Dis. Model. Mech.* **9**, 463–471 (2016).

58. Roman, O., Seres, J., Pometlova, M. & Jurcovicova, J. Neuroendocrine or behavioral effects of acute or chronic emotional stress in Wistar Kyoto (WKY) and spontaneously hypertensive (SHR) rats. *Endocr. Regul.* **38**, 151–155 (2004).

59. Reckelhoff, J. F., Zhang, H. & Srivastava, K. Gender differences in development of hypertension in spontaneously hypertensive rats: Role of the renin-angiotensin system. *Hypertension* **35**, 480–483 (2000).

60. Rudic, R. D. & Fulton, D. J. Pressed for time: The circadian clock and hypertension.

J. Appl. Physiol. **107**, 1328–1338 (2009).

61. Woon, P. Y. *et al.* Aryl hydrocarbon receptor nuclear translocator-like (BMAL1) is associated with susceptibility to hypertension and type 2 diabetes. *Proc. Natl. Acad. Sci. U. S. A.* **104**, 14412–14417 (2007).

62. Tanaka, S. *et al.* The adrenal gland circadian clock exhibits a distinct phase advance in spontaneously hypertensive rats. *Hypertens. Res.* **42**, 165–173 (2019).

63. Morris, C. J., Purvis, T. E., Mistretta, J., Hu, K. & Scheer, F. A. J. L. Circadian Misalignment Increases C-Reactive Protein and Blood Pressure in Chronic Shift Workers. *J. Biol. Rhythms* **32**, 154–164 (2017).

64. Curtis, A. M. *et al.* Circadian variation of blood pressure and the vascular response to asynchronous stress. *Proc. Natl. Acad. Sci. U. S. A.* **104**, 3450–3455 (2007).

65. Marques, F. Z. *et al.* Gene expression profiling reveals renin mRNA overexpression in human hypertensive kidneys and a role for microRNAs. *Hypertension* **58**, 1093–1098 (2011).

66. Eckel-Mahan, K. & Sassone-Corsi, P. Metabolism and the circadian clock converge. *Physiol. Rev.* **93**, 107–135 (2013).

67. Wang, M. The role of glucocorticoid action in the pathophysiology of the Metabolic Syndrome. *Nutr. Metab.* **2**, (2005).

68. Reinke, H. & Asher, G. Circadian Clock Control of Liver Metabolic Functions. *Gastroenterology* **150**, 574–580 (2016).

69. Froy, O. Metabolism and circadian rhythms - Implications for obesity. *Endocr. Rev.* **31**, 1–24 (2010).

70. Duez, H. & Staels, B. Rev-erb-α: An integrator of circadian rhythms and metabolism. *J. Appl. Physiol.* **107**, 1972–1980 (2009).

71. Marcheva, B. *et al.* Circadian clocks and metabolism. *Handb. Exp. Pharmacol.* **217**, 127–155 (2013).

72. Stephan, F. K. & Zucker, I. Circadian rhythms in drinking behavior and locomotor activity of rats are eliminated by hypothalamic lesions. *Proc. Natl. Acad. Sci. U. S. A.* **69**, 1583–1586 (1972).

73. Vollmers, C. *et al.* Time of feeding and the intrinsic circadian clock drive rhythms in hepatic gene expression. *Proc. Natl. Acad. Sci. U. S. A.* **106**, 21453–21458 (2009).

74. Schmutz, I., Ripperger, J. A., Baeriswyl-Aebischer, S. & Albrecht, U. The mammalian clock component PERIOD2 coordinates circadian output by interaction with nuclear receptors. *Genes Dev.* **24**, 345–357 (2010).

75. Grimaldi, B. *et al.* PER2 controls lipid metabolism by direct regulation of PPARγ. *Cell Metab.* **12**, 509–520 (2010).

76. Zhang, E. E. *et al.* Cryptochrome mediates circadian regulation of cAMP signaling and hepatic gluconeogenesis. *Nat. Med.* **16**, 1152–1156 (2010).

77. Adamovich, Y., Aviram, R. & Asher, G. The emerging roles of lipids in circadian control. *Biochim. Biophys. Acta - Mol. Cell Biol. Lipids* **1851**, 1017–1025 (2015).

78. Kyrou, I. & Tsigos, C. Stress mechanisms and metabolic complications. *Horm. Metab. Res.* **39**, 430–438 (2007).

79. Rabasa, C. & Dickson, S. L. Impact of stress on metabolism and energy balance. *Curr. Opin. Behav. Sci.* **9**, 71–77 (2016).

80. Martí, O., Martí, J. & Armario, A. Effects of chronic stress on food intake in rats: Influence of stressor intensity and duration of daily exposure. *Physiol. Behav.* **55**, 747–753 (1994).

81. Harris, R. B. S., Palmondon, J., Leshin, S., Flatt, W. P. & Richard, D. Chronic

disruption of body weight but not of stress peptides or receptors in rats exposed to repeated restraint stress. *Horm. Behav.* **49**, 615–625 (2006).

82. Pecoraro, N., Reyes, F., Gomez, F., Bhargava, A. & Dallman, M. F. Chronic stress promotes palatable feeding, which reduces signs of stress: Feedforward and feedback effects of chronic stress. *Endocrinology* **145**, 3754–3762 (2004).

83. McEwen, B. S. The Weathering Hypothesis of Aging: Part II. *Cyberounds* (2002). Available at: http://www.cyberounds.com/cmecontent/art43.html.

84. Khurana, S. *et al.* Fetal programming of adrenal PNMT and hypertension by glucocorticoids in WKY rats is dose and sex-dependent. *PLoS One* **14**, (2019).

85. Grandbois, J. *et al.* Phenylethanolamine N-methyltransferase gene expression in adrenergic neurons of spontaneously hypertensive rats. *Neurosci. Lett.* **635**, 103–110 (2016).

86. Paxinos, G. & Watson, C. *The Rat Brain in Stereotaxic Coordinates: Sixth Edition*. *Elsevier Academic Press* (2006).

87. Livak, K. J. & Schmittgen, T. D. Analysis of relative gene expression data using real-time quantitative PCR and the 2-ΔΔCT method. *Methods* **25**, 402–408 (2001).

88. Landgraf, D., Wang, L. L., Diemer, T. & Welsh, D. K. NPAS2 Compensates for Loss of CLOCK in Peripheral Circadian Oscillators. *PLoS Genet.* **12**, e1005882 (2016).

89. Palmisano, B. T., Stafford, J. M. & Pendergast, J. S. High-Fat feeding does not disrupt daily rhythms in female mice because of protection by ovarian hormones. *Front. Endocrinol. (Lausanne).* **8**, Article 44 (2017).

90. Erzberger, A., Hampp, G., Granada, A. E., Albrecht, U. & Herzel, H. Genetic redundancy strengthens the circadian clock leading to a narrow entrainment range. *J. R. Soc. Interface* **10**, 20130221 (2013).

91. Jeanneteau, F. & Chao, M. V. Are BDNF and glucocorticoid activities calibrated? *Neuroscience* **239**, 173–195 (2013).

92. Lamia, K. A. *et al.* Cryptochromes mediate rhythmic repression of the glucocorticoid receptor. *Nature* **480**, 552–556 (2011).

93. Sapolsky, R. M. & Meaney, M. J. Maturation of the adrenocortical stress response: Neuroendocrine control mechanisms and the stress hyporesponsive period. *Brain Res. Rev.* **11**, 65–76 (1986).

94. Lee, Y. *et al.* Coactivation of the CLOCK-BMAL1 complex by CBP mediates resetting of the circadian clock. *J. Cell Sci.* **123**, 3547–3557 (2010).

95. Ripperger, J. A. & Schibler, U. Rhythmic CLOCK-BMAL1 binding to multiple E-box motifs drives circadian Dbp transcription and chromatin transitions. *Nat. Genet.* **38**, 369–374 (2006).

96. Doi, M., Hirayama, J. & Sassone-Corsi, P. Circadian Regulator CLOCK Is a Histone Acetyltransferase. *Cell* **125**, 497–508 (2006).

97. Ferguson, A. V., Latchford, K. J. & Sanon, W. K. The paraventricular nucleus of the hypothalamus - A potential target for integrative treatment of autonomic dysfunction. *Expert Opin. Ther. Targets* **12**, 717–727 (2008).

98. Asai, M. *et al.* Circadian profile of Per gene mRNA expression in the suprachiasmatic nucleus, paraventricular nucleus, and pineal body of aged rats. *J. Neurosci. Res.* **66**, 1133–1139 (2001).

99. Arnsten, A. F. T. Stress signalling pathways that impair prefrontal cortex structure and function. *Nat. Rev. Neurosci.* **10**, 410–422 (2009).

100. Yamaguchi, S. *et al.* Role of DBP in the Circadian Oscillatory Mechanism. *Mol. Cell. Biol.* **20**, 4773–4781 (2000).

101. Wang, Y. L. *et al.* Effects of circadian rhythm disorder on the hippocampus of SHR and WKY rats. *Neurobiol. Learn. Mem.* **168**, (2020).

102. Folkow, B., Hallback-Norlander, M., Martner, J. & Nordborg, C. Influence of amygdala lesions on cardiovascular responses to alerting stimuli, on behaviour and on blood pressure development in spontaneously hypertensive rats. *Acta Physiol. Scand.* **116**, 133–139 (1982).

103. Takeda, K. *et al.* Sympathetic inhibition and attenuation of spontaneous hypertension by PVN lesions in rats. *Brain Res.* **543**, 296–300 (1991).

104. Chun, L. E., Woodruff, E. R., Morton, S., Hinds, L. R. & Spencer, R. L. Variations in phase and amplitude of rhythmic clock gene expression across prefrontal cortex, hippocampus, amygdala, and hypothalamic paraventricular and suprachiasmatic nuclei of male and female rats. *J. Biol. Rhythms* **30**, 417–436 (2015).

105. Lim, A. S. P. *et al.* Sex difference in daily rhythms of clock gene expression in the aged human cerebral cortex. *J. Biol. Rhythms* **28**, 117–129 (2013).

106. Douma, L. G. *et al.* Female C57BL/6J mice lacking the circadian clock protein PER1 are protected from nondipping hypertension. *Am. J. Physiol. Integr. Comp. Physiol.* **316**, R50–R58 (2018).

107. Astiz, M. & Oster, H. Perinatal Programming of Circadian Clock-Stress Crosstalk. *Neural Plast.* **2018**, 5689165 (2018).

108. Mendez, N. *et al.* Gestational chronodisruption impairs circadian physiology in rat male offspring, increasing the risk of chronic disease. *Endocrinology* **157**, 4654–4668 (2016).

109. Peters, R. V. *et al.* The control of circadian rhythms and the levels of vasoactive intestinal peptide mRNA in the suprachiasmatic nucleus are altered in spontaneously

hypertensive rats. *Brain Res.* **639**, 217–227 (1994).

110. Rosenwasser, A. & Plante, L. Circadian activity rhythms in SHR and WKY rats: strain differences and effects of clonidine. *Physiol. Behav.* **53**, 23–29 (1993).

111. Kuo, T. B. J., Shaw, F. Z., Lai, C. J., Lai, C. W. & Yang, C. C. H. Changes in sleep patterns in spontaneously hypertensive rats. *Sleep* **27**, 406–412 (2004).

112. Coogan, A. N., Baird, A. L., Popa-Wagner, A. & Thome, J. Circadian rhythms and attention deficit hyperactivity disorder: The what, the when and the why. *Prog. Neuro-Psychopharmacology Biol. Psychiatry* **67**, 74–81 (2016).

113. Jung-Hynes, B., Huang, W., Reiter, R. J. & Ahmad, N. Melatonin resynchronizes dysregulated circadian rhythm circuitry in human prostate cancer cells. *J. Pineal Res.* **49**, 60–68 (2010).

114. Thompson, L. P. & Al-Hasan, Y. Impact of oxidative stress in fetal programming. *J. Pregnancy* **2012**, (2012).

115. Sauer, A. V., Brigida, I., Carriglio, N. & Aiuti, A. Autoimmune dysregulation and purine metabolism in adenosine deaminase deficiency. *Front. Immunol.* **3**, (2012).

116. El Ridi, R. & Tallima, H. Physiological functions and pathogenic potential of uric acid: A review. *J. Adv. Res.* **8**, 487–493 (2017).

117. Mazzali, M. *et al.* Uric acid and hypertension: Cause or effect? *Curr. Rheumatol. Rep.* **12**, 108–117 (2010).

118. Bremer, J. Carnitine. Metabolism and functions. *Physiol. Rev.* **63**, 1420–1480 (1983).

119. Robaczewska, J. *et al.* Role of glutathione metabolism and glutathione-related antioxidant defense systems in hypertension. *J. Physiol. Pharmacol.* **67**, 331–337 (2016).

120. Fukai, T. & Ushio-Fukai, M. Superoxide dismutases: Role in redox signaling,

vascular function, and diseases. *Antioxidants Redox Signal.* **15**, 1583–1606 (2011).

121. Lamothe, J. *et al.* The Role of DNMT and HDACs in the Fetal Programming of Hypertension by Glucocorticoids. *Oxid. Med. Cell. Longev.* **2020**, 5751768 (2020).

122. Wyrwoll, C. S., Mark, P. J., Mori, T. A., Puddey, I. B. & Waddell, B. J. Prevention of programmed hyperleptinemia and hypertension by postnatal dietary ω-3 fatty acids. *Endocrinology* **147**, 599–606 (2006).

Appendices

Appendix 1. Saline male vs Dex male raw metabolite data of significant results

Name	Molecular Weight	RT [min]	Ratio: (DM) / (SM)	P-value
1-[(9Z)-octadecenoyl]-2-[(4Z,7Z,10Z,13Z,16Z,19Z)-docosahexaenoyl]-sn-glycero-3-phosphocholine	831.57634	12.968	0.265	0.00054184
4-Formyl-2-methoxyphenyl hydrogen sulfate	232.00407	5.906	3.004	0.00351615
	649.43133	10.972	0.445	0.00708704
	782.56389	13.032	0.307	0.00823096
	808.57807	12.886	8.995	0.00883183
DL-Carnitine	161.10507	0.752	0.487	0.01061418
DL-TYROSINE	181.0736	1.068	0.63	0.01128288
Xanthine	152.03346	1.115	0.623	0.0124001
	474.29015	10.685	0.602	0.02156628
(E)-p-coumaric acid	164.04733	1.064	0.68	0.02293774
	565.31405	10.595	0.247	0.0234832
Dihexyverine	321.26642	10.613	0.306	0.02482968
DL-Tryptophan	204.08954	2.705	0.77	0.02914266
4149853	371.3033	10.799	0.203	0.03287597
9,10-Dimethoxy-1,2,3,6,7,12,15,16-octadehydrogalanthan-6-ium	266.11997	6.04	0.55	0.03435221
Xanthine	152.03274	1.088	0.634	0.0356631
	600.3371	10.947	0.241	0.03704887
	809.58238	13.189	0.228	0.03816212
SL3675000	262.22936	10.778	0.186	0.03849424
Uracil	112.02624	1.028	0.464	0.04046308
Hypoxanthin	136.03828	1.059	0.717	0.0405606
LysoPC(18:3(9Z,12Z,15Z))	517.31415	10.781	0.355	0.04166692
	442.18924	7.337	2.307	0.042561
3,16,23-Trihydroxy-12,29-dioxooleanan-21-yl 2-(methylamino)benzoate	637.39498	10.892	0.565	0.04479033
.alpha.-Aminoadipic acid	161.06873	0.791	0.212	0.0472026
Eicosapentanoic acid	302.22421	10.569	0.43	0.04859053

Appendix 2. Saline female vs Dex female raw metabolite data of significant results

Name	Molecular Weight	RT [min]	Ratio: (DF) / (SF)	P-value: (DF) / (SF)
2,3,4,5-Tetrahydroxypentanal	150.05415	1.023	6.228	1.3135E-07
3,16,23-Trihydroxy-12,29-dioxooleanan-21-yl 2-(methylamino)benzoate	637.39498	10.892	0.278	8.9726E-06
	609.36384	10.503	0.404	2.1542E-05
1,2-DILINOLEOYL-SN-GLYCERO-3-PHOSPHATIDYLETHANOLAMINE	739.515	12.616	0.006	6.1809E-05
spermidine	145.15781	0.974	1.869	8.4361E-05
	649.43133	10.972	0.374	9.8836E-05
	128.13133	0.974	1.827	0.0001056
ophthalmic acid	289.12773	1.004	4.303	0.00035531
O-(Hydroxy{(2R)-3-(tetradecanoyloxy)-2-[(9Z)-9-tetradecenoyloxy]propoxy}phosphoryl)-L-serine	677.42625	10.97	0.491	0.00121946
Creatinine	113.05918	1.009	1.905	0.00122754
N-[(2S,3R,4E)-1-{[4-O-(beta-D-Galactopyranosyl)-beta-D-glucopyranosyl]oxy}-3-hydroxy-4-octadecen-2-yl]dodecanamide	805.54891	12.409	0.216	0.00175637
	244.15345	1.174	1.805	0.0022134
Benserazide	257.10248	1.008	2.048	0.00288048
(2S,4R,4aS,4bR,6aS,8aR,11aR,15bS,15cS,17aS)-4-Hydroxy-2-(2-hydroxy-2-propanyl)-9,9,11,11,15b,15c-hexamethyl-12-oxo-3,4,5,6,6a,7,8,8a,9,11,11a,12,15,15b,15c,16,17,17a-octadecahydro-2H-[2]benzofuro[5,6-e]chromeno[5',6':6,7]indeno[1,2-b]indole-4a(4bH)-carbaldehyde	617.36883	10.611	0.463	0.00292188
	621.39993	11.107	0.5	0.00338076
	579.35326	10.733	0.576	0.00433824
Adenosine	267.09668	2.669	1.97	0.00473755
	593.36885	10.751	0.539	0.00502002
Adenine	135.05404	2.672	1.911	0.0109412
Elaidolinolenic acid	278.22449	9.748	0.308	0.01164811
Pregabalin	159.12588	1.002	1.723	0.01502947
	313.10272	2.674	2.081	0.01516026

3-Hydroxy-3-[(3-methylbutanoyl)oxy]-4-(trimethylammonio)butanoate	261.1575	1.251	1.486	0.0186267
Choline	103.10006	0.951	1.683	0.02210976
propionylcarnitine	217.13125	1.71	2.059	0.02685635
	175.12076	1.011	1.579	0.03285393
	635.3796	10.615	0.581	0.03286697
Hypoxanthin	136.03851	1.328	1.634	0.03538884
L-(+)-ERGOTHIONEINE	229.08838	0.976	1.558	0.03850724
Glutathione disulfide	612.15218	1.021	1.775	0.04162925
Nicotinamide	122.04825	1.599	1.464	0.04325364
5-Nitro-o-toluidine	152.05852	1.304	1.449	0.0448727
Benzoxazolone	135.03216	1.3	1.415	0.0460894
	829.54576	11.411	0.417	0.04699072
7-Chloro-5-(2-fluorophenyl)-1-(2-methoxyethyl)-1,3-dihydro-2H-1,4-benzodiazepin-2-one	346.08638	2.492	1.525	0.0472046
	574.11782	1.319	1.621	0.04741469
Caprolactam	113.08438	4.698	1.394	0.04861032
L-(-)-methionine	149.05102	1.029	1.667	0.04927301

Appendix 3. Saline female vs saline male raw metabolite data of significant results

Name	Molecular Weight	RT [min]	Ratio: (SF) / (SM)	P-value: (SF) / (SM)
196633	221.06081	8.594	0.117	1E-15
coenzyme Q2	318.18361	8.14	318.642	1E-15
10-GINGEROL	350.24589	8.55	92.479	1E-15
3, 5-Tetradecadiencarnitine	367.2722	8.905	76.421	1E-15
cerenox	241.0864	6.229	0.004	1E-15
(20S)-17,20-Dihydroxypregn-4-en-3-one	332.23506	8.547	138.132	1E-15
10-GINGEROL	350.24575	8.898	24.279	1E-15
clomazone	239.0713	7.221	0.089	1E-15
(1S,2R)-3-(4-Chlorophenyl)-3,5-cyclohexadiene-1,2-diol	222.04485	7.222	0.087	1E-15
clomazone	239.07136	6.107	0.101	5.0882E-13
	194.04996	6.107	0.112	6.567E-13
(1S,2R)-3-(4-Chlorophenyl)-3,5-cyclohexadiene-1,2-diol	222.04483	6.7	0.141	1.5687E-11
clomazone	239.07137	6.717	0.139	7.2535E-11

4-Formyl-2-methoxyphenyl hydrogen sulfate	232.00407	5.906	23.53	9.5519E-11
	323.15788	6.709	0.023	9.7808E-10
(+)-cephalosporin C	415.10378	7.666	0.052	1.2905E-09
	321.16094	6.707	0.023	2.2741E-09
propionylcarnitine	217.13125	1.71	5.529	3.4074E-09
(+)-Alantolactone	232.14641	8.449	6.187	1.2901E-08
Pirprofen	251.07117	8.052	0.364	1.6946E-08
	208.06565	7.56	0.127	2.8759E-07
3,7-Dihydroxy-2-(3-hydroxyphenyl)-5-chromanesulfinic acid	322.0518	7.134	0.143	6.7475E-07
2-Deoxy-2-(glycoloylamino)-6-O-phosphono-beta-D-mannopyranose	317.04926	7.931	154.783	7.1536E-07
Benzoxazolone	135.03216	1.3	0.318	3.746E-06
clomazone	239.07175	8.061	0.211	4.3556E-06
5-Nitro-o-toluidine	152.05852	1.304	0.321	5.7843E-06
2-(2-Chlorophenyl)-6-hydroxy-2-(methylamino)cyclohexanone	253.08697	7.391	0.263	6.0396E-06
D-PANTOTHENIC ACID	219.11047	1.331	0.305	8.6453E-06
13-KODE	294.21986	9.713	0.201	1.1753E-05
Gefitinib	446.15268	7.886	0.141	1.5055E-05
2172	391.23565	8.798	9.095	2.3617E-05
Xanthosine	284.07598	1.273	0.363	2.8086E-05
2,3,4,5-Tetrahydroxypentanal	150.05415	1.023	0.242	4.2858E-05
Benserazide	257.10261	0.731	0.329	5.6376E-05
Choline	103.10006	0.951	0.495	6.2836E-05
	513.29548	7.918	4.529	7.8136E-05
Pirprofen	251.07124	5.816	0.262	0.00011766
	512.29218	7.861	4.066	0.00012464
	121.06421	1.456	0.438	0.00015671
Tributyl citrate acetate	402.22257	1.792	0.39	0.00015909
	208.06557	6.827	0.386	0.00041287
METIPRANOLOL	309.19377	8.035	1.684	0.00042013
N-(tert-Butoxycarbonyl)-L-leucine	231.14695	1.851	2.997	0.0004714
5955761	287.20946	7.702	1.814	0.00067753
2-(6'-methylthio)hexylmalic acid	264.10433	1.498	0.387	0.0007738
(4S)-4-[(2E)-2-Octenoyloxy]-4-(trimethylammonio)butanoate	285.19403	7.448	2.765	0.00080983
	663.16487	1.46	0.382	0.0008131
6-(2-Chloroethyl)-2,5,7-trimethyl-1-indanone	236.09852	7.263	0.211	0.00102419

felbamate	238.0949	7.821	4.107	0.00102516
4H-Cyclopenta(def)chrysene	240.09163	7.825	4.067	0.00109128
Olprinone	250.08722	6.256	0.319	0.0010943
	239.0884	7.812	4.08	0.00110775
Anastrozole	293.16282	6.383	4.684	0.00134084
lubabegron	499.19725	7.934	0.11	0.0013586
Athamantin	430.20284	8.42	7.102	0.00150191
	244.15345	1.174	0.581	0.00158334
	234.09265	8.13	0.476	0.00192155
Benserazide	257.10248	1.008	0.515	0.00198983
	248.10788	8.703	4.315	0.00227704
O-heptanoylcarnitine	273.19376	7.055	4.03	0.00229667
Ketamine	237.09164	7.801	2.9	0.00244037
Adenosine monophosphate	347.06317	1.895	0.445	0.00253073
	280.04636	1.093	0.502	0.0029692
Adenylthiomethylpentose	297.0896	6.215	1.665	0.00300478
bamifylline	385.20989	1.72	0.247	0.00325093
L-Hexanoylcarnitine	259.17836	6.46	3.281	0.00363008
Palmitelaidic acid	254.22662	9.683	0.429	0.00395922
1,2-Dioleoyl-sn-glycero-3-phospho-L-serine	787.53594	11.592	0.103	0.00429294
	250.10487	8.703	4.291	0.00431093
	619.38453	10.854	0.443	0.00493303
	119.07374	1.839	0.574	0.00501341
Xanthine	152.03274	1.088	0.542	0.00560849
	771.54117	11.906	0.119	0.00598636
(E)-p-coumaric acid	164.04733	1.064	0.581	0.00624659
Xanthine	152.03346	1.115	0.605	0.00642568
2-Hydroxyfelbamate	254.09009	1.014	0.222	0.00679927
6-Chloroindole	151.01878	7.811	3.099	0.00695341
Uracil	112.02624	1.028	0.511	0.00840199
	221.02175	0.942	2.276	0.00860134
DL-TYROSINE	181.0736	1.068	0.558	0.00874341
Pregabalin	159.12588	1.002	1.632	0.00919584
METIPRANOLOL	309.19365	7.812	1.295	0.00920268
N-(4-Chlorobenzyl)-N-ethyl-2-pyridinamine	246.09231	7.613	0.396	0.01255114
Uridine	244.06966	1.099	0.624	0.01418995
	371.23084	5.289	0.27	0.01441244
	845.54082	11.4	0.284	0.01577175

protionamide	180.07219	6.474	0.29	0.01663512
2,2'-Iminodipropan-1-ol	133.11033	0.968	0.277	0.01903824
13S-hydroxyoctadecadienoic acid	296.23561	10.196	0.232	0.01948727
4'-Phosphopantetheine	358.09653	2.224	0.475	0.02043289
Ricinoleic Acid	298.25103	10.447	0.269	0.02288367
8-hydroxy-deoxyguanosine	283.09173	1.406	4.5	0.02397873
norketamine	223.07631	7.858	0.616	0.0244402
DL-Phenylalanine	165.07878	1.838	0.608	0.02524767
DL-Glutamic acid	147.05273	0.998	0.574	0.02645511
L-Proline	115.06364	0.981	0.584	0.02709891
Uracil	112.02756	1.099	0.71	0.02739632
	829.54576	11.411	0.206	0.0277043
	827.53047	11.39	0.269	0.02823545
MFCD00055031	206.04975	7.844	0.624	0.03015383
4-amino-2-hydroxyamino-6-nitrotoluene	183.06594	0.741	1.667	0.03537848
	730.53337	12.534	0.346	0.03787721
DL-Glutamic acid	147.05212	0.992	0.609	0.03931819
demecycline	430.13367	1.382	0.509	0.03968451
	773.5569	12.162	0.34	0.0399598
Adenosine monophosphate	347.06311	1.045	3.448	0.04176953
D-Gluconic acid	196.05794	1.026	0.544	0.04269252
	516.32357	9.4	2.006	0.04659024
13S-hydroxyoctadecadienoic acid	296.23557	9.757	0.472	0.04663023
	649.43133	10.972	0.461	0.04663666
2-methylbutyrylcarnitine	245.1626	4.264	1.447	0.04999916